The Association of PARP1 Enzymatic Inhibition and Chromatin Complex Formation with Radiosensitization by PARP Inhibitors and Their Combination with ATR Inhibition in Pancreatic Cancer

by

Carl G. Engelke

A dissertation submitted in partial fulfillment
of the requirements of the degree of
Doctor of Philosophy
(Molecular and Cellular Pathology)
in the University of Michigan
2020

Doctoral Committee:

Professor Arul M. Chinnaiyan, Co-Chair
Professor Theodore S. Lawrence, Co-Chair
Professor Gary D. Hammer
Associate Professor Meredith A. Morgan
Assistant Professor Corey W. Speers
Professor Scott A. Tomlins

Carl G. Engelke
cengelke@umich.edu
ORCID iD: 0000-0002-4510-7528

DEDICATION

This dissertation is dedicated to my family: to my wife and partner, Téa Prokes, and to my parents, Alexandra Krikos and David Engelke. The love and support you have shown me has meant more than I could ever express.

ACKNOWLEDGEMENTS

First and foremost, I would like to acknowledge and thank my mentors. I have had the very good fortune to be mentored not by one, but three wonderful scientists and advisors: Meredith Morgan, Ted Lawrence, and Arul Chinnaiyan. They have provided me a scientific home and contributed to my development as a scientist in ways that I appreciate and will continue to appreciate throughout my life. From troubleshooting experiments and organizing testable hypotheses, to managing projects and understanding the scientific field and how it moves, they have contributed to my education. Each has provided me unique research opportunities and scientific insight and I will always be grateful to them.

I would also like to thank the other three members of my thesis committee. Gary Hammer, Corey Speers, and Scott Tomlins have provided me not only with scientific guidance during our many formal committee meetings and informal discussions, but also wisdom about what it means to be a physician scientist and how to navigate the path ahead of me.

The work presented in this dissertation would not have been possible without the effort and assistance of many members of the Morgan lab, whom I would like to thank here. The investigations into PARP trapping in combination with radiation and ATR inhibition is a project I shared with our laboratory manager, Leslie Parsels. In addition to the enormous body of work she contributed to this project, she has been a constant source of support and scientific feedback. Josh Parsels is another member of the lab who contributed many experiments to the

work presented in this dissertation; in addition, I appreciated his patience and tutelage in many techniques where he demonstrates wizardry, including animal experiments and microscopy. Finally, I would like to thank Qiang Zhang for his guidance in my earlier investigations into ubiquitin ligases, which do not appear in this dissertation. It goes without saying that in addition to the ways that I appreciate all members of the lab from the perspective of our professional collaboration, I also consider them friends.

I would like to thank the various organizations that have supported me during my time in graduate school. The MSTP has helped me navigate the transitions between medical school and graduate school and has helped me stay on course during this long journey. Specifically, I would like to thank director Ron Koenig and assistant directors Justine Hein and Ellen Elkin, in addition to the associate directors and office staff. The Molecular and Cellular Pathology training program, its director Zaneta Nikolovska-Coleska, and administrator Laura Labut have provided me enormous help navigating the hurdles of graduate school. The Department of Radiation Oncology and Michigan Center for Translational Pathology have provided me scientific homes for the past five and a half years, for which I am grateful.

My family has been a constant source of support during graduate school and throughout my life. My parents have always encouraged me to follow my passions. They encouraged my curiosity and provided me every opportunity to explore and learn as I grew up. They supported and encouraged me when I went to music school and in my brief career as a professional musician, and again when I changed careers to pursue an MD and later a PhD.

When I began graduate school, I could not have imagined that I would meet and marry the wonderful woman who is now my wife. Téa Prokes has been an incredible, loving, and

supportive partner in my life since we met. I love her and look forward to the adventures that await us in the next chapter of our lives.

TABLE OF CONTENTS

LIST OF FIGURES

LIST OF ILLUSTRATIONS

ABSTRACT

Pancreatic cancer has a five-year overall survival rate of less than 10%. Locoregional progression is responsible for death in up to a third of all patients, highlighting the need for local control. The use of chemotherapeutic agents in combination with radiation represents a current standard of care for locally advanced PDAC, but new therapies are urgently needed.

PARP inhibitors have shown promise as radiosensitizing agents preclinically, both alone and in combination with chemotherapeutic or molecularly targeted agents. Work has demonstrated that their antitumor effect may be the product of their enzymatic inhibition or ability to form PARP1-DNA complexes at DNA damage sites known as PARP trapping. These complexes have been implicated as the cause for both therapeutic efficacy as well as many dose-limiting toxicities seen clinically.

In our work, we investigated the radiosensitizing properties of PARP inhibitors in pancreatic cancer cell line models. Using olaparib, which inhibits PARP at both low and high concentrations but only traps at high concentrations, we demonstrated that pancreatic cancer cells proficient in homologous recombination were only radiosensitized by high concentrations of olaparib. While we demonstrated that olaparib possesses the ability to inhibit enzymatically at both high and low concentrations, it is known to trap only at high. The ability to form PARP1-DNA complexes correlated with increased DNA double strand breaks at higher olaparib concentrations.

We discovered that the radiosensitizing potency of three PARP inhibitors, veliparib, olaparib, and talazoparib, corresponded to their described increasing potency as PARP trappers. Deletion of PARP1 failed to phenocopy the radiosensitizing effects of PARP inhibitors and protected cells from cytotoxicity from talazoparib. In order to more fully characterize PARP trapping, we adapted the proximity ligation assay to measure trapped PARP1 *in situ* by measuring the proximity of PARP1 and total histone H2AX in treated cells.

To further potentiate the radiosensitizing effects of PARP inhibition, we leveraged the knowledge that PARP inhibition causes replication stress. ATR is known to regulate the cellular response to replication stress and fork stability. Thus, we sought to combine PARP inhibition with the ATR inhibitor AZD6738. The combinatorial effect of ATR and PARP inhibition in HR proficient cell lines to radiosensitize and damage DNA was most pronounced at trapping concentrations of olaparib. Further, this effect required presence of the PARP1 protein. Combined treatment in mice bearing pancreatic cancer xenografts with olaparib, AZD6738, and radiation substantially inhibited tumor growth relative to all other treatment groups while causing minimal toxicity. These findings strongly recommend the merits of clinical investigation into the efficacy of combined ATR and PARP inhibition with radiation for locally advanced disease and suggest that the PARP inhibitors with greater PARP trapping potency may be most efficacious.

CHAPTER 1:

Introduction

Our laboratory focuses on the use of pharmacologic agents to improve the efficacy of therapeutic radiation for the treatment of pancreatic cancer. As such, our field has broadly focused on the stages of pancreatic cancer where radiation holds the most promise for treatment and the inherent makeup of pancreatic cancer that would render it susceptible to specific types of intervention. Past work has found that the use of anti-metabolite agents such as gemcitabine or 5-fluorouracil sensitizes pancreatic cancer to ionizing radiation through an increase in DNA damage. Since then, we have undertaken efforts to further increase the efficacy of these therapies through the introduction of molecularly targeted agents directed at proteins involved in pathways that influence DNA repair. My own work in the lab began with investigating inhibitors of cell cycle checkpoint proteins checkpoint kinase 1 and Wee1 kinase, the latter of which has gone on to show promise clinically in combination with chemoradiation. More recent work has focused on the inhibition of two sensors and master regulators of the DNA damage response—poly (ADP-ribose) polymerase 1 and ataxia telangiectasia mutated and Rad3-related—in combination with radiation, which will be presented in this dissertation.

1.1 Radiation and locoregional control in pancreatic cancer

90% of cancers of the pancreas are pancreatic ductal adenocarcinoma (PDAC) [1]. Among the most lethal cancers, it has a 5 year survival less than 10% [2]. Most of those in that 10% are among those able to undergo surgical resection [3]. Among the difficulties leading to these poor outcomes is the relative paucity of symptoms, leading to late-stage diagnosis in most patients [4]. To make matters worse, pancreatic cancer tends to be inherently aggressive and prone to early metastasis. Its typical mutational landscape and microenvironment render it highly resistant to conventional therapies. Finally, definitive surgical resection is difficult due to the tendency for invasion of critical local structures, leading to the famous “surgeon’s three rules” [5].

A relatively small number of PDACs (5-6%) contain germline mutations, the most frequent of which tend to be genes involved in DNA repair [6], [7]. Overwhelmingly, the most recurrently mutated gene in PDAC is KRAS, demonstrating an oncogenic activating mutation in greater than 90% of patients. Other recurrently mutated genes include TP53, SMAD4, and CDKN2A, which are reported at various frequencies but almost always above 50% [8]–[13]. Another hallmark of pancreatic cancers is the thick desmoplastic stroma surrounding tumor cells. It is estimated that up to 90% of pancreatic tumor volume is comprised of cancer-associated fibroblasts [14]. For this reason, study of the tumor microenvironment in PDAC represents a vital contribution to our understanding of the disease, but is beyond the scope of the work presented here (reviewed in [15]–[17]).

The standard of treatment for local PDAC with well-defined margins is surgical resection, but this only represents 10-20% patients at the time of diagnosis [18]. The remainder fall into the category of locally advanced or metastatic cancer. For these, the historical standard has been antimetabolite therapies such as Gem and 5-FluoroUracil

(5-FU) either alone or with radiation [19]. The recent introduction of a multidrug regimen consisting of folinic acid, 5-FU, irinotecan, and oxplatin (FOLFIRINOX) has improved outcomes [20] and despite increased toxicities associated with the more aggressive regimen has still measurably improved quality of life for patients [21]. Together with the addition of albumin-bound paclitaxel (nab-paclitaxel) to gemcitabine [22], [23], these represent the current standard of care.

While most non-resectable disease is metastatic, necessitating the use of aggressive systemic therapy, radiation represents an important therapeutic modality for local disease. However, the role of radiation in the locally advanced setting was called into question by a recent trial LAP07 [24], which showed no difference in median overall survival (OS) between chemotherapy and chemoradiotherapy. However, other trials suggest benefits of added radiation, with a study by the Eastern Cooperative Oncology group demonstrating an improvement in median OS from 9.2 months with gemcitabine alone to 11.1 months with gemcitabine plus radiation [25]. The importance of locoregional control in the setting of pancreatic cancer is underlined by the fact that up to one third of patients die from local disease progression [26] and that chemotherapy alone is unable to cure gross disease. Taken together the data suggest that as our systemic therapies continue to improve and reduce metastatic disease burden, the efficacy of radiation in the local setting will become more readily appreciable. Above all, they underline the inadequacy of our current approaches and the desperate need for advancement.

1.2 The DNA Damage Response

Therapeutic radiation has an upper limit of tolerability as a monotherapy due to surrounding normal tissue toxicity. Therefore, it becomes important to search for ways to enhance the tumor cell sensitivity to radiation while sparing normal tissues. One of the basic hallmarks of cancer is genomic instability and mutation [27], [28]. While this property is an advantage for growth and adaptation, it is also a liability as it renders the cancer cell vulnerable to therapeutic interventions. Specifically, these genomic vulnerabilities render the cell more susceptible to increased genomic stress and targeting of its remaining DNA safeguards. Normal tissues, meanwhile, are able to tolerate greater amounts of damage and removal of one or two redundant protective systems (reviewed in [29]). Much of the work, therefore, has focused on targeting weaknesses in the DNA damage repair and cell cycle checkpoint pathways, and the exploitation of replicative stress to preferentially sensitize cancer cells to radiotherapy.

Cellular ionizing radiation most frequently causes damage to the DNA backbone, creating a single-stranded break (SSB) or double-stranded break (DSB). SSBs are more common and repaired through SSB repair where they are sensed by poly (ADP-ribose) polymerase 1 (PARP1), which recruits repair factors including XRCC1 and Lig3. DSBs are more lethal [30] and are repaired by two main pathways: non-homologous end joining (NHEJ) or homologous recombination (HR) repair (**Illustration 1.2a**). NHEJ is the faster, error-prone repair pathway available to the cell throughout the cell cycle. It begins with the recognition and stabilization of DNA ends by the KU70 and KU80 heterodimers and initial recruitment of DNA-dependent protein kinase (DNA-PK). The repair process proceeds, recruiting other necessary factors, to ligate together blunt ends of the DNA and repair the breach. While the process is fast and the integrity of the DNA backbone

preserved, deletions can be introduced in genes through loss of material to generate blunt ends. For this reason, it is most frequently employed to repair simple DSBs. At complex or single-ended DSBs the chances of generating a deletion or ligating to a distal location in the genome is much greater.

During the S and G2 phases of the cell cycle, HR is available for the repair of DSBs. Using sister chromatids as a template, this process is able to repair even complex DNA lesions with high fidelity. After recognition of the insult by ataxia telangiectasia mutated (ATM) and Mre11-Rad50-Nbs1(MRN) complex, 5' ends of the DNA are resected and bound with replication protein a (RPA). RPA is bound by ATRIP, which in turn attracts ataxia telangiectasia mutated and RAD3-related (ATR) to sites of resolving DSBs. RAD51 recruitment to the site by BRCA2 allows sister chromatid strand invasion to provide a template for homology, ensuring high fidelity resolution.

A third type of DSB repair exists, known as alternative end joining (Alt-EJ), which may compensate in the absence of NHEJ or HR activity. Alt-EJ does not rely on the components of these pathways, but rather repairs lesions with slow kinetics through the actions of PARP1, XRCC1, Lig3, and other proteins that are still being elucidated. In some cases, Alt-EJ may be facilitated by regions of DNA sequence microhomology [31].

Another type of DNA backbone break occurs physiologically during replication, when the DNA strands are separated by helicase and newly synthesized DNA trails behind. At replication forks, single strand breaks caused by unligated Okazaki fragments account for a majority of cellular PARP1 activity. Replication forks that encounter an unpassable genomic lesion can become stalled, generating large stretches of single-stranded DNA

and activating ATR. Unresolved stalled replication forks can collapse to generate complex DSBs, which must then be repaired through HR.

In order to accommodate the repair of deleterious genomic lesions, the cell passes through several cycle checkpoints where it can arrest and repair damage (**Illustration 1.2b**). These checkpoints are activated by ATM and ATR, making them master regulators of the DNA damage response. The G1 checkpoint is crucial to prevent entry into S phase with unresolved damage, and relies on the phosphorylation and activation of p53 by ATM. The frequent mutation of p53 in pancreatic cancer leads the cell to rely heavily on its intra-S and G2/M checkpoints to prevent mitotic progression with catastrophic damage. ATR and ATM work in tandem through checkpoint kinase 1 (Chk1) and checkpoint kinase 2 (Chk2), respectively, to activate the intra-S and G2/M checkpoints. Wee1 kinase additionally regulates the G2/M checkpoint through inhibitory phosphorylation of Cdk1.

1.3 Chemoradiation

Conventional chemotherapeutic agents were among the first to be found to sensitize cancer cells *in vitro* to radiation [32]–[34] in the 1950's. A decade later, promising results were achieved in human trials by combining 5-FU with radiation in gastrointestinal cancers [35], [36]. Shortly thereafter, the same group investigated adding a regimen of 5-FU to radiotherapy for locally advanced unresectable pancreatic adenocarcinoma [37]. They found a significant survival benefit improving median survival from 23 weeks to either 33 weeks or 39 weeks depending on the dose of radiation. The combination of 5-FU and radiation was also investigated in the adjuvant setting for resected pancreatic adenocarcinoma, improving median survival from 11 months to 20 months [38]. A pilot

study in the neoadjuvant setting [39] demonstrated improved rates of resectable disease following radiation combined with 5-FU and mitomycin-C.

The increasing use of gemcitabine in pancreatic cancer led to its investigation in preclinical studies, where it demonstrated powerful radiosensitization [40], [41]. A retrospective analysis comparing radiation in combination with 5-FU or gemcitabine demonstrated higher toxicities in the gemcitabine-radiation group but a small but statistically insignificant median overall survival advantage [42]. These results underscored the relatively narrow therapeutic index for optimal chemoradiation.

Cisplatin is the most widely used chemotherapeutic in combination with radiation. Cisplatin is an inorganic platinum agent that forms intra-strand crosslinks on DNA, leading to impaired replication and DNA damage, which accounts for most of its toxicity [43]. As a single agent, these adducts are most frequently repaired by the nucleotide excision repair (NER) pathway. However, it has been established that the lesions induced by the radiosensitizing effects of cisplatin mostly involve NHEJ [44], and these adducts develop into complex DSBs following radiation induced DNA damage [45]. Similarly, temozolomide forms methyl adducts at specific positions on guanine and adenine which are normally repaired by Mismatch Repair (MMR). In conjunction with radiation, it inhibits DNA repair [46] and increases DSBs [47].

In pancreatic cancer, antimetabolites such as 5-FU and gemcitabine are the standard agents used in combination with radiation. In their active forms, both of these agents misincorporate into DNA, and inhibit enzymes involved in maintenance of the cellular nucleotide pool, thymidylate synthase and ribonucleotide reductase, respectively. The addition of these agents deplete available nucleotides and shift cells into incomplete

S-phase, where replication forks collide with radiation-induced SSBs to produce complex DSB that are repaired slowly [48], [49].

Despite all of the improvements in radiation efficacy delivered by traditional chemotherapeutics, their current delivery at maximally tolerated doses suggests that we have already or nearly realized their maximum therapeutic potential. However, with the development of molecularly targeted agents directed toward proteins involved in the DNA damage response, opportunities exist to improve the DNA damaging efficacy of chemoradiation without corresponding increases in toxicity.

1.4 Checkpoint kinase 1 (Chk1) and Wee1 kinase (Wee1)

Upon DNA damage, Chk1 is phosphorylated at S317 and S345 and hence activated by ATR [50]. In turn, Chk1 phosphorylates CDC25A, leading to a decrease in CDK2 activity and activation of the S-phase cell cycle checkpoint [51]. Additional phosphorylation events on CDC25B and CDC25C lead to their degradation and decreased CDK1/cyclinB activity and G2/M arrest [52], [53]. In yeast, Chk1 also acts to phophorylate Wee1 kinase to activate and further potentiate G2 arrest [54], [55], though it is not clear that it performs this function in humans. Additionally, studies have reported that it is involved in homologous recombination repair [56], [57] and the protection of replication fork integrity [58].

Specific inhibitors of Chk1/2 (AZD7762) and Chk1 (MK8776) were developed as anti-cancer therapeutics to exploit its cell cycle function by forcing cells through mitosis with damage [59]. Chk1 inhibition is most effective in the setting of cancers that already possess cell cycle defects. It is described to have synthetic lethality with the Fanconi

anemia pathway [60] and Rad17 [61] and Wee1 [62]. However, further investigation demonstrated that increased DNA damage and inhibition of HR are major contributors to the efficacy of Chk1 inhibitors [56].

Chk1 inhibition was first found to chemosensitize by the inhibitor UCN-01 [63], an agent originally developed to inhibit members of the protein kinase C family, but with many targets. More selective agents have been used in combination with gemcitabine and irrinotecan ([64]) and radiation [57] preclinically. In agreement with its proposed mechanism of forced mitotic entry, it preferentially sensitizes in p53 mutant cancers [65]–[67], which lack a functional G1 checkpoint. It has also been found to chemoradiosensitize in preclinical pancreatic cancer models [68]. Inhibitors have undergone clinical investigation in combination with gemcitabine (NCT00937664 NCT00413686 NCT00839332 NCT01139775 NCT01341457 NCT00779584 NCT00437203) and chemoradiation (NCT02555644).

Similar to Chk1, Wee1 functions to regulate Cdk1/CycB control of the G2/M checkpoint (reviewed in [69]). Growth factor signals in active cells maintain this check on mitotic entry through phosphorylation at S642 of CDK1 by Akt to activate [70]. In turn, it phosphorylates CDK1 on Y15 to maintain an inactive state [71], [72]. In the absence of unresolved DNA damage, Wee1 is targeted for degradation by phosphorylation from PLK1 to release CDK1 inhibition [73]. Wee1 is another protein at the nexus of many genomic integrity pathways besides cell cycle arrest, and has described roles in cell division coordination [74] replication stability [75], [76] and HR [77].

AZD1775 (previously MK1775) was developed as a specific Wee1 inhibitor [78]. It sensitizes with a variety of DNA damaging agents such as 5-FU [79] gemcitabine [80],

[81], and radiation [82]–[84], and increases the sensitivity to chemoradiation ([85]). Like Chk1 inhibition, Wee1 inhibitors preferentially radiosensitize p53 mutant tumors [83], [84], [86]. In an effort to move beyond the toxicities associated with traditional chemotherapeutics, AZD1775 has also been combined with other DDR inhibitors as a radiosensitizer including PARP1 [87] and Chk1 [88].

Many trials are currently ongoing combining AZD1775 with DNA damaging chemotherapeutics or molecularly targeted agents. A dose escalation trial was recently completed here at the University of Michigan in which 34 pancreatic cancer patients were given four cycles of gemcitabine and AZD1775, adding radiation to cycles 2 and 3 [89]. Median overall survival was extended to 21.7 months from 13.6 months reported by the LAP07 trial for gemcitabine alone [24].

1.5 Ataxia telagiectasia mutated and Rad3 related (ATR)

ATR is recruited to sites of RPA-bound single-stranded DNA—such as those found at HR strand resection or stalled replication forks—with its partner ATRIP to begin its regulation of the DNA damage response [90], [91]. Further work found that a strong element of the recruitment signal is the junction between single-stranded DNA and double-stranded DNA [92]. ATR's sensing of these junctions suggests that it plays a much more important role in the resolution of replication stress than simply DSB repair, as with ATM and DNA-PK [93]. Once bound to target sites, ATR is further activated by cofactors TOPB1 [94], [95] and ETAA1 [96], [97].

Downstream, ATR functions mainly through its phosphorylation and activation of Chk1, activating cell cycle arrest and promoting DNA repair, as discussed earlier.

However, several additional functions of ATR contribute to the resolution of replication stress outside of the ATR/CHK1 axis. Locally, ATR functions to maintain the stability of stalled replication forks to prevent “collapse” [98]. While not fully understood, this mechanism is thought to involve the dual actions of modulating the function of supportive helicases at replication forks [99]–[101] and recruiting HR repair proteins to the site [102], [103].

Additionally, ATR acts to support DNA replication by negatively regulating aberrant initiation of dormant DNA replication origins through its phosphorylation of minichromosome maintenance complex (MCM) proteins [104] and Fanconi anemia group I protein (FANCI) [105]. It also acts to ensure a sufficient supply of deoxynucleotides (dNTPs) for replication, in direct opposition to the stressful actions of anti-metabolites described above. It accomplishes this by elevating cellular levels of ribonucleotide reductase regulatory subunit M2 (RRM2) through increased transcription and decreased proteasomal degradation [106], [107]. Additional evidence for these pathways of protection is demonstrated by the cellular rescue of ATR-deficiency by increased dNTP synthesis [108].

The cellular functions of ATR are much broader than its downstream effector Chk1, and multiple studies have demonstrated the essentiality of the enzyme [109], [110]. Therefore, it was harder to envision the targeted specificity of an ATR inhibitor delivering sufficient therapeutic window to be viable clinical candidates for the treatment of malignancy. Nevertheless, recent years have seen the development of potent and selective inhibitors of ATR and their rapid adoption into preclinical and clinical studies (reviewed in [111]).

Among the applications of ATR inhibition as a single agent, use in the p53- or ATM-deficient settings seem to be especially effective [112]–[117]. Encouragingly, for pancreatic cancer, oncogenic KRAS also seems to lend sensitivity to ATR inhibition through its contribution to replication stress [118]. This study found that oncogenic Ras combined with ATR inhibition leads to an increase in genomic instability beyond what could be explained by increased cell cycling rates. A possible explanation involves ATR's role in preventing the aberrant initiation of replication origins induced by oncogene activity.

A number of studies have found that ATR inhibition *in vitro* radiosensitizes in pancreatic cancer [119], [120]. However, the role of radiation in combination with ATR loss is modest when compared with replication stress-inducing agents [121], suggesting that the more plentiful single-stranded breaks induced by radiation at physiologically-tolerated doses may not suffice to deliver optimal therapeutic efficacy. Attention has quickly turned to how ATR inhibitors may be used in combination with other targeted agents such inhibitors of Chk1 [122], Wee1 [123], IGF1R [124], BET family proteins [125], [126], and PARP [127], [128].

Using a combination of molecularly targeted agent and radiation to generate a background of replicative stress and DNA DSBs has the potential to "prime" cancer cells for collapse with the addition of ATR inhibition, and is an area that warrants investigation.

1.6 Poly (ADP-ribose) polymerase 1 (PARP1)

PARP1 is the first member in a family of 17 proteins, which have diverse cellular roles including DNA repair, transcriptional control, chromatin regulation, and many others

(reviewed in [129]–[131]). PARP1 is the most abundant and active member of the family [132]. In response to genomic insult, PARP1 is recruited to breaks in the DNA backbone through recognition by zinc finger motifs [133], inducing a conformational change that activates its enzymatic function [134]. Once there, it polymerizes long branched chains of poly(ADP-ribose) using NAD^+ (known as PARylation), which it then attaches to Glu, Lys, and Asp of target proteins. PARP1 also rapidly auto-PARylates, leading to dissociation from chromatin.

These long, negatively-charged branched chains serve as scaffolds for the recruitment of DNA repair factors such as XRCC1 [135], CHD4 [136], and APLF [137] to sites of damage. Protein localization and docking is mediated by a variety of known PAR binding motifs (reviewed in [138]) though our knowledge of these PAR binding proteins continues to expand [139]. In addition to its well-described actions in SSB repair through BER pathway [140], [141], PARP1 has been suggested to have roles in MMR [142] and NER [143].

Investigation of PARP1 as a potential target in cancer has led to the elucidation of varied, emerging roles in the resolution of DSBs (reviewed in [144]). PARylation at sites of DNA damage facilitates the rapid recruitment of MRN [145] to promote HR, in which strand resection is followed by BRCA1/2-mediated Rad51 complex formation [146]. PARP1 has become established as an essential component of alternative end joining [147] and evidence has also suggested roles in classical NHEJ [148] and facilitating the resolution of stalled replication forks [149], [150].

Despite intermittent interest in the development of PARP inhibitors clinically due to their association with the DNA damage response, the field fully took off with the

publication of two seminal studies demonstrating the exquisite sensitivity of BRCA-mutant cancers to PARP inhibition [151], [152] and subsequent single-agent clinical deployment of olaparib [153]. The interaction between PARP inhibitors and BRCA mutations realized the potential for synthetic lethality between a pharmacologic agent and a genetic alteration, and remains the only such example to have made the successful transition from laboratory to FDA-approved clinical usage [154]. The concept of synthetic lethality was originally proposed nearly a century ago [155] wherein two individually survivable genetic variations occurred concomitantly to result in a loss of viability. Increasingly sophisticated genomic technology has allowed us to search for new genes that exhibit synthetic lethality in combination with known alterations in cancer cells [156], [157]. These candidate genes could then be exploited using specific, molecularly targeted pharmacologic agents. Any novel and truly synthetic lethal combinations would represent a perfect therapeutic window: a day-and-night difference between a drug's effect on the patient's normal tissue and the cancer bearing that specific mutation.

Currently, the only labeled indications for use of PARP inhibitors are for breast, ovarian, prostate, and pancreatic cancers with BRCA loss or existing platinum sensitivity. However, because there is no standardized clinical assay for somatic BRCA status, germline BRCA status is the only widespread method for the patient selection. These limitations highlight the need to improve testing and expand the definition of "BRCAness" to recommend other molecular defects synthetic lethal with PARP inhibition [158]. Subsequently, it was found that cancers with HR defects were broadly sensitive to PARP inhibition [159]–[161]. This has led to efforts to define an assay for the functional status of homologous recombination competency in patients outside of the status of single

individually defined genes, including sequencing signatures [162], [163], mutational burden [164], and Rad51 focus formation [165], [166]. In time, one of these alternate approaches may become a standard laboratory test for all patients with cancer in much the same way that receptor status is assayed in breast cancer.

Most work on the efficacy of single-agent olaparib in ovarian [167], breast [168], and prostate cancer [169], [170] has focused on the setting of well-defined BRCA mutations or frequent alteration of HR genes. Classically, this has been attributed to the persistence of SSB lesions in PARP inhibited cancer cells, which are then converted to DSBs by collision with replication forks [171]. However, this may be an oversimplification that will become more nuanced as we continue to learn about the biology of PARPs [172], [173].

Before the discovery of synthetic lethality in HR mutant cancers, PARP inhibitors were evaluated as agents to sensitize to cytotoxic agents irrespective of HR status. These studies were challenged by the high toxicity associated with PARP inhibitors at doses required for efficacy, especially in combination with traditional chemotherapeutics [174]. Some evidence exists at the preclinical stage for the efficacy of this combination [175], [176]. Clinical evaluation continues despite a temporary setback in which iniparib failed to show benefit in combination with Gemcitabine/carboplatin [177]. It was later demonstrated that iniparib does not inhibit PARP enzymes [178].

Given the immediate and essential functions of PARP1 in response to ionizing radiation [179]–[181], PARP inhibitors have also been combined with radiation preclinically [182], [183] and in numerous clinical trials, both as a single agent and as a chemoradiosensitizer. The rationale for radiosensitization by PARP inhibitors is similar to that in BRCA deficient cells; replication fork collision converts persistent SSB insults into

DSBs [184], [185]. But again, this may reflect a simplified understanding of PARP inhibitor mechanistic action [186] and bears elucidation due to implications for clinical practice discussed in this work.

Illustration 1.1

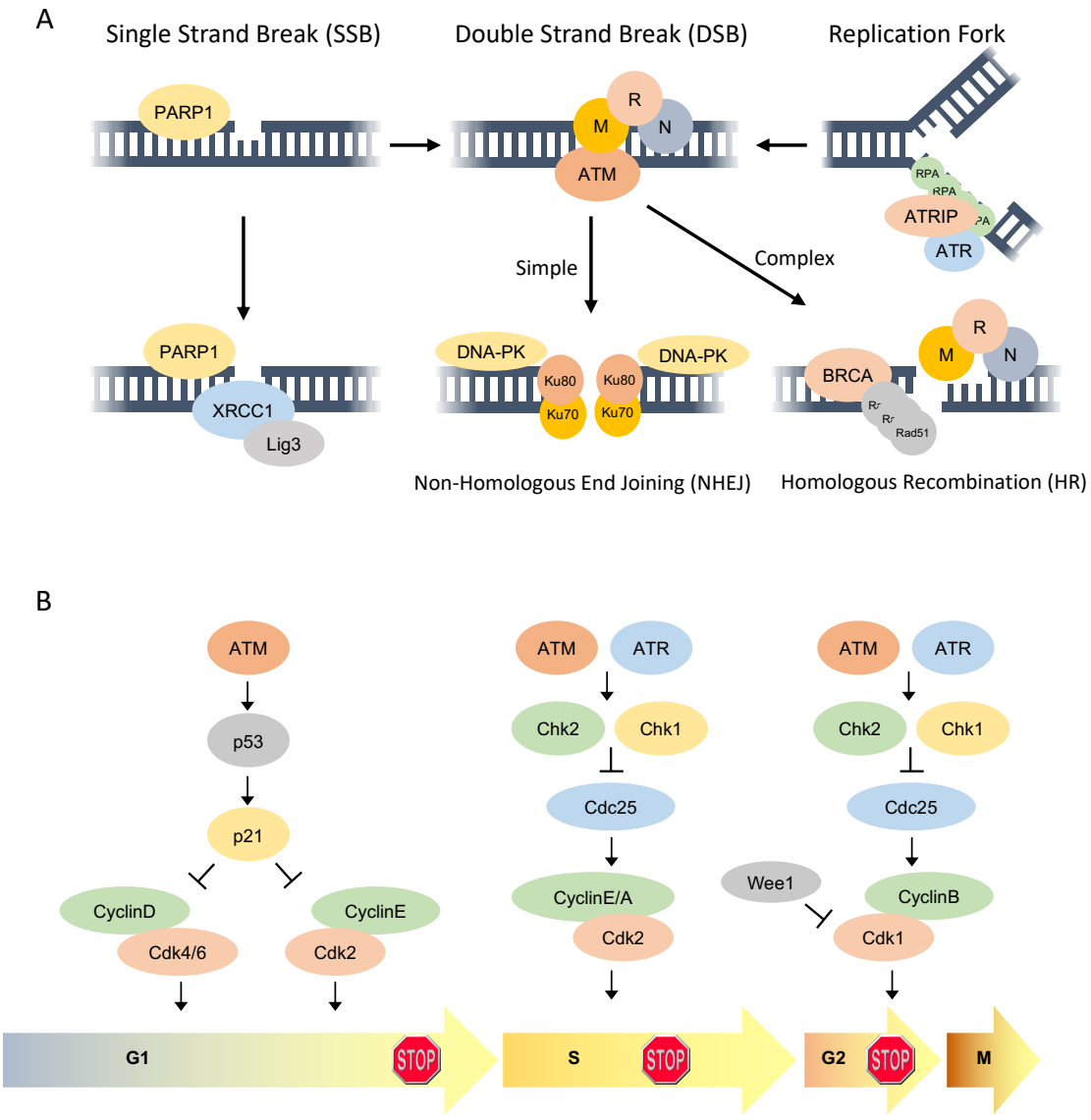

Illustration 1.1 – The DNA damage response and cell cycle checkpoints protect the cell from ionizing radiation. (A) Radiation induces single-strand breaks (SSBs) either directly or indirectly as intermediates of base excision repair. These breaks are sensed by PARP1, which recruits repair factors such as XRCC1 and Lig3 to sites of damage. Double-strand breaks (DSBs) are sensed by ATM and the MRE11-RAD50-NBS1 (MRN) complex. Simple DSBs are repaired with fast kinetics by non-homologous end-joining (NHEJ), where ends of DNA are bound by Ku70/80 heterodimers to recruit DNA-PK. Homologous recombination (HR) operates with high fidelity under slow kinetics and is partly responsible for repair of complex 2-ended DSBs and exclusively responsible for repair of 1-ended DSBs. MRN resects 5' DNA strands to allow RAD51 mediated sister chromatid invasion. Stalled replication forks are stabilized by ATR, and if unresolved can be converted to complex DSBs. (B) Cell cycle checkpoints are activated in response to

DNA damage to prevent propagation of cells with damaged DNA and to permit time for DNA repair. The major checkpoints include those occurring in G1, S and G2. While ATM activation is the initial response to radiation-induced DNA DSBs, ATR is subsequently activated and contributes to a sustained cell cycle checkpoint response. Adapted from Morgan and Lawrence [29].

CHAPTER 2:

The Association of PARP1 Enzymatic Inhibition and Chromatin Complex Formation with Radiosensitization by PARP Inhibitors

2.1 Introduction

Inhibition of poly (ADP-ribose) polymerase 1 (PARP1) as a strategy for treating cancer has emerged as a leading example of the use of molecularly targeted agents. It is perhaps the most famous example of synthetic lethality between a therapeutic agent and a genetic mutation for its activity in BRCA mutant cancers [151], [152].

Investigation into the function of PARP1 stretches back to 1963 following the observation that addition of nicotinamide mononucletide to kidney nuclei induced the inclusion of C14 adenine into the RNA fraction of the cell [187]. While initially characterized as an RNA polymerase, the enzyme was shown to catalyze the formation of polyA-like structures in a DNA-dependent manner. Later, it was discovered that enzymatic function of PARP1 was triggered by DNA damage [188], [189]. Further early characterization proposed a role for PARP1 in the DNA damage response and demonstrated that pharmacologic inhibition could propagate the effects of radiation [190]–[192].

PARP1 functions in the DNA damage response primarily through recruitment to sites of DNA damage followed by the polymerization and deposition of long branched

chains of poly (ADP-ribose) (PAR) on chromatin associated proteins and itself; these negatively-charged moieties serve as scaffolds for the recruitment of other DDR factors (**Illustration 2.1a-c**). PARylation has been shown to play a role in numerous diverse DNA repair pathways, including base excision repair, alternative end joining, non-homologous end joining, and homologous recombination (reviewed in [193]).

A variety of specific PARP inhibitors have been developed. While they share relatively similar properties as enzymatic inhibitors, they display large differences in cytotoxicity and clinical tolerability. Variation in size and structure of the molecules are thought to account for these distinctions by affecting their ability to modify the PARP1 NAD^+ binding site and hence the ability of PARP1 to dissociate from chromatin following recruitment. Veliparib, the smallest inhibitor, does not display an appreciable reduction in its observed off-rate at clinically relevant concentrations while talazoparib, which is the largest and possesses a rigid structure, increases retention the most. The formation of these PARP1-DNA complexes has come to be called "PARP trapping." Current understanding proposes that more potent trappers such as talazoparib block the NAD^+ binding site, preventing its use for auto-PARylation and dissociation from chromatin ([186], **Illustration 2.1d-f**). This secondary mechanism of action is also dependent on concentration independently from its enzymatic inhibition. Olaparib, which displays an intermediate trapping phenotype relative to veliparib and talazoparib, enzymatically inhibits PARP1 at concentrations in the mid-nanomolar range but traps only at micromolar concentrations [194].

PARP trapping has been proposed as a major mechanism of the observed cytotoxicity of PARP inhibitors in preclinical studies [194]. In patients, a common major

adverse event seen is the development of hematologic toxicities [195]. Cytopenias have been observed more frequently in patients treated with more potent trappers such as talazoparib [196] and niraparib [197], as opposed to olaparib [198], [199]. Accordingly, these dose-limiting-toxicities are thought to derive from the formation of cytotoxic DNA-PARP1 complexes. Preclinical evidence exists to support the toxicity of PARP trapping in bone marrow [200].

Several studies have been published combining PARP inhibition by veliparib with radiation clinically to treat cancers of the brain, gastrointestinal system, and breast, frequently in combination with another therapeutic agent (reviewed in [201]). One trial combined olaparib with cetuximab and radiation for the treatment of squamous cell carcinoma. Other trials of PARP inhibitors plus radiotherapy are ongoing. As we pursue these inhibitors as radiosensitizing agents, it is important that we clarify whether their efficacy with radiation is due to their inhibition of enzymatic activity or ability to form toxic adducts. An answer to this question has implication for the selection and dosage of PARP inhibitors used in combination with radiation.

2.2 Results

We began our study of the radiosensitizing properties of PARP inhibitors by performing clonogenic survival assays in four cell line models of pancreatic cancer (**Figure 2.1**). Given the close association of PARP inhibition with homologous recombination (HR) and usage in HR-deficient (HRD) cancers, we first tested the radiosensitizing properties of olaparib in two HRD models. One cell line, Capan-1.NEO (Capan-1), is deficient in HR due to the deletion of one allele of BRCA2 and 6174delT

mutation in the other [202], [203]. The other model utilized a normally homologous recombination-proficient cell line, MiaPaCa2, stably transfected with doxycycline-inducible shRNA directed toward Rad51, a necessary component of HR, which, when treated with doxycycline, renders the cell effectively HRD. This model is referred to in the text as MPC2.HRP under normal conditions and MPC2.HRD under conditions of doxycycline treatment. Treatment with 10nM olaparib—a concentration demonstrated to enzymatically inhibit PARP1 in previous work in our laboratory—beginning one hour prior to radiation and continuing through 24 hours post-radiation modestly sensitized Capan-1 and MPC2.HRD cells to radiation up to 8 Gy (**Figure 2.1a-b**).

Radiation enhancement is quantified as an enhancement ratio (ER) of the mean inactivation dose, which is defined as the area under the survival curve, of the untreated cells divided by the mean inactivation dose of the treatment group [204]. Radiation survival curves used to generate ERs are normalized to the toxicity of the treatment group in the absence of radiation, meaning that significant cytotoxicity may compromise a treatment's ability to demonstrate radiation enhancement. Ten nM olaparib produced an ER of 1.26±0.06 in Capan-1 cells and 1.17±0.03 in MPC2.HRD cells, which represent reasonable single-agent radiosensitization.

We shifted our focus to homologous recombination-proficient (HRP) models of pancreatic cancer. MiaPaCa2 and Panc1, like ~85% of pancreatic cancers [10], [205], are proficient in HR. Additionally, they carry mutations in KRAS and p53, as do most pancreatic cancers. In these cell lines we saw little radiosensitization by 10nM olaparib, generating enhancement ratios of 1.11±0.04 in MPC2.HRP and 1.03±0.07 in Panc1. However, the increased tolerance of PARP inhibitors in HR proficient cell lines allowed

for investigation with higher concentrations of olaparib without the cytoxicity limitations of HRD models. When treated on the same schedule with 3uM olaparib—concentrations achieved in patients in clinical trials [206]—radiation sensitivity for both cell lines deepened, with enhancement ratios of 1.43±0.08 for MPC2.HRP and 1.29±0.06 for Panc1.

The difference in radiosensitizing potency of olaparib between the HRP and HRD cell line models cannot be explained based solely on the extent of enzymatic inhibition. The enzymatic activity of PARPs after treatment with olaparib can be measured using a western blot for poly (ADP-ribose). We found that 10nM and 3uM olaparib create nearly identical enzymatic inhibition in MiaPaCa2 and Panc1 cells (**Figure 2.2a-b**; this western blot contains conditions of treatment with ATR inhibitor AZD3768 that will be discussed in Chapter 3).

The discrepancy between radiosensitization and enzymatic inhibition is consistent with early findings in the development of olaparib. Work in HRP cancer models demonstrated that cytotoxicity EC50 values were much higher than enzymatic IC50 values for the drug leading to the discovery that high concentration olaparib decreases the kinetic off-rate from chromatin of the PARP1 protein known as “PARP trapping.” We next evaluated the effects of olaparib on PARP1-DNA binding in response to radiation-induced DNA damage. Relative to untreated control cells, we found that radiation alone caused an increase in chromatin associated PARP1, an effect which likely reflects the transient association of PARP1 with DNA damage sites. Furthermore, olaparib caused a modest increase in PARP1-DNA binding in response to radiation with minimal change in the amount of PARP1 in whole cell lysates (**Figure 2.2c-d**). The subtle effect measured

by chromatin fractionation increased the difficulty of appreciating the lack of trapping by lower concentrations of olaparib. However, using alkylating agents, other groups have demonstrated that lower concentrations of olaparib display minimal trapping potential even at concentrations as high as 100nM [194], [207], [208].

Profound differences between the effects of high and low concentration of olaparib can also be observed in its effects on the cell cycle and resolution of DNA damage. In response to 6 Gy, cells undergo G2 cell cycle arrest that is fully resolved 24 hours-post RT (**Figure 2.3 a-b**). However, we found that cells treated with 3uM olaparib remained in complete G2 arrest at this time in both MiaPaCa2 and Panc1 cells. Ten nM olaparib also delayed resolution of cell cycle arrest, but to a lesser extent. We hypothesized that this delayed resolution could be due to unresolved DNA damage at this timepoint. γH2AX flow cytometry data supported this hypothesis (**Figure 2.3 c-d**). It demonstrates similar induction of damage among all treatment groups, but elevated DNA damage associated with 3uM olaparib and a mild elevation with 10nM olaparib at late time points.

We confirmed this finding through the use of a physical assay for DNA double strand breaks. Following suspension in agarose and neutral lysis, nuclear DNA with greater double-strand break damage will migrate further in an electrophoretic field, generating “comets,” for which the assay is named. Comet assays in our pancreatic cancer cell lines required optimization in handling due to their high background genomic instability. The use of trypsin, vortexing, or lysis above 4˚C caused long comet tails in all conditions, obscuring differences between the treatment groups. Quantification of comet results measured the Olive Tail Moment (OTM), named for the original developer of the assay [209], which combines length and intensity of the tail relative to the nucleus into a

numerical score. Comparison between replicates of treatment groups was accomplished with the inclusion of a positive control of cells treated with 8 Gy on ice immediately prior to processing to simulate maximum DNA damage at that dose. This internal control was used to normalize different experiments before combining. Comet assay results demonstrated significantly elevated DSB DNA damage in cells treated with 3uM olaparib relative to 10nM olaparib and DMSO 24 hours after radiation (**Figure 2.4**).

We further sought to characterize the radiosensitizing potency of different PARP inhibitors with respect to their enzymatic inhibition and PARP trapping properties. Veliparib, olaparib, and talazoparib are all under clinical investigation and have been described to have significantly different trapping potencies in increasing order as listed. This potency mirrors the reported cytotoxicity of these agents in most cancers. The availability of three clinical-grade inhibitors with low, middle, and high PARP trapping potency was both a tool to help us explore PARP trapping biology and also gave our work greater relevance to clinical decision-making about how and why to choose among these options when crafting treatment plans for patients in the setting of radiation therapy.

We determined the radiosensitizing efficacy of each inhibitor by performing clonogenic survival experiments in MiaPaCa2 and Panc1 cells at a range of concentrations to determine the radiation enhancement of the inhibitor at 4 Gy radiation (**Figure 2.5**). Olaparib and talazoparib demonstrated a concentration-dependent increase in radiation enhancement, beginning at lower concentrations and reaching greater enhancement ratios at high concentrations. Strikingly, veliparib produced negligible radiation enhancement across the entire range of tested concentrations in both cell lines.

The absence of radiosensitization by veliparib in either cell line model stands in contrast with its enzymatic inhibition. Concentration-response curves for each drug demonstrate that all three inhibitors achieve complete enzymatic inhibition of PARP1 at a concentration of 3uM or lower (**Figure 2.6**). While radiosensitization and enzymatic inhibition trend together in olaparib and talazoparib, there are differences in the concentration ranges where these changes occur. Taken together with the lack of radiosensitization by veliparib, these results suggest a mechanism beyond catalytic inhibition contributes to radiosensitization.

In order to study the effects of enzymatic inhibition independently from trapping, we generated a genetic model in which the loss of the PARP1 protein would effectively mimic complete enzymatic inhibition without the ability to trap. We deleted PARP1 homozygously from MiaPaCa2 cells using CRISPR-Cas9 technology to create two clones that are PARP1$^{-/-}$: MPC2 Null#1 and MPC2 Null#2. In tandem, we created a MiaPaCa2 clone stably transfected with the Cas9 enzyme without guide RNA as a control cell line. PARP1-null cells do not express PARP1 nor do they exhibit cellular PARylation (**Figure 2.7a**; again, this western blot contains conditions of treatment with ATR inhibitor AZD3768 that will be discussed in Chapter 3). While the Null#1 and Null#2 clones display increased radiation sensitivity relative to Cas9 at high radiation doses, the effect of PARP1 depletion does not replicate the radiosensitizing effects of 3uM olaparib (**Figure 2.7b**). Further, olaparib has little effect on radiation sensitivity in PARP null cells (**Figure 2.7c**). The persistent DNA damage elevation at 16 and 24 hours after radiation seen in the Cas9 control cells treated with 3uM olaparib is not present in the MPC2 Null#1 cells (**Figure 2.7d**).

We also created a cell line using MPC2 Null#1 stably transfected with wild-type PARP1 (MPC2.#110) to study the effects of exogenously reintroduced PARP1 protein in the setting of a null background. We found that while PARP1 deletion conferred complete resistance to the cytotoxic effects of 30nM talazoparib and partial resistance to 300nM talazoparib, reintroduction of the protein partially restored sensitivity (**Figure 2.8**).

One challenge in studying the biology of PARP trapping has been the difficulty of experimentally measuring trapped PARP on the chromatin following radiation. The gold standard assay for the detection of PARP-DNA complexes is chromatin fractionation followed by western blot, which has been both demonstrated and referenced earlier in this chapter. This approach requires a large amount of starting cellular material that is fresh and unfixed, which must be processed immediately with highly accurate and reproducible pipetting and handling. Further, the amount of trapping observable by chromatin fractionation combined with radiation—as opposed to an alkylating agent such as methyl methanesulfonate (MMS) or temozolomide (TMZ)—was very subtle, even under robust trapping conditions. This difficulty in the context of radiation was corroborated in correspondence with peers in the field. Finally, the method only allows for the processing of small batches of samples, limiting the number of productive comparisons that can be made at one time between various conditions that can affect trapping.

One other accepted method for the measurement of PARP trapping is the use of laser microirradiation in combination with fluorescently-labeled PARP1. Briefly, a high intensity laser is used either to pulse a spot in or draw a line across the nucleus of a single cell, generating a DNA damage “scratch.” It is then possible to observe the recruitment of

fluorescently labeled proteins to that point or line and observe the kinetics of recruitment of various factors involved in the DNA damage response. Measurement of PARP trapping using this technique measures the length of retention at the site of DNA damage of PARP1. While this assay delivers additional, valuable information about the kinetics of PARP1-DNA complexes in response to DNA damage, the quality of damage is very different from the ionizing radiation delivered in the therapeutic setting. We found that PARP1 was retained at the site of DNA damage for over 30 minutes under conditions of no drug treatment, well beyond what is seen in the literature [210]. We speculate that this could be a result of the high intensity of radiation delivered to the site generating insurmountable damage that altered the traditionally observed on/off kinetics of the PARP1 enzyme. This was not a productive tool for us in the timeframe of this work but could be helpful to shed light on the disassociation of PARP-DNA complexes in the future if we are able to attenuate the radiation delivered to more relevant doses.

Ultimately, we utilized a new assay developed by Hopkins *et al.* [200], [208]. Detection of trapped PARP utilizes the proximity ligation assay (PLA) technique. In this procedure, fixed cells or tissues are probed with primary antibodies against two proteins of interest. Then they are incubated with secondary antibodies conjugated to oligonucleotide linkers. If the two proteins reside within 400Å the linkers can be ligated to form a circular template which is then polymerized and probed with fluorescently labeled oligos, allowing for the mass amplification of signal. Using this technique, single protein-protein interactions can be visualized with high sensitivity by light microscopy. Hopkins *et al*. selected the pairing of antibodies against PARP1 and a panel of chromatin proteins, mainly comprised of histones. They reported experimental success using high content

robotic handling and imaging for their samples, achieving the highest sensitivity and specificity of trapped PARP detection by pairing anti-PARP1 with either anti-total H2AX (tH2AX) or γH2AX.

We were interested to adapt this technique for more routine laboratory use in non-high-throughput settings. We chose to focus wholly on the proximity detection of PARP1 and tH2AX. As demonstrated in figure 2.3c-d earlier and reported elsewhere, increasing concentration of PARP inhibitors elevate levels of DNA damage and would present a confounding effect on detection using the γH2AX antibody. In piloting this approach, we also chose to focus on cells grown on coverslips in 12-well plates, which would allow the greatest amount of experimental flexibility *in vitro*. Ultimately, we were able to reproducibly demonstrate differences in PLA signal between robust non-trapping and trapping conditions: 0.01% MMS and 0.01% MMS + 100nM talazoparib (**Figure 2.9**).

2.3 Conclusions

We have demonstrated that while low concentrations of olaparib sensitize homologous recombination deficient cell line models of pancreatic cancer to ionizing radiation, HR proficient cell lines require high concentration olaparib for sensitization. These differences in sensitivity do not correspond to differences in enzymatic inhibition, which is nearly complete at both concentrations. Instead, high concentration olaparib leads to increased retention of PARP1 at chromatin, a phenomenon that has come to be called “PARP trapping” in the literature. Trapping concentrations induce prolonged G2 cell cycle arrest in HRP cell lines up to 24 hours, while this effect is attenuated at low concentrations of olaparib that only inhibit enzymatically. Prolonged arrest can be

explained by a delay in DNA damage resolution at trapping concentrations seen by γH2AX flow. Increased DNA double strand break damage 24 hours following radiation can be appreciated for cells treated with trapping concentrations of olaparib by comet assay.

Concentration response curves in MiaPaCa2 and Panc1 cells for radiation enhancement after treatment with a PARP inhibitor demonstrate great radiosensitizing potency for talazoparib and nearly none for veliparib, with in intermediate potency for olaparib. These potencies correspond to each agent's described trapping potency in the literature. However, differences in potency of enzymatic inhibition between the three drugs is mild, and all three achieve total inhibition at submicromolar concentrations. Genetic deletion of PARP1 from HR proficient cells does not replicate radiosensitizing properties of high concentration olaparib, and the presence of PARP1 protein is required for radiosensitization by olapaib. The delayed resolution of DNA damage in response to PARP inhibition was not seen in PARP1-null cells.

The kinetics of trapped PARP detection using the chromatin fractionation assay following radiation were surprisingly long. Other groups have found success in assaying for trapped PARP 4-6 hours following treatment; their samples remain under constant conditions of DNA damage due to the presence of an alkylating agent. A logical hypothesis would be that following radiation, which is delivered in a single hit temporally, an early timepoint would yield the greatest contrast between retained and released PARP1. However, we found the opposite to be true. The greatest amount of signal under trapping conditions relative to control occurred when samples were collected 24 hours following radiation. It is unclear whether this represents an artifact of the collection and

assay process or whether substantial time must pass after radiation for trapped PARP to accumulate. If the latter, this may suggest that some element of the repair process or the progression through one or more specific phases of the cell cycle promote PARP trapping.

Finally, we adapted a new assay for PARP trapping using the proximity ligation assay. This new assay will be an improvement on current methods in its ability to handle multiple samples, reduced reliance on handling skills of the researcher, ability to assess trapping in cellular context, and ability to assess trapping in fixed animal and human tissues. The potential advantages of using the PLA to measure levels of trapped PARP over chromatin fractionation are various. First, while the handling requirements of chromatin fractionation limit experimental batch size, two dozen PLA samples can easily be processed together, if not more. Additionally, the treatment and fixation of cells for the PLA assay can be performed without the necessity of immediately moving on to processing samples, allowing for greater flexibility and convenience. In theory, sample handling for the PLA should be less reliant on the handling of the technician as chromatin fractionation. This property, once the assay is completely standardized, should lend it greater repeatability between operators. Finally, and most importantly from a scientific perspective, the ability to detect trapped PARP in the setting of fixed cells and tissues in conjunction with visualization of the cellular context will broaden the experimental opportunities for exploring PARP trapping. The obvious application for this advance in technology is the application to *in situ* tissue samples from both experimental animals and human patients. Beyond that, the capacity for evaluating trapped PARP in cellular context will broaden our understanding of cellular heterogeneity in the PARP trapping response

and allow us to assay in mixed populations of cells such as we see in normal tissue, delivering similar benefits as the use of single-cell sequencing technologies.

2.4 Experimental Procedures

Data shown in this work is the product of collaboration and represents the work of many members of the laboratory, past and present. Leslie A. Parsels performed work contributing to the clonogenic cell survival assays, immunoblotting, and chromatin fractionation. Joshua D. Parsels contributed to clonogenic survival assays. Sheryl Flanagan contributed to PAR immunoblots. CRISPR-Cas9 PARP1-null and control cell lines were generated by Qiang Zhang.

Cell Culture and drug solutions

MiaPaCa2 and Panc1 cells were obtained from and authenticated by the American Type Culture Collection. Capan1.NEO is a clonal cell line expressing the neomycin resistance gene obtained from S. Powell (Memorial Sloan Kettering Cancer Center, New York, NY) [203]. Cells were grown in either DMEM (MiaPaCa2 and Panc1; Invitrogen), or IMDM medium (Capan1.NEO; Invitrogen) supplemented with 10% fetal bovine serum (Premium Select; Atlanta Biologicals). Olaparib was dissolved in DMSO and stored in aliquots at −20°C.

Clonogenic survival assays

Cells were treated with drugs/radiation and then replated at cloning densities. Cells were grown for 9-14 days and then fixed and stained with methanol-acetic acid and trypan

blue and scored for colonies of >50 cells. Cell survival curves were fitted using the linear quadratic equation and the mean inactivation dose was calculated through an integration to infinity of an extrapolation of cell survival curves [204]. The mean inactivation dose, therefore, represents the area under cell survival curves and more heavily weights low rather than high doses of radiation. The radiation enhancement ratio was calculated as the quotient of the mean inactivation dose under control conditions divided by that under experimental conditions. An enhancement ratio greater than 1 indicated radiosensitization.

Immunoblotting

Whole cell lysates were prepared in RIPA buffer (150 mM NaCl, 1% NP-40, 0.5% sodium deoxycholate, 0.1% SDS, 25 mM Tris pH 7.4) supplemented with both PhosSTOP phosphatase inhibitor and Complete protease inhibitor cocktails (Roche) as previously described [211]. To assess PARP1 bound to chromatin, cells were fractionated using a series of salt stringency buffers as previously described [207]. Briefly, nuclei from approximately 3×106 irradiated and drug-treated cells were isolated by gentle lysis in 100 µL ice-cold hypotonic buffer (50 mM HEPES, pH 7.9, 10 mM KCl, 1.5 mM MgCl2, 0.34 M sucrose, 10% glycerol, 1 mM DTT, 0.1% Triton X-100, protease inhibitors), followed by slow-speed centrifugation (1,300 × g at 4°C for 4 min). Washed nuclei were then lysed in ice-cold buffer B (50 mM HEPES, pH 7.9, 100 mM KCl, 2.5 mM MgCl2, 0.05% Triton X-100, protease inhibitors) and insoluble chromatin was collected by centrifugation (10 min, 15,000 × g, 4°C) and washed once in buffer C (50 mM HEPES, pH 7.9, 250 mM KCl, 2.5 mM MgCl2, 0.05% Triton X-100, protease inhibitors) and once in buffer D (50 mM HEPES,

pH 7.9, 500 mM KCl, 2.5 mM MgCl2, 0.1% Triton X-100, protease inhibitors). The chromatin pellet was then resuspended with Buffer B supplemented with 5 mM CaCl2 and incubated at 37°C for 10 min with 3 units of micrococcal nuclease, centrifuged, and processed for Western blot analysis as previously described [212].

Neutral Comet Assay

Cells were treated with AZD6738 and/or olaparib for one hour prior to 8 Gy radiation and 24 hours post-radiation. Neutral comet assay was performed according to the manufacturer's protocol (Trevigen, USA). Briefly, cells were scraped, mixed 1:10 with 1% molten LMAgarose, pipetted onto a CometSlide and submerged in neutral lysis buffer overnight at 4˚C. Slides were rinsed 3x with TBE and subjected to neutral electrophoresis for 35 minutes at 25V. Slides were incubated in 2.5 ug/ml propidium iodide for 20 minutes, then rinsed in 70% ethanol and allowed to dry overnight. Slides were viewed by epifluorescence microscopy. At least 50 cells were counted and imaged. Comet Assay IV software (Instem) was used to quantify the average tail moment.

Flow Cytometry

Cells were trypsinized, washed with ice-cold PBS, and fixed at a concentration of 2 × 106 cells/mL in ice-cold 70% ethanol. For γH2AX analysis, samples were incubated with a mouse anti-γH2AX-specific antibody (clone JBW301; Millipore) overnight at 4°C followed by incubation with a FITC-conjugated secondary antibody (Sigma) as previously described (27). γH2AX positivity was quantified by setting a gate on the control, untreated sample to define a region of positive staining for γH2AX of approximately 5%. This gate

was then overlaid on the drug/radiation-treated samples. Samples were stained with propidium iodide to measure total DNA content and analyzed on a FACScan flow cytometer (Becton Dickinson) with FlowJo software (Tree Star).

Proximity Ligation Assay

Cells were plated on round coverslips in a 12-well plate. Following treatment with drug(s), samples were fixed for 10 minutes in 2% formaldehyde. Following fixation, cells were blocked and permeablized for one hour in 2% bovine serum albumin (Sigma), 5% normal donkey serum (), and 0.2% TritonX-100 in PBS. Slides were incubated overnight at 4˚C in 1:250 total H2AX () and 1:250 PARP1 in Duolink antibody diluent (Sigma). The following day, samples were incubated for one hour at 37˚C with Duolink secondary probes according to the manufacturer's protocol. Following incubation with secondary probes, ligation and polymerization were performed according to Duolink protocol using In Situ Detection Reagents Red according to manufacturer's protocol; all washes were performed seven times with 1x PBS. Following polymerization and final washes, Samples were incubated with DAPI and mounted to slides for visualization by microscope.

2.5 Data and Figures

Figures begin next page

Figure 2.1

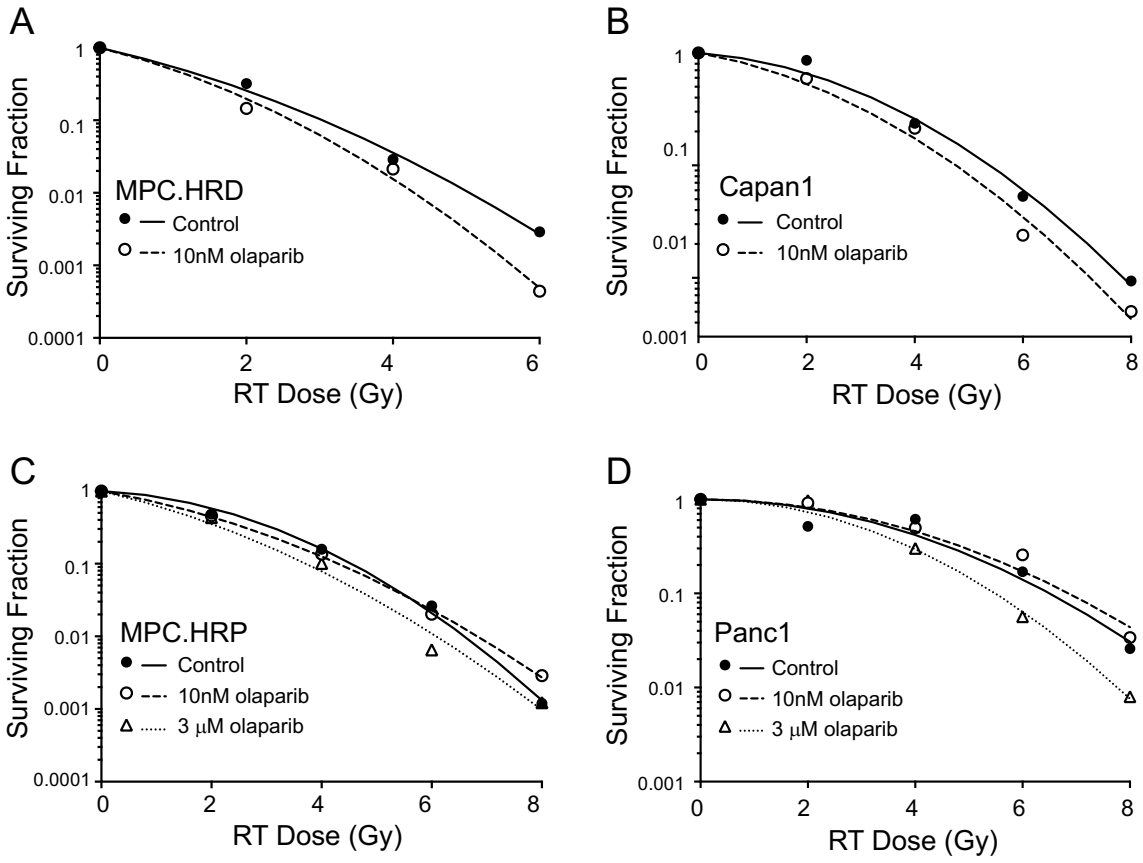

E

Condition	RER	Cytotoxicity
MiaPaCa-2 RAD51 shRNA		
HRP (no dox)	*1.0*	*1.0*
Olaparib (10 nmol/L)	1.11 ± 0.04	0.88 ± 0.04
Olaparib (3 μmol/L)	1.43 ± 0.08[a]	0.80 ± 0.04
HRD (+ dox)	*1.0*	*1.0*
Olaparib (10 nmol/L)	1.17 ± 0.03	0.80 ± 0.05
Panc-1		
Olaparib (10 nmol/L)	1.03 ± 0.07	0.83 ± 0.09
Olaparib (3 μmol/L)	1.29 ± 0.06[a]	0.80 ± 0.12
Capan-1		
Olaparib (10 nmol/L)	1.26 ± 0.06	0.92 ± 0.12

Figure 2.1 Sensitization to radiation by olaparib in pancreatic cancer cells - MPC.HRD (A**),** Capan-1 (B), MPC.HRP (C), and Panc1 (D) cells were treated with 10nM or 3uM olaparib for one hour prior to radiation (RT; 0-8 Gy) and 24 hours after radiation, whereupon they were processed for evaluation of clonogenic survival. (E) Enhancement ratio and cytoxocicity for cell lines and treatments in A-D. Data are the mean ± SEM for n=3-6 independent experiments.

Figure 2.2

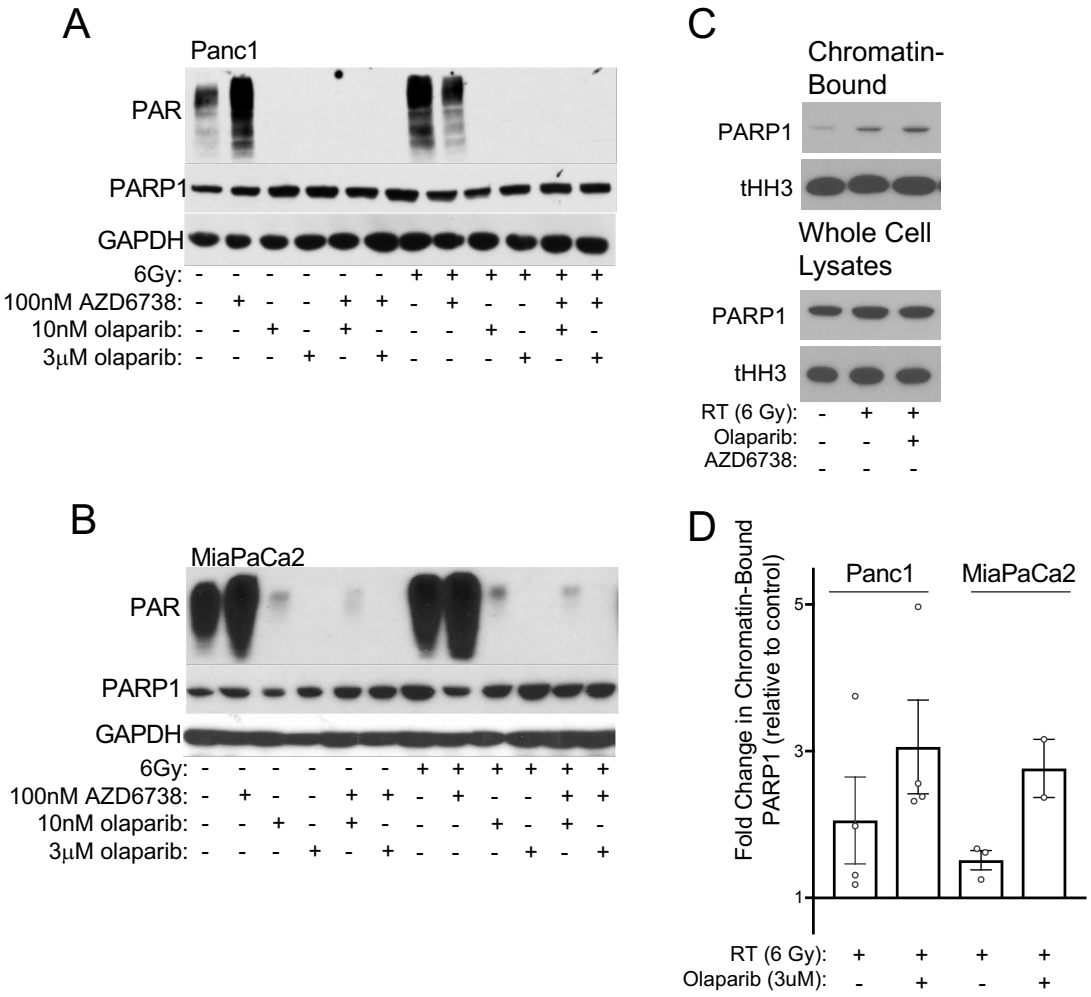

Figure 2.2 Cellular PARP changes after treatment with olaparib and radiation - Western blots showing whole-cell lysate of Panc1 (A) and MiaPaCa2 (B) cells treated with a combination of 6Gy radiation, 100nM AZD6738. and either 10nM or 3uM olaparib for one hour before radiation and 24 hours post-radiation. (C) Cellular fractionation on Panc1 cells treated with a combination of 6Gy radiation and 3uM olaparib for one hour before radiation and 24 hours post-radiation. Immunoblotting was performed on these fractions for PARP1 and total histone H3 (tHH3). These are shown in comparison to whole cell lysates under the same conditions. (D) Chromatin-bound PARP1 in Panc1 and MiaPaCa2 cells were quantified by densitometry and are represented as fold change relative to untreated controls. Results are the mean of n=4 (Panc1) or n=2 (MiaPaCa2) ± SE.

Figure 2.3

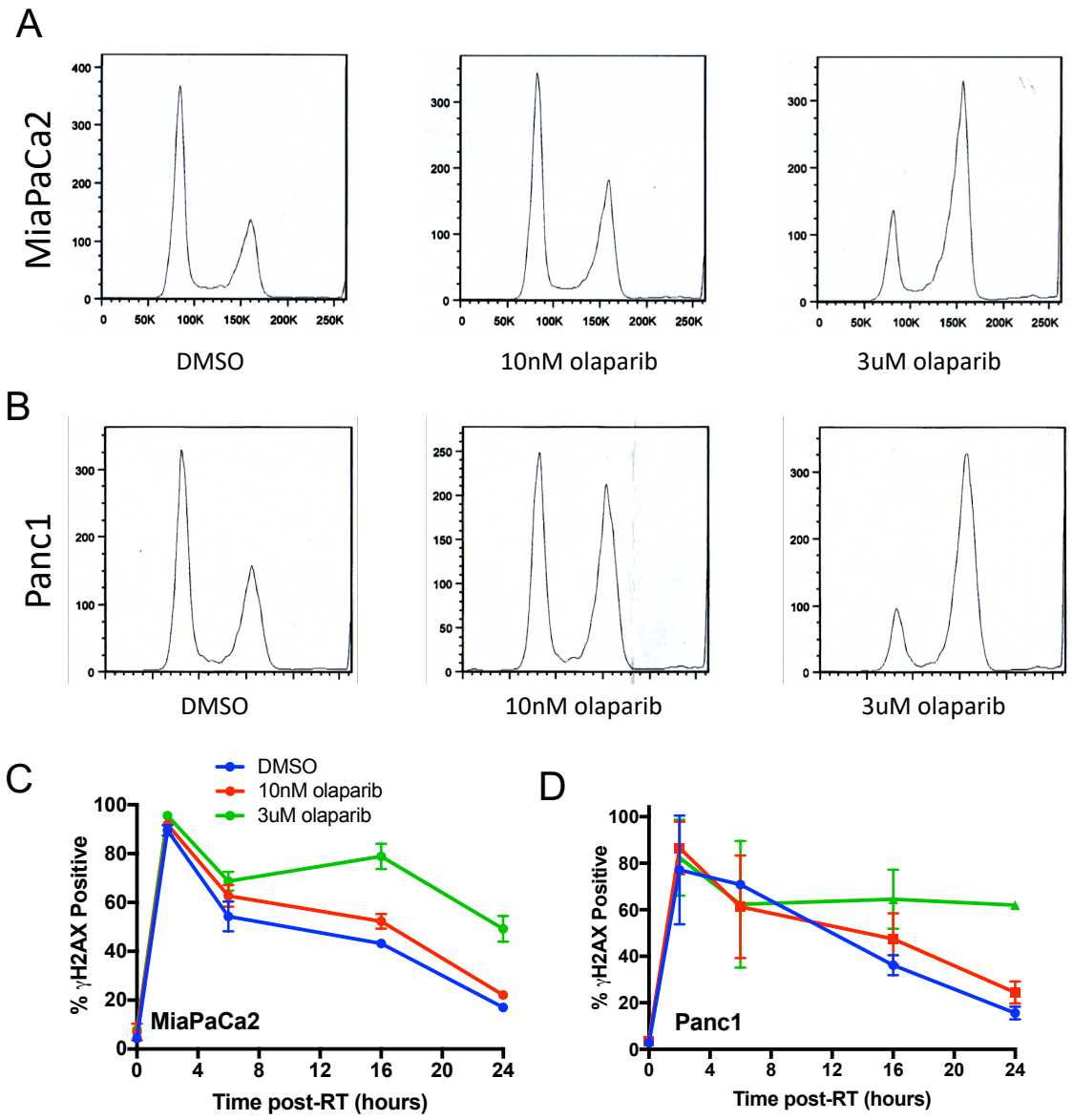

Figure 2.3 High concentration olaparib causes G2 arrest and delayed DNA damage resolution – MiaPaCa2 (A) and Panc1 (B) cells were treated with 10nM or 3uM olaparib prior to 6 Gy radiation. 24 hours after irradiation cells were fixed for flow cytometry and analyzed for DNA content by propidium iodide stain. MiaPaCa2 (C) and Panc1 (D) cells were treated with 10nM or 3uM olaparib prior to 6 Gy radiation. At the indicated times post-RT cells were fixed for flow cytometry and analyzed for gH2AX positivity. Data shown are the mean from n=2 independent experiments ± SE.

Figure 2.4

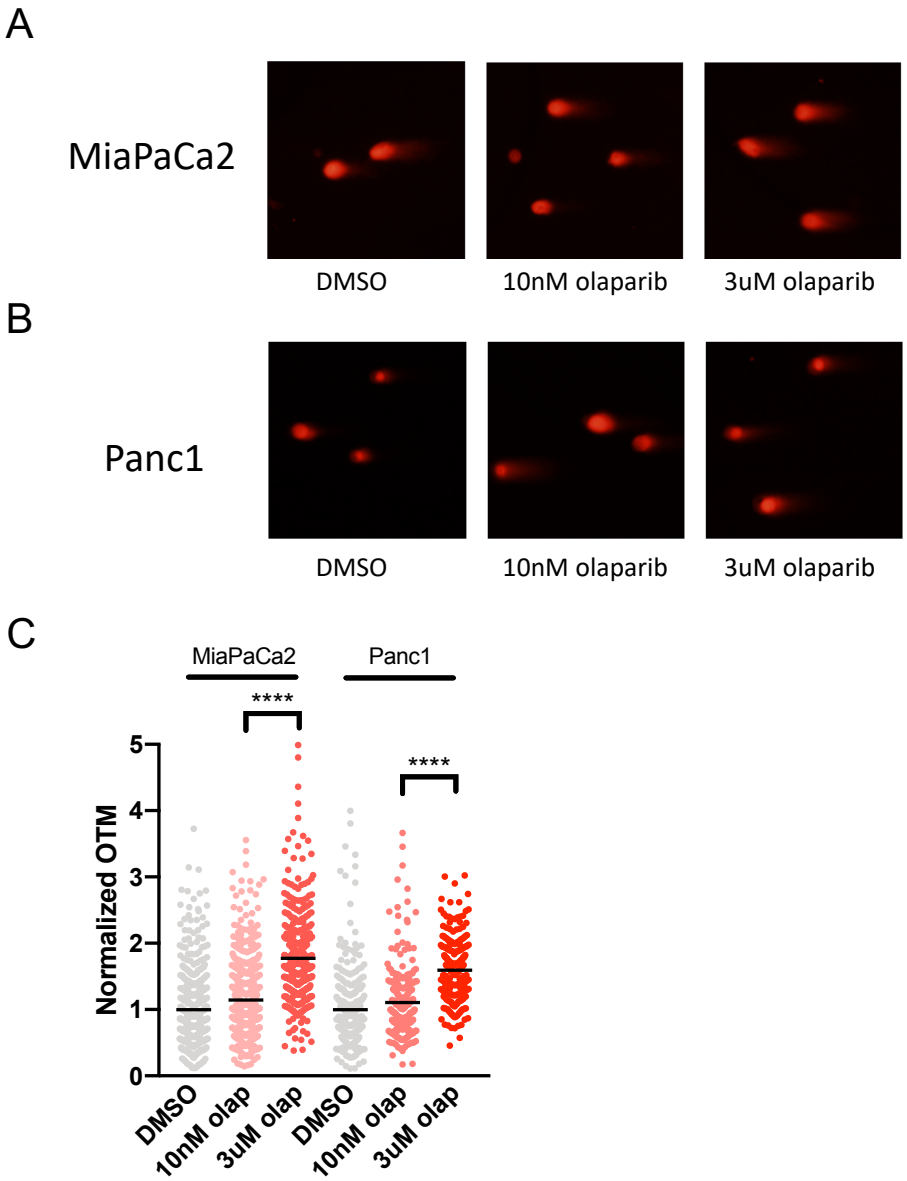

Figure 2.4 High concentration olaparib prevents repair of DNA double strand breaks following radiation - MiaPaCa2 and Panc1 cells were treated with 10nM or 3uM olaparib for one hour prior to 8 Gy radiation and 24 hours post-radiation. DNA double-strand breaks were evaluated by neutral comet assay. Representative comet images are shown for MiaPaCa2 (A) and Panc1 (B). (C) Comet Olive tail moment (OTM) was determined and normalized to DMSO control for MiaPaCa2 and Panc1. Results represent the aggregation of n=3 experiments normalized using an internal positive control irradiated on ice with mean ± SE.

Figure 2.5

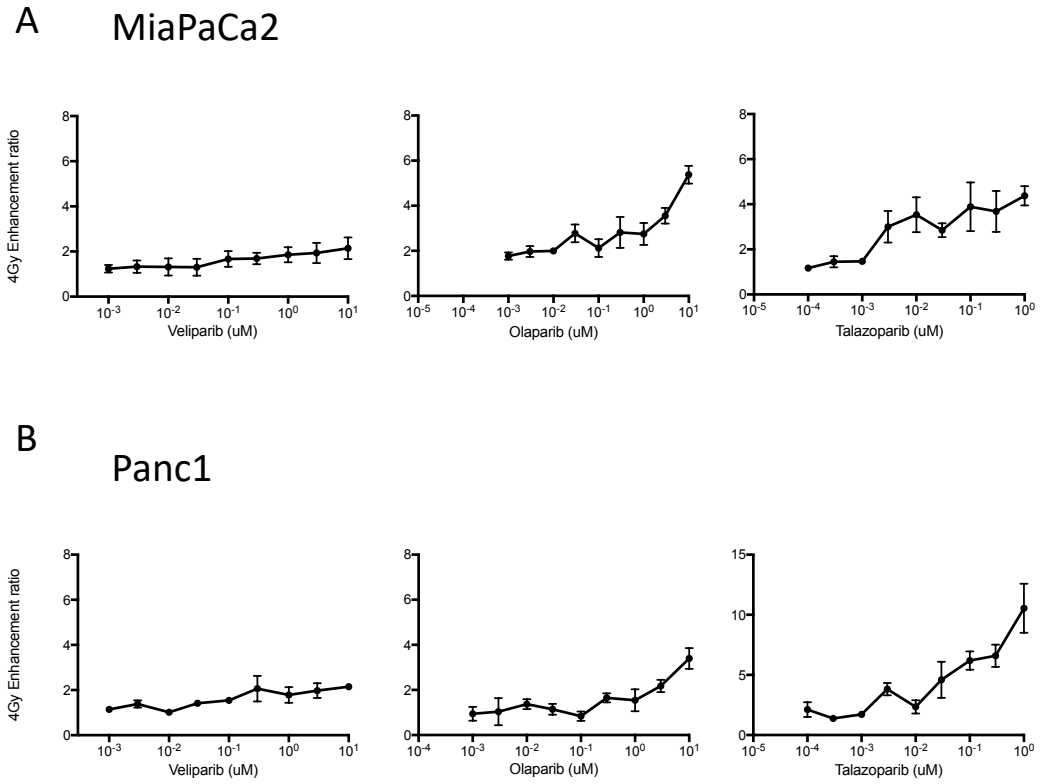

Figure 2.5 Radiosensitizing potency of PARP inhibitors – MiaPaCa2 (A) and Panc1 (B) cells were treated with various concentrations of veliparib, olaparib, or talazoparib for one hour prior to 4 Gy radiation and 24 hours after radiation, whereupon they were processed for clonogenic survival. Data represent the mean ± SE of 3 independent experiments.

Figure 2.6

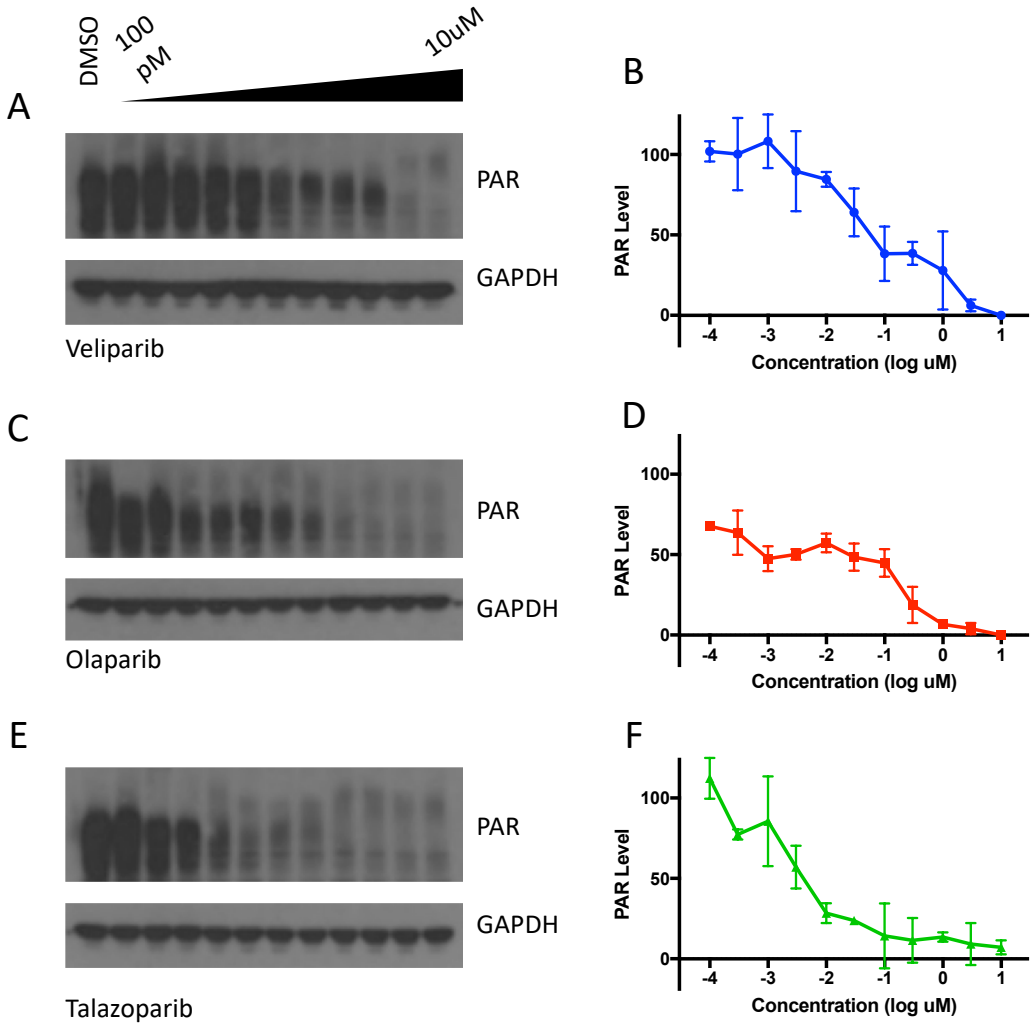

Figure 2.6 Enzymatic inhibition potency of PARP inhibitors - MiaPaCa2 cells were treated with increasing concentrations of veliparib (A), olaparib (C), and talazoparib (E) for six hours. Cells were collected for immunoblot and probed with antibodies to PAR and GAPDH. Quantitation of cellular PAR levels after 6-hour treatment with veliparib (A), olaparib (D), and talazoparib (F) by densitometry. PAR immunoblot intensity was individually against GAPDH and collectively against DMSO control. Data represent the mean ± SE of two experiments.

Figure 2.7

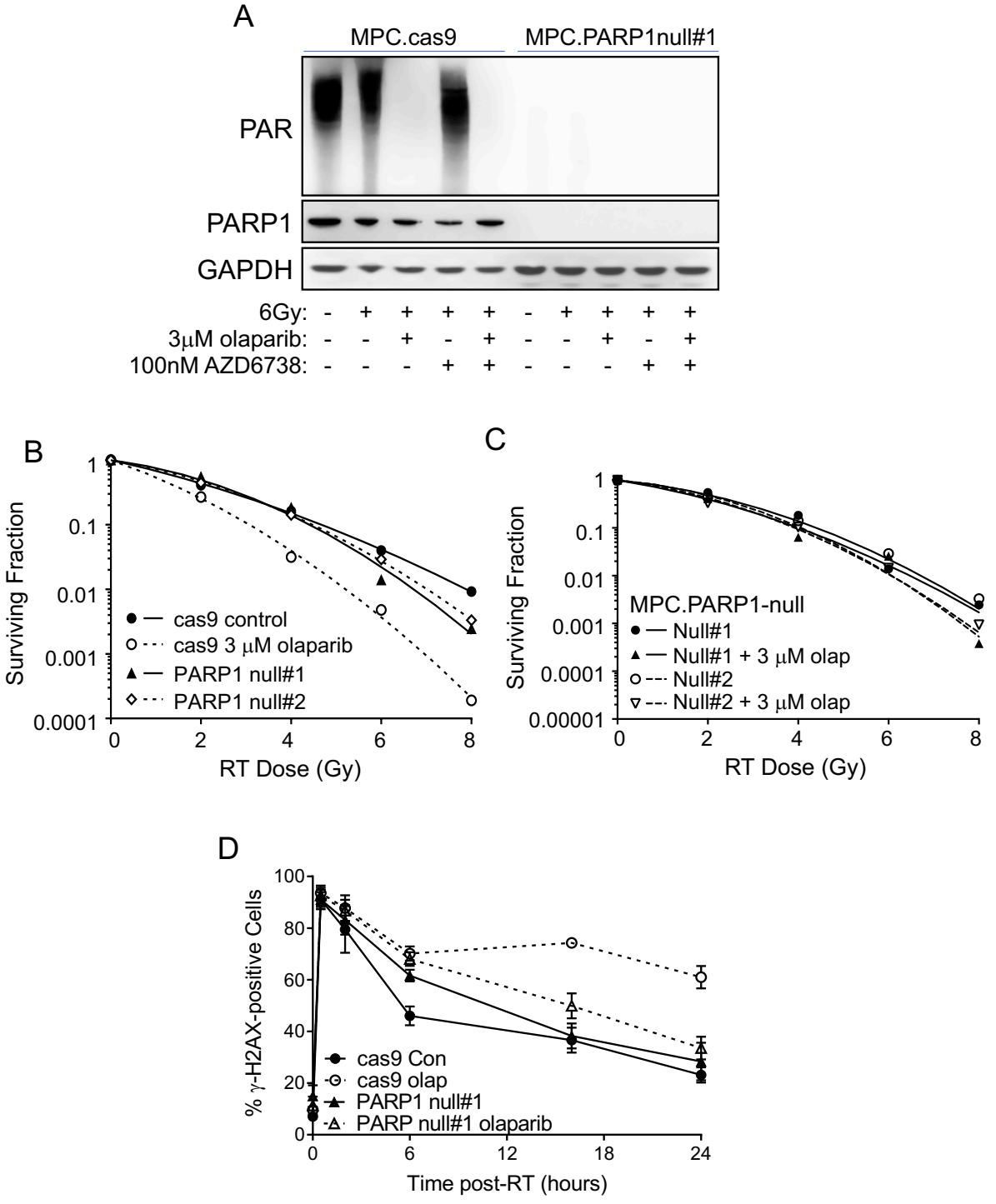
A
MPC.cas9
MPC.PARP1null#1
PAR
PARP1
GAPDH
6Gy: - + + + + - + + + +
3μM olaparib: - - + - + - - + - +
100nM AZD6738: - - - + + - - - + +
B
Surviving Fraction
1
0.1
0.01
0.001
0.0001
cas9 control
cas9 3 μM olaparib
PARP1 null#1
PARP1 null#2
0
2
4
6
8
RT Dose (Gy)
C
Surviving Fraction
1
0.1
0.01
0.001
0.0001
0.00001
MPC.PARP1-null
Null#1
Null#1 + 3 μM olap
Null#2
Null#2 + 3 μM olap
0
2
4
6
8
RT Dose (Gy)
D
% γ-H2AX-positive Cells
100
80
60
40
20
0
cas9 Con
cas9 olap
PARP1 null#1
PARP null#1 olaparib
0
6
12
18
24
Time post-RT (hours)

Figure 2.7 PARP trapping is required for radiosensitization and DNA damage – (A) Western blot showing whole cell lysate of MPC Cas9 and MPC PARP1 null#1 cells were treated with 3uM olaparib or 100nM AZD6738 for one hour prior to radiation and 24 hours following radiation. (B) Clonogenic survival of Cas9 control cell line ± 3uM olaparib and PARP1 null clones #1 and #2. (C) PARP1 null#1 and null#2 cells were treated with 3uM olaparib for one hour prior to radiation and 24 hours post-radiation, whereupon they were processed for clonogenic survival. (D) Cas9 control cells and PARP1 null#1 cells were treated with 3uM prior to 6 Gy radiation. At the indicated times post-RT cells were fixed for flow cytometry and analyzed for gH2AX positivity. Data shown are the mean from n=2-4 independent experiments ± SE.

Figure 2.8

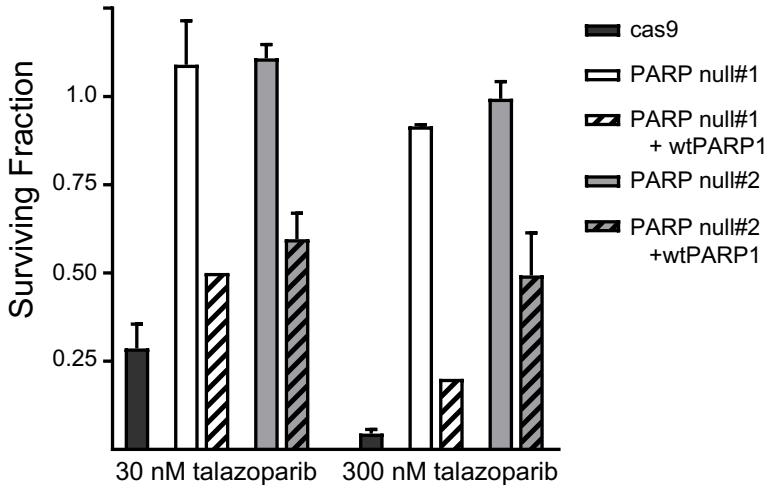

Figure 2.8 PARP inhibitor resistance by PARP1 deletion is reversed by exogenous expression of PARP1 - Cas9, PARP null#1, PARP null#1 reconstituted with wild-type PARP1, PARP null#2, and PARP null#2 reconstituted with wild-type PARP1 cells were treated with 30 nM talazoparib for 72 hours. Following treatment, cell were collected for clonogenic survival analysis. Data represent the mean ± SE of 3-5 experiments except for PARP null#1 + wt PARP1 which represents a single experiment.

Figure 2.9

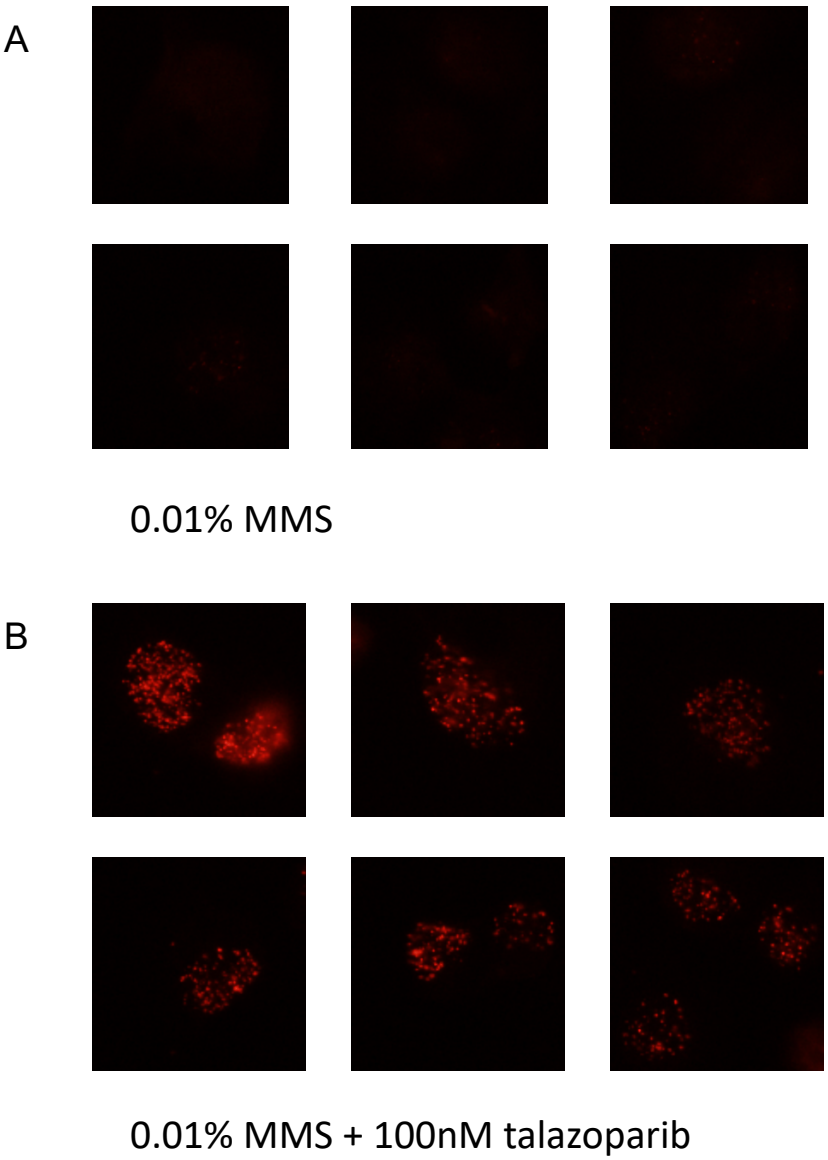

Figure 2.9 The proximity ligation assay as a measure of PARP trapping in cells – Cells were treated with 0.01% MMS (A) or 0.01% MMS (B) plus 100nM talazoparib for five hours. Following treatment, cells were fixed and processed for the proximity ligation assay for total H2AX and PARP1. PLA signal is shown as red. Representative images from n=3 experiments are shown.

Illustration 2.1

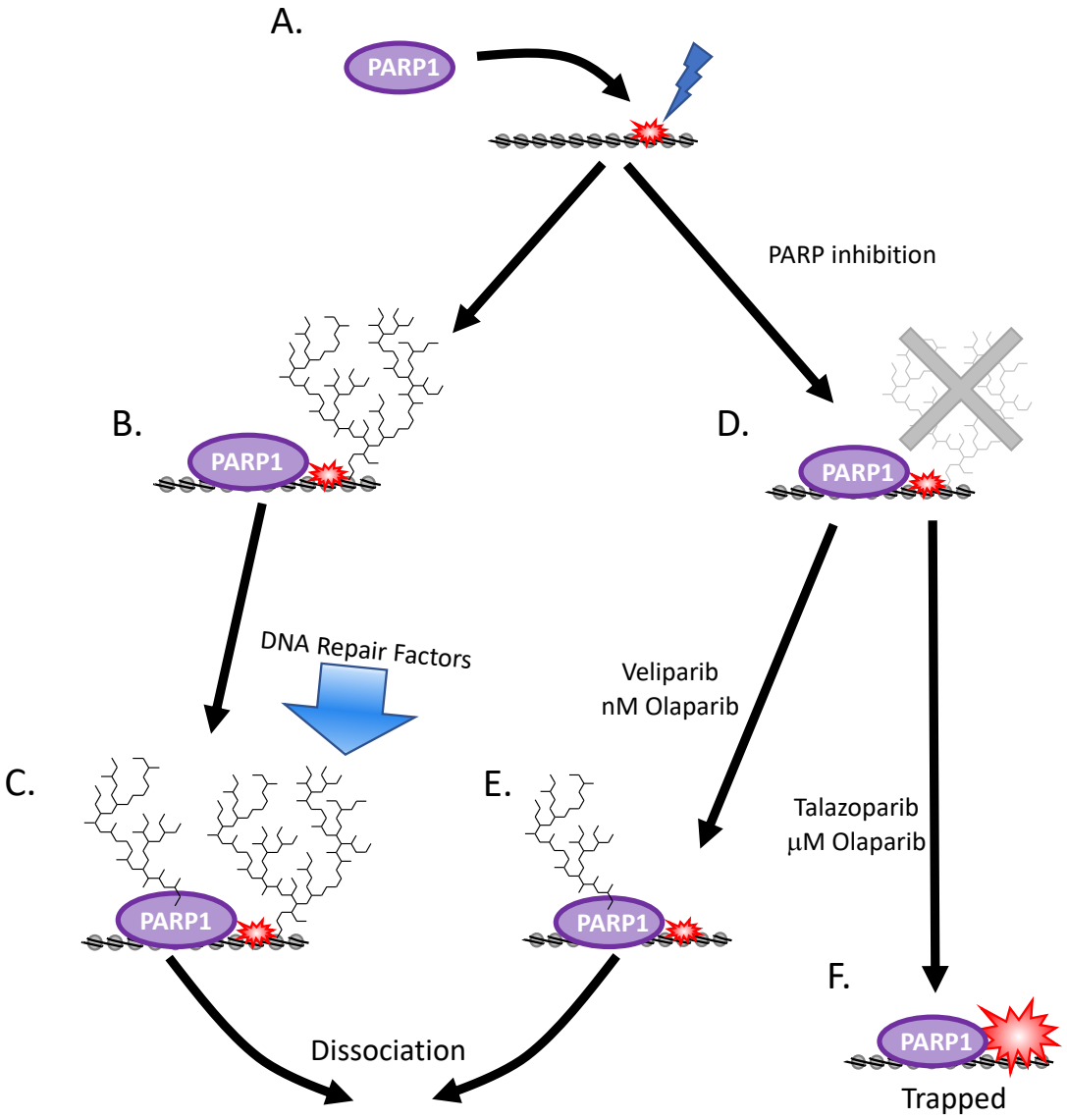

Illustration 2 .1 PARP1 response to DNA damage and consequences of inhibition. In response to ionizing radiation, poly (ADP-ribose) polymerase 1 (PARP1) is recruited to sites of DNA damage (A). There, it catalyzes the formation of large, negatively-charged, branched-chain moieties known as poly (ADP-ribose) (PAR) on chromatin (B), which serves as a docking station for factors involved in the repair of DNA (C). PARP1 then auto-PARylates and dissociates from the DNA. In the presence of a PARP inhibitor, the formation of PAR is prevented (D). After inhibition by veliparib or nanomolar concentrations of olaparib, PARP1 auto-PARylates and dissociates from chromatin (E). However, after treatment with talazoparib or micromolar concentrations of olaparib, PARP1 is not able to auto-PARylate and becomes trapped on chromatin, leading to increased DNA damage (F).

Chapter 3:

Combined Inhibition of ATR and PARP As a Radiosensitizing Strategy in Pancreatic Ductal Adenocarcinoma

3.1 Introduction

Local failure is responsible for up to 1/3 of pancreatic cancer related mortality [26] and chemotherapy alone is insufficient for the treatment of gross local disease. While radiation affords improved local disease control [24], the median survival of patients receiving standard concurrent chemoradiation therapy is only approximately 1 year [24], [25], [213]. Therefore, progress in the treatment of locally advanced pancreatic cancer will need to address the gross primary tumor. Hence, radiation sensitizing strategies are important for improved local control and will become increasingly important in light of improvements in systemic therapy [20], [22].

Given that radiation kills tumor cells by the induction of DNA double strand breaks (DSBs) [30], the DNA damage response (DDR) is a promising/logical target for radiosensitization [29] . While extensive preclinical data support the efficacy of DDR inhibitors as tumor radiosensitizers [85], [214], [215], recent clinical data also support this concept in pancreatic cancer patients treated with the combination of a WEE1 inhibitor with chemoradiation [89]. Subsequent laboratory studies have focused on strategic combinations of DDR inhibitors, in lieu of cytotoxic chemotherapy, concurrent with

radiation, with the goal of reducing toxicity while improving tumor efficacy. Specifically, our prior work has demonstrated the efficacy of the combination of WEE1 and PARP inhibitors with radiation in pancreatic cancer [87]. Furthermore, mechanistic studies have revealed that replication stress is the key mechanism of radiosensitization by combined treatment with WEE1 and PARP inhibitors [212].

Based on the importance of replication stress to tumor radiosensitization [212], [216], ATR (Ataxia telangiectasia and Rad3-related) and PARP1 (poly (ADP-ribose) polymerase 1) are promising targets for radiosensitization. ATR is a central mediator of the DNA replication stress response that is activated by RPA (replication protein A)-coated ssDNA (single stranded DNA) that occurs at sites of stalled replication forks as well as DNA damage sites [217], [218]. In cooperation with ATRIP and CHK1, ATR promotes the stabilization and restart of stalled replication forks, inhibits the initiation of aberrant replication forks, and pauses cell cycle progression until the completion of DNA replication (**Illustration 3.1**). Similarly, PARP1 has several important functions in DNA replication including stabilization, restart, and homologous recombination repair of stalled DNA replication forks [149], [150], [219], as well as regulation of DNA replication fork speed [220], [221]. Furthermore, the activity of several pharmacological inhibitors of PARP1 has been attributed to their ability to prevent the release PARP1 from DNA damage sites also known as PARP trapping a process thought to create an obstacle for ongoing DNA replication forks.

While HR (homologous recombination) repair deficiencies are a predictor of PARP inhibitor sensitivity, the mutations conferring these repair defects such as those occurring in BRCA1/2 are relatively rare in pancreatic cancer [11]. Therefore, strategies to extend

the efficacy of PARP inhibitors to otherwise resistant HR proficient pancreatic cancers are warranted.

In the study we investigated the activity of the combination of ATR and PARP inhibitors with radiation in HR proficient (as well as HR deficient) pancreatic cancers. When we found that catalytic inhibition of PARP1 was insufficient for the interaction of ATR and PARP inhibitors on radiosensitization in HR proficient pancreatic cancers, we went on to investigate the contribution of PARP1 protein and its DNA binding to radiosensitization both in vitro and in pancreatic tumor models. In addition, we investigated the contributions of replication stress and unrepaired DSBs to radiosensitization by combined inhibition of ATR and PARP. Furthermore, the tolerability and therapeutic efficacy of combined ATR and PARP inhibition with radiation were confirmed in animal models. The results of this study form the foundation for future clinical trials combining ATR and PARP inhibitors with radiation.

3.2 Results

To establish the efficacy of radiosensitization by combined ATR and PARP inhibitors we began by defining similarly cytotoxic concentrations of ATR and PARP inhibitors in both HR proficient and deficient pancreatic cancer cells. To this end, we employed the previously described RAD51shRNA MiaPaCa2 cells that, following doxycycline treatment, displayed reduced levels of RAD51 and sensitivity to both PARP inhibition and radiation, consistent with functional HR deficiency. We found that the ATR inhibitor AZD6738 similarly sensitized both the HR proficient (HRP) and deficient (HRD) MiaPaCa2 cells to PARP inhibition by olaparib (**Figure 3.1a-b**). Much higher, albeit

clinically relevant [153], concentrations of olaparib (1-10uM) were required to achieve similar sensitization in HR proficient cells to that observed in HR deficient cells (10-100nM). This finding is in agreement with the concentrations of olaparib required for sensitization by AZD6738 in HR proficient Panc1 cells and BRCA2 mutant, HR deficient Capan1 cells (**Figure 3.1c-d**).

Using similarly cytotoxic concentrations of AZD6738 (100nM) in combination with olaparib (10nM in HRD and 3uM in HRP), we next assessed radiosensitization following a concurrent treatment (1h pre, 24h post-RT). While either agent alone produced modest radiosensitization, combined treatment with ATR and PARP inhibitors was highly effective in inducing radiosensitization with enhancement ratios ranging from 1.67±0.07 to 1.83±0.14 and 1.43±0.11 to 1.47±0.13 in HR proficient and deficient pancreatic cancer cells, respectively (**Figure 3.2a-d, Table 3.1a**).Given that lower concentrations of olaparib (10nM) in combination with ATR inhibitor induced significant radiosensitization in HR deficient cells, we also tested the effects of a low olaparib concentration in HR proficient cells. In MiaPaCa2 (HRP) cells, olaparib alone produced minimal radiosensitization that was enhanced by the combination with AZD6738 (ER: 1.4±0.1) (**Figure 3.2e, Table 3.1a**) although to a much lesser extent than in combination with a high olaparib concentration (3uM; ER: 1.83±0.1). Similarly, in Panc1 cells a low concentration of olaparib given in combination with AZD6738 did not radiosensitize (ER: 1.06±0.04; **Figure 3.2f, Table 3.1a**), whereas high concentration olaparib produced significant radiosensitization in combination with AZD6738 (ER: 1.7±0.07). These data demonstrate marked differences in the olaparib concentration required for maximal radiosensitization in HR proficient and

deficient cells in the context of combined therapy with ATR inhibitor. This may reflect different, concentration-dependent mechanisms of action.

We next sought to evaluate the differential effects of low versus high olaparib concentrations on PARP1 activity with a focus on HR proficient cells which represent the majority of pancreatic cancer [153] and those most likely to benefit from the combination of ATR and PARP inhibitors given their resistance to PARP inhibitor monotherapy. Our work in Chapter 2 demonstrated that increased radiosensitization by 3uM olaparib relative to 10nM olaparib is mainly attributable to the presence of persistent PARP1-DNA complexes. We saw the same increased combinatorial efficacy of PARP and ATR inhibition when olaparib was used in trapping ranges, despite a no significant difference in enzymatic inhibition. Taken together, these data suggest that radiosensitization by the combination of ATR and PARP inhibitors is not only a function of PARP catalytic inhibition but also is associated with PARP1-DNA binding.

Previous work has established that PARP1 protein is required for the trapping effect and thus cytotoxicity of PARP inhibitors [194]. Therefore, in order to test the requirement for PARP1 protein in radiosensitization by olaparib and AZD6738, we deleted PARP1 from MiaPaCa2 cells by CRISPR-Cas9. MiaPaCa2 Cas9 cells were sensitized by olaparib alone (3uM; ER 1.59±0.09), an effect that was potentiated by AZD6738 (ER 2.1±0.17) (**Figure 3.3a, Table 3.1b**). In contrast, in PARP null MiaPaCa2 cells olaparib failed to radiosensitize, either alone (ER 1.07±0.07) or in combination with AZD6738 (ER 1.20±0.03) (**Figure 3.3b, Table 3.1b**). Together, these demonstrate that PARP1 protein is required for radiosensitization by olaparib and AZD6738, supporting the concept that

the combinatorial efficacy of ATR and PARP inhibitors is mediated by PARP1 DNA binding rather than catalytic inhibition.

Given the requirement for PARP1 protein in radiosensitization by ATR and PARP inhibitors, and its ability to form potentially cytotoxic PARP1-DNA complexes, we next compared the consequences of PARP catalytic inhibition and PARP1-DNA binding by using high or low olaparib concentrations in combination with AZD6738 and radiation. As we have demonstrated earlier, high but not low concentrations of olaparib caused a delay in the resolution of radiation-induced γH2AX (**Figure 3.4a-b**). However, while we expected that ATR inhibition would further potentiate DNA damage, combination with ATR inhibitor reduced the γH2AX signal. This finding is consistent with elevated replication stress and subsequent ATR-dependent H2AX phosphorylation [222]. Given that unrepaired DSBs are the lethal lesions induced by radiation, we next sought to physically measure DSBs after radiation using neutral comet assays in both MiaPaCa2 and Panc1 cells. In contrast to low concentrations of olaparib which had no effect on the resolution of radiation-induced DSBs in MiaPaCa2 or Panc1 cells, high concentrations of olaparib caused a significant increase in persistent DSBs following radiation (**Figure 3.4c-d**). In the absence of radiation, drug alone caused only mild elevation of DNA damage in MiaPaCa2 and Panc1 (**Figure 3.4e-f**). More importantly, AZD6738 treatment caused a significant increase in unrepaired DSBs following radiation but only when given in combination with a high olaparib concentration. These data demonstrate that PARP catalytic inhibition alone is insufficient to cause persistent DSBs in response to radiation and suggest that the maximal interaction of ATR and PARP inhibitors leading to

unrepaired DSBs and radiosensitization requires not only PARP catalytic inhibition but also PARP1 association with DNA.

To investigate the mechanism leading to unrepaired DSBs following ATR and PARP inhibition, we assessed DNA replication stress using DNA fiber combing. Given the requirement of PARP1 protein and concentrations of olaparib in excess of those required for PARP catalytic inhibition to produce maximal DSBs and radiosensitization, we hypothesized that PARP1 protein and its DNA binding create an obstacle for active DNA replication forks that is further exacerbated by inhibition of ATR, ultimately resulting in fork stalling/collapse and lethal DSBs. To test the effects of ATR and PARP inhibition on DNA replication stress [219], MiaPaCa2 cells were treated under radiosensitizing conditions with AZD6738 and olaparib and at the end of treatment active DNA replication forks were labeled with IdU and CIdU (**Figure 3.5a-b**). Surprisingly and in contrast to our initial hypothesis, treatment with AZD6738, olaparib, and radiation did not result in DNA replication fork stalling or collapse (**Figure 3.5c**). Instead, high concentrations of olaparib increased the speed of replication fork progression, suggesting, consistent with a prior study, that PARP1-DNA complexes do not impede DNA replication [220] (**Figure 3.5d**). This increase in replication velocity was associated with activation of the ATR-mediated replication stress response marked by increased ATR (T1989) and CHK1 (S345) phosphorylation (**Figure 3.5e**). Inhibition of ATR significantly inhibited DNA replication speed, an effect that is consistent with the role of ATR in preventing excessive origin firing which impedes DNA replication rates [223]. Furthermore, these effects of ATR inhibition were dominant even in combination with high concentrations of olaparib that otherwise stimulated DNA replication rates. Taken together, these data demonstrate increased

replication rates following a high olaparib concentration that are severely reduced by ATR inhibition. In light of the persistent DSBs associated with combined ATR and PARP inhibition, these data suggest that ATR is required for mitigating the replication stress caused by faster DNA replication rates following PARP inhibition such that combined inhibition of ATR and PARP has detrimental effects on DNA replication ultimately leading to DSBs.

Based on the substantial radiosensitizing efficacy of ATR and PARP inhibitors in vitro, we next tested the therapeutic efficacy and tolerability of combined AZD6738, olaparib and radiation in animal tumor models. Nude mice bearing MiaPaCa2-derived tumor xenografts were treated with daily AZD6738, olaparib, and radiation. While radiation alone or in combination with AZD6738 or olaparib had a modest effect on tumor growth, the combination of AZD6738, olaparib, and radiation had a profound effect on tumor growth (**Figure 3.6a**). Tumors treated with this combination displayed a significantly increased time to tumor volume tripling relative to all other groups including radiation combined with either single agent (**Figure 3.6b**). Noteworthy, 28% of the tumors treated with the combination of AZD6738, olaparib, and radiation had complete responses that lasted for the duration of the study (80 days). These results were in the absence of any significant toxicity as reflected by mouse weights, with the average weight loss being less than 5% for any treatment group (**Figure 3.6c**). Taken together these data demonstrate that the combination of ATR and PARP inhibitors is a highly active radiosensitizing strategy with a favorable toxicity profile.

3.3 Conclusions

In this study we sought to investigate the efficacy of combined inhibition of ATR and PARP1 in combination with radiation for the treatment of pancreatic cancer. We began by assessing the combined cytotoxicity of AZD6738 and olaparib, inhibitors of ATR and PARP1, respectively. We found that the combination was well tolerated even at high concentrations of olaparib by cell lines proficient in HR, but HRD cell lines were rapidly sensitized to olaparib by AZD6738. Similarly, we found that low concentration olaparib was sufficient to sensitize HRD pancreatic cancer cell lines to radiation in combination with AZD6738 but HRP cell lines required high concentrations to achieve this combined radiosensitizing effect. Based on our previous work characterizing the effects of high versus low concentration of olaparib on enzymatic inhibition and the formation of PARP1-DNA complexes, we hypothesized that combinatorial efficacy in HR proficient cells was based on the ability of olaparib to trap PARP1 to chromatin. In agreement with this observation, a genetic model of PARP1 loss was not sensitized to radiation by AZD6738, demonstrating that loss of enzymatic activity through deletion does not replicate the combinatorial effects of olaparib. Further, the requirement for PARP1 protein was confirmed by the failure of high concentration olaparib and AZD3768 to radiosensitize in PARP1-null cells.

Work to uncover the mechanism of this combined sensitization showed an increase in double-strand DNA damage at 24 hours following radiation in cells treated with high concentration olaparib, but not low concentration. This effect was further potentiated by the addition of AZD6738, which did not have an effect on its own or in combination with non-trapping concentrations of olaparib. We hypothesized that this increase in damage could be caused by the removal of ATR's described functions in the

resolution of replication stress exhibited by olaparib-induced elevation in fork speed and markers of stress. Finally, we demonstrated the combined efficacy of ATR and PARP inhibition with radiation in mice bearing tumor xenografts. Tumors in the group receiving the triple combination therapy demonstrated superior response to all other treatment groups, including a 28% cure rate. Toxicity of the combination was minimal as measured by animal weight.

At the time of writing, eight active and recruiting trials are investigating the combination of olaparib and AZD6738 including one in pancreatic cancer. Many of these trials are founded on work by Kim *et al*. [127] exploring the preclinical combination of ATR and PARP inhibition in the setting of BRCA-mutant ovarian cancer. A strong emphasis on HR status in the development of PARP inhibitors has meant that it has come into play during the patient stratification (NCT03330847) and inclusion criteria (NCT02576444) for some of these trials. Given the intimate involvement of both targets in the DNA damage response, we hope that the remarkable response we have seen in our own preclinical tumor study will encourage thought about combining these drugs with radiation as a means for tackling HR proficient cancers, and that the mechanistic rationale will help guide dosages and schedules into effective therapeutic ranges. Major dose limiting toxicities in PARP inhibitor trials have been related to cytopenias [224], [225] a phenotype that has been attributed to PARP trapping [200]. Some of these adverse effects may have to be risked in order to harness the maximum efficacy of PARP inhibitors in their combination with ATR inhibition.

It is not immediately clear which predictive biomarkers may best serve to select patients for treatment with this combined therapy. Sensitivity to PARP inhibition,

discussed in Chapter 1, or ATR inhibition, which may be predicted through certain genetic mutations including ATM [226], by themselves would enhance the anti-tumor activity of the combination. However, based on the mechanistic rationale for the combination, markers of inherent replication stress are likely to serve as biomarkers for tumors that will respond to the triple combination. Currently, no clinically-deployed assay serves as a reliable indicator of replication stress levels. Due to their direct activation in response to replication stress, IHC for phosphorylated ATR (T1989) and Chk1 (S345). Our data demonstrate the activation of these pathways after cellular treatment with radiation and trapping levels of PARP inhibitor (**Figure 3.5e**). Other research has suggested that replication stress could be measured through the expression level of a panel of five proteins involved in the replication stress response in FFPE tissues [227]. Finally, levels of chromosomal instability, one consequence of replication stress in cancers, measured in circulating tumor DNA was reflective of therapeutic response in a study of gastric cancer [228]. It is possible a similar assay could be used as a proxy measurement for replication stress.

3.4 Experimental Procedures

Much of the data shown in this chapter is also displayed in Chapter 2 of this work. The two projects were pursued concurrently and often experiments produced results relevant to both. For convenience of comparison, those data are shown again in the results section of this chapter.

Data shown in this work is the product of collaboration and represents the work of many members of the laboratory, past and present. Leslie A. Parsels performed work

contributing to the clonogenic cell survival assays, immunoblotting, and DNA fiber spreading. Joshua D. Parsels contributed to clonogenic survival assays and assisted with tumor growth studies. Sheryl Flanagan contributed to PAR immunoblots. CRISPR-Cas9 PARP1-null and control cell lines were generated by Qiang Zhang.

Cell Culture and drug solutions

MiaPaCa2 and Panc1 cells were obtained from and authenticated by the American Type Culture Collection. Capan1.NEO is a clonal cell line expressing the neomycin resistance gene obtained from S. Powell (Memorial Sloan Kettering Cancer Center, New York, NY) [203]. Cells were grown in either DMEM (MiaPaCa2 and Panc1; Invitrogen), or IMDM medium (Capan1.NEO; Invitrogen) supplemented with 10% fetal bovine serum (Premium Select; Atlanta Biologicals). Olaparib and AZD6738 (AstraZeneca) were each dissolved in DMSO and stored in aliquots at −20°C. For in vivo studies, AZD6738 is dissolved in 40% propylene glycol. Olaparib was diluted as needed in 2-hydroxypropyl-β-cyclodextrin (Kleptose).

Clonogenic survival assays

Cells were treated with drugs/radiation and then replated at cloning densities. Cells were grown for 9-14 days and then fixed and stained with methanol-acetic acid and trypan blue and scored for colonies of >50 cells. Cell survival curves were fitted using the linear quadratic equation, and the mean inactivation dose calculated [204]. The radiation enhancement ratio was calculated as the quotient of the mean inactivation dose under

control conditions divided by that under experimental conditions. An enhancement ratio greater than 1 indicated radiosensitization.

Immunoblotting

Whole cell lysates were prepared in RIPA buffer (150 mM NaCl, 1% NP-40, 0.5% sodium deoxycholate, 0.1% SDS, 25 mM Tris pH 7.4) supplemented with both PhosSTOP phosphatase inhibitor and Complete protease inhibitor cocktails (Roche) as previously described [211]. Samples were processed for Western blot analysis as previously described [212].

Neutral Comet Assay

Cells were treated with AZD6738 and/or olaparib for 1 h prior to and 24 h post-8 Gy RT. Neutral comet assay was performed according to the manufacturer's protocol (Trevigen, USA). Briefly, cells were scraped, mixed 1:10 with 1% molten LMAgarose, pipetted onto a CometSlide (Trevigen, USA) and submerged in neutral lysis buffer (Trevigen, USA) overnight at 4˚C. Slides were rinsed 3 times with TBE (90 mM Tris base, 90 mM boric acid, 2 mM EDTA, pH 8.0) and subjected to neutral electrophoresis for 35 minutes at 25V. Slides were incubated in 2.5 ug/ml propidium iodide for 20 minutes, then rinsed in 70% ethanol and allowed to dry overnight. Images were acquired using an Olympus ix73 inverted microscope with a 10x objective. The tail moments from at least 50 cells were measured for each experimental condition. Comet Assay IV software (Instem) was used to quantify the Olive tail moment. Tail moment for each replicate experiment was normalized to an internal control condition of cells collected for neutral

comet assay immediately following irradiation with 8 Gy radiation. Tail moment values for replicates of each condition were then pooled and all conditions were normalized to DMSO control.

Flow Cytometry

Cells were trypsinized, washed with ice-cold PBS, and fixed at a concentration of 2 × 106 cells/mL in ice-cold 70% ethanol. For γH2AX analysis, samples were incubated with a mouse anti-γH2AX-specific antibody (clone JBW301; Millipore) overnight at 4°C followed by incubation with a FITC-conjugated secondary antibody (Sigma) as previously described (27). γH2AX positivity was quantified by setting a gate on the control, untreated sample to define a region of positive staining for γH2AX of approximately 5%. This gate was then overlaid on the drug/radiation-treated samples. Samples were stained with propidium iodide to measure total DNA content and analyzed on a FACScan flow cytometer (Becton Dickinson) with FlowJo software (Tree Star).

DNA Fiber Spreading

MiaPaCa2 cells treated as depicted in Fig. 4D were pulse-labeled with 25 uM 5-iododeoxyrudine (IdU) for 30 min, followed by two gentle washes with pre-warmed PBS and a second pulse with 250 uM 5-chloro-2'-deoxyuridine (CldU) for 30 min. Labelled cells were collected and fibers spread on silane-coated slides (Lab Scientific 7801B) as previously described [229] with modifications noted below. Two slides were spread and stained for each experimental condition. IdU was detected with a mouse anti-BrdU antibody (Becton Dickinson, 347580) and CldU with a rat anti-BrdU antibody (BIORAD,

OBT0030G). Secondary antibodies were Alexa Fluor 594 anti-mouse (Invitrogen, A11062) used at a 1:1000 dilution and Alexa Fluor 488 anti-rat (Invitrogen, A21470) used at a 1:200 dilution. Images of well-spread fibers were acquired using an Olympus ix73 inverted microscope with a 60x objective. For each experimental condition, double-labelled replication forks from 3-8 fields/slide were analyzed manually using ImageJ software (NIH). Fork measurements from two independent experiments were pooled and the total number of DNA fibers from both experiments is presented.

Tumor Growth Studies

Animals were handled according to a protocol approved by the University of Michigan Committee for Use and Care of animals. MiaPaCa-2 cells (5×106) were suspended in a 1:1 mixture of 10% FBS/DMEM:Matrigel (BD Biosciences) and injected subcutaneously, bilaterally into the flanks of 3-5 week old, female, athymic nude mice. Treatment was initiated when the average tumor volume reached 100mm3. Tumor size was measured two times per week; tumor volume (TV) was calculated according to the equation: $TV = \pi / 6 (ab2)$, where a and b are the longer and shorter dimensions of the tumor, respectively. Measurements were made until the tumor volume increased by approximately a factor of 4.

3.5 Figures and Data

Figures begin next page

Figure 3.1

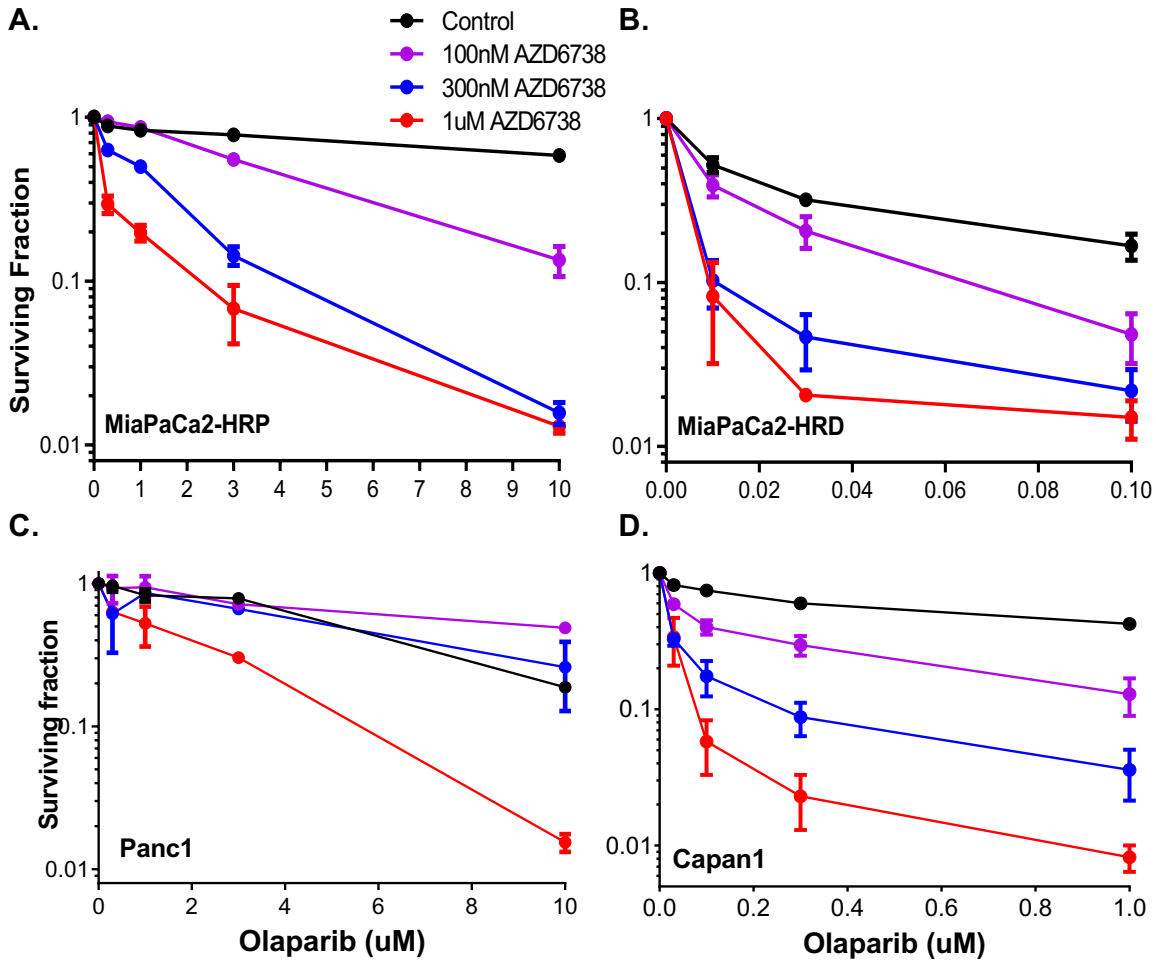

Figure 3.1 The interaction of ATR and PARP inhibitors on cytotoxicity in HRP and HRD pancreatic cancers - MiaPaCa2-HRP (A), MiaPaCa2-HRD (B), Panc1 (C), and Capan-1 (D) cells were treated with indicated concentrations of olaparib and AZD6738 for 72 hours, whereupon they were collected and processed for clonogenic survival. Results represent the mean ± standard error of 3-4 experiments.

Figure 3.2

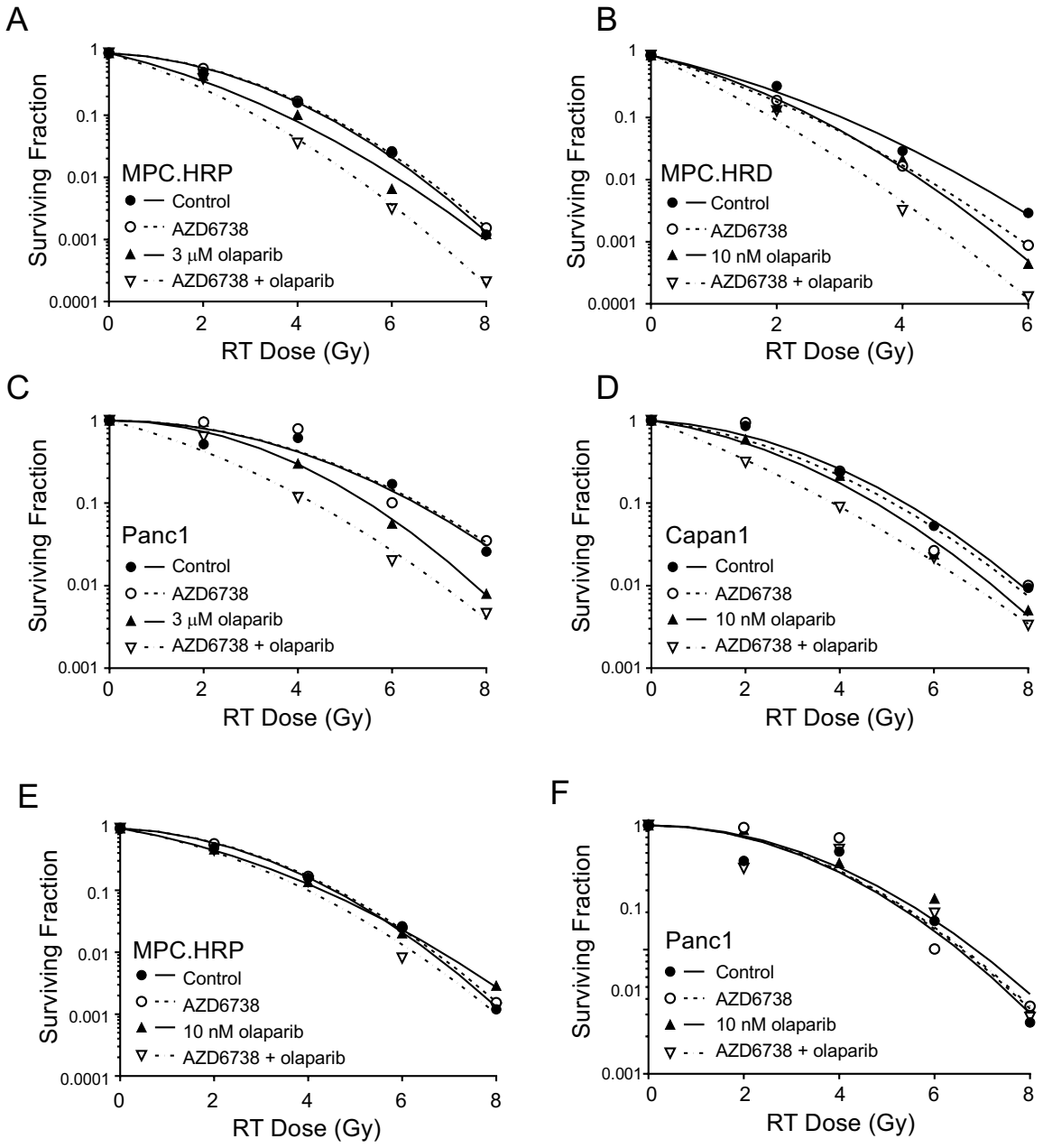

Figure 3.2 Sensitization to radiation by olaparib and AZD6738 in pancreatic cancer cells - MPC.HRP (A,E), MPC.HRD (B), Panc1 (C,F), and Capan1 (D) cells were treated with 100nM AZD6738 and/or olaparib for one hour prior to radiation (RT; 0-8 Gy) and 24 hours after radiation, whereupon they were processed for evaluation of clonogenic survival. MPC.HRP and Panc1 cells were treated with 3uM olaparib while MPC.HRD and Capan1 cells were treated with 10nM olaparib.

Figure 3.3

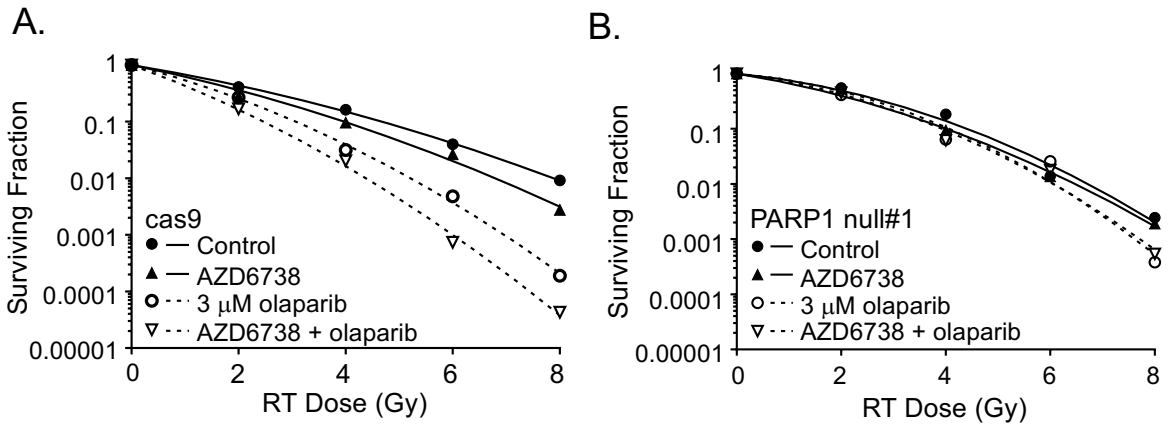

Figure 3.3 PARP1 null cells are not radiosensitized by olaparib and AZD6738 – MiaPaCa2 Cas9 control cells (A) and PARP1 null#1 cells (B) were treated with 100nM AZD6738 and/or 3uM olaparib for one hour prior to radiation and 24 hours post-radiation, whereupon they were processed for clonogenic survival.

Figure 3.4

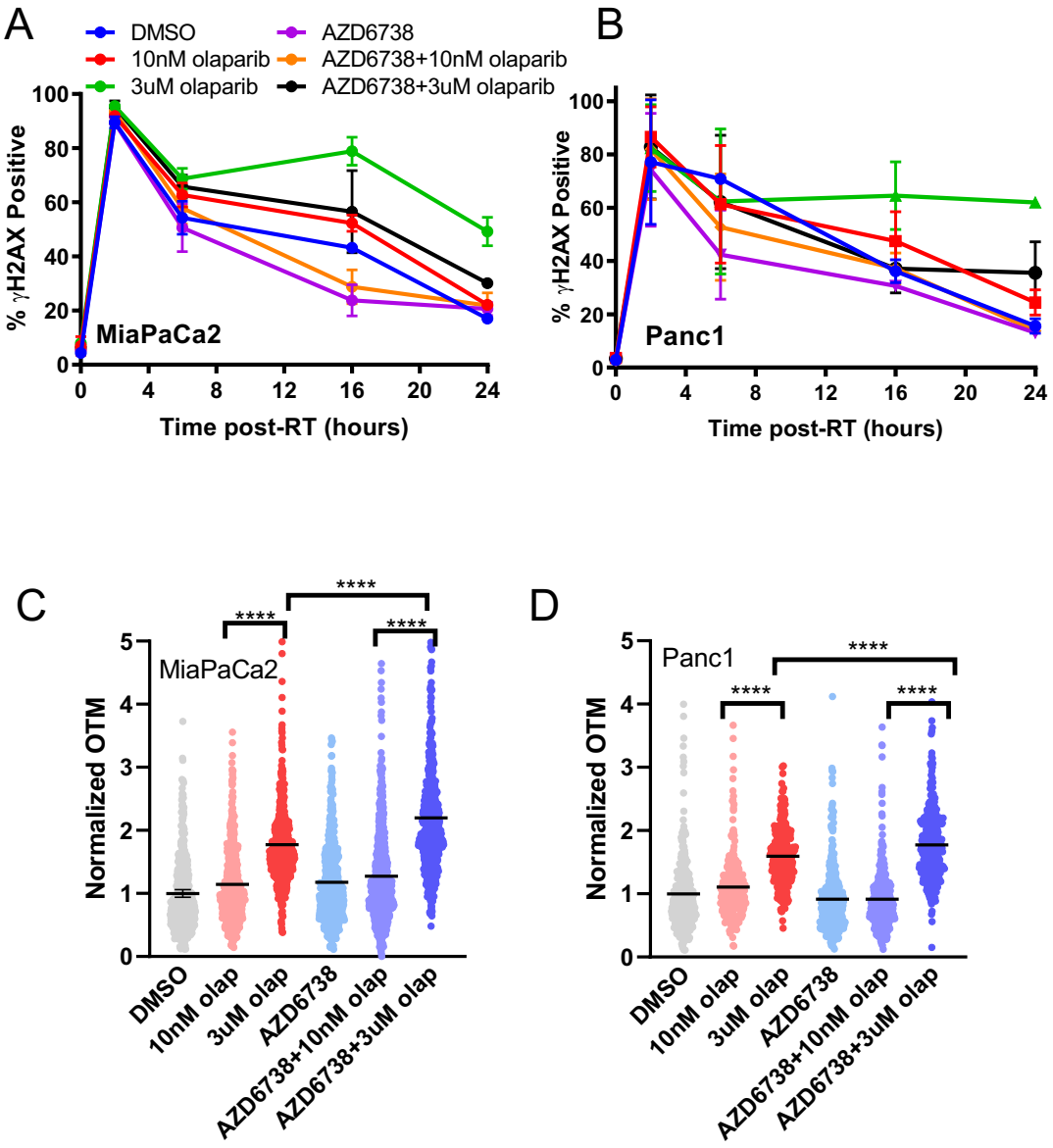
A
DMSO
10nM olaparib
3uM olaparib
AZD6738
AZD6738+10nM olaparib
AZD6738+3uM olaparib
% γH2AX Positive
MiaPaCa2
Time post-RT (hours)
B
% γH2AX Positive
Panc1
Time post-RT (hours)
C
Normalized OTM
MiaPaCa2
****
****
****
DMSO
10nM olap
3uM olap
AZD6738
AZD6738+10nM olap
AZD6738+3uM olap
D
Normalized OTM
Panc1
****
****
****
DMSO
10nM olap
3uM olap
AZD6738
AZD6738+10nM olap
AZD6738+3uM olap

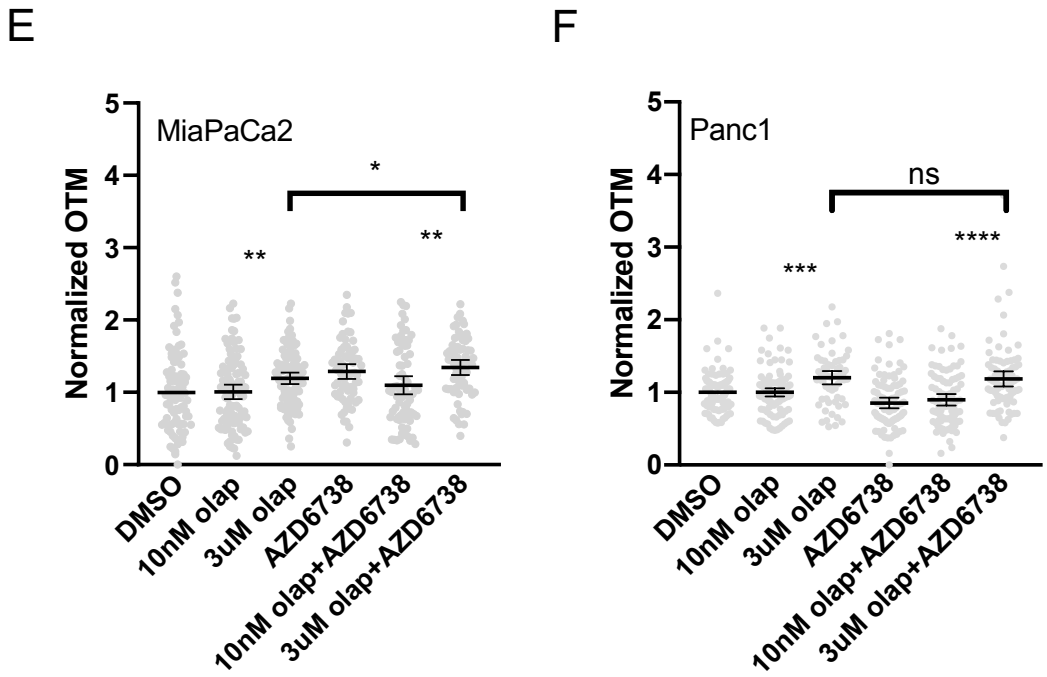

Figure 3.4 ATR and PARP inhibition delay the resolution of DNA following radiation – MiaPaCa2 (A) and Panc1 (B) cells were treated with 100nM AZD6738 and 10nM or 3uM olaparib one hour prior to 6 Gy radiation. At the indicated times post-RT cells were fixed for flow cytometry and analyzed for gH2AX positivity. Data shown are the mean from n=2 independent experiments ± SE. MiaPaCa2 (C) and Panc1 (D) cells were treated with 100nM AZD6738 and/or olaparib at the indicated concentrations for one hour prior to 8 Gy radiation and 24 hours post-radiation. DNA double-strand breaks were evaluated by neutral comet assay. Comets Olive tail moment (OTM) was determined and normalized to DMSO control. Results represent the aggregation of n=3 experiments normalized using an internal positive control irradiated on ice with mean ± SE. MiaPaCa2 (E) and Panc1 (F) cells were treated with 100nM AZD6738 and/or olaparib at the indicated concentrations without radiation for 24 hours. DNA double-strand breaks (DSBs) were evaluated by neutral comet assay. Comets Olive tail moment (OTM) was determined and normalized to DMSO control.

Figure 3.5

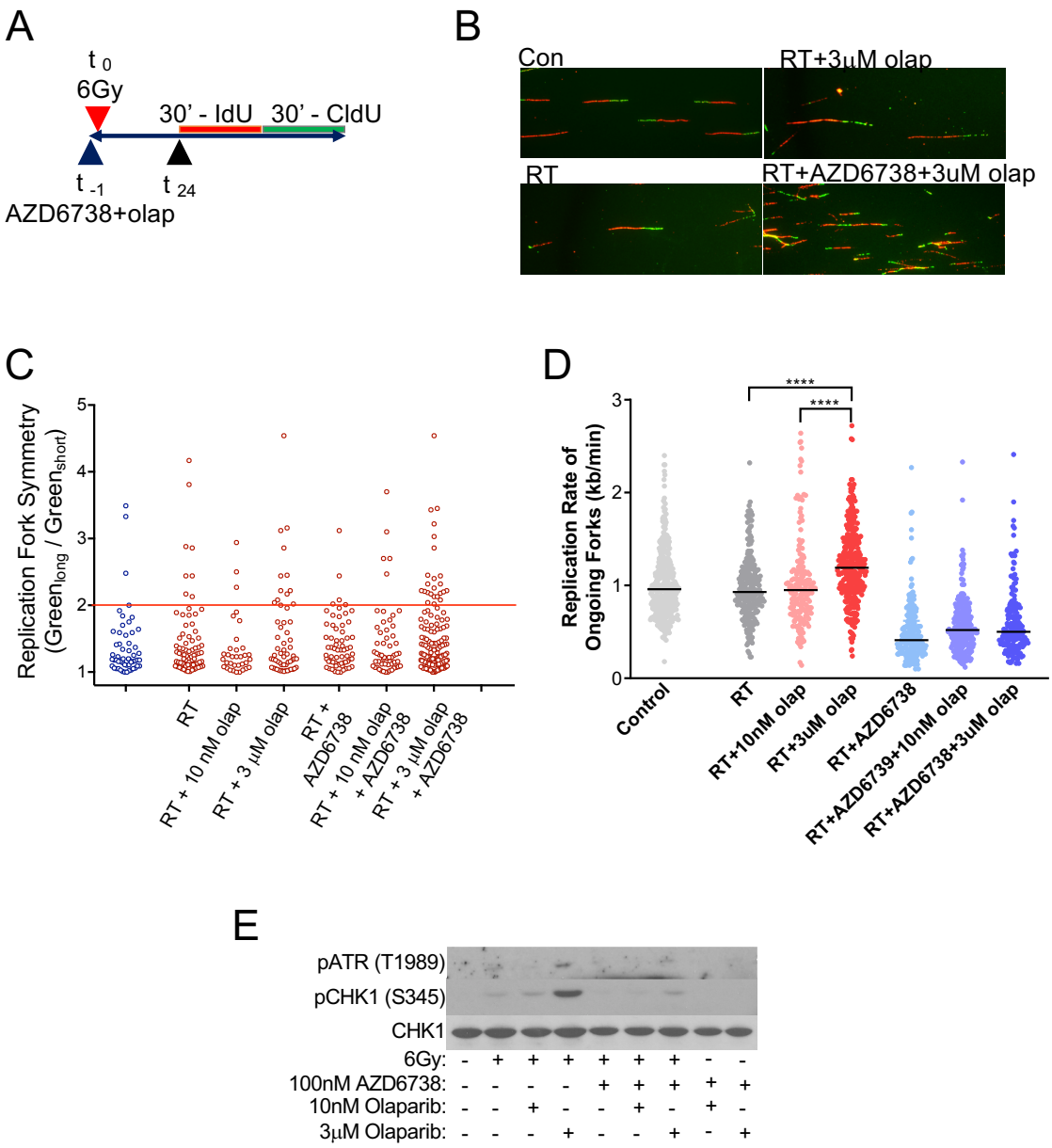

Figure 3.5 The effect of combined ATR and PARP1 inhibition on replication stress – Treatment schedule (A) and representative images (B) of DNA fibers from MiaPaCa2 cells 24 h after treatment with 6 Gy radiation, 10 nM or 3 uM olaparib and 300 nM AZD6738. (C) Replication fork symmetry was calculated for individual forks labeled with an IdU track flanked on both sides by CldU tracks as the ratio of CldU track lengths. A track ratio of 1 indicates symmetrical fork elongation and greater than 2 indicates highly asymmetrical fork elongation. (D) Replication fork speed was calculated for individual forks labelled with an IdU track flanked by a single CldU track. Errors bars represent the

median ± interquartile range from over 150 forks scored in two biological replicates. Statistical differences between distributions were assessed using the nonparametric Mann-Whitney rank sum test. (E) Western blot of whole cell extract from MiaPaCa2 cells treated with 100 nM AZD6738 and 10 nM or 3 uM olaprib for one hour prior to 6 Gy radiation and 24 hours after radiation.

Figure 3.6

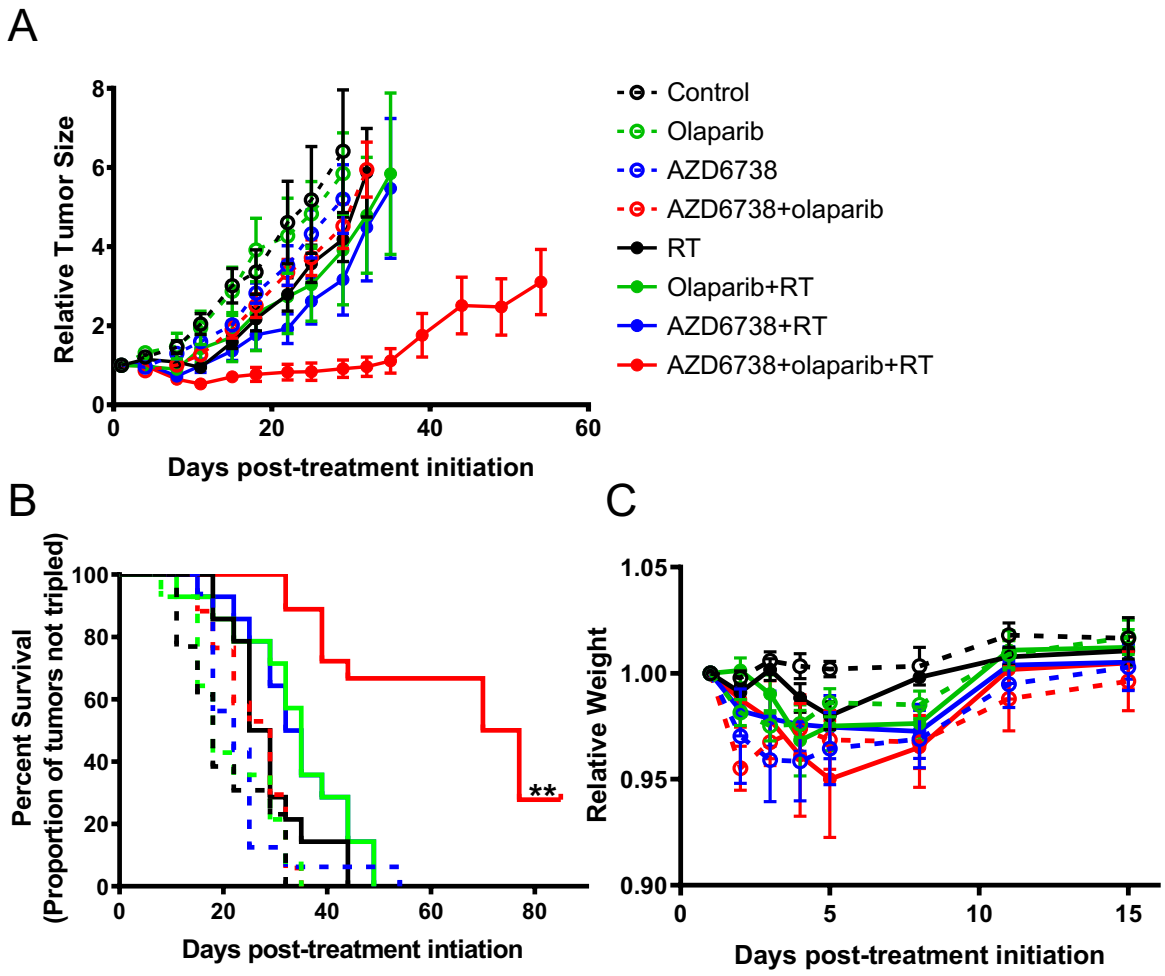

Figure 3.6 Radiosensitization of pancreatic tumor xenografts by AZD6738 and olaparib - Athymic nude mice bearing bilateral, flank MiaPaCa-2 xenografts were treated with AZD6738 (25mg/kg) and olaparib (50mg/kg) one hour pre-RT, and radiation (RT; 1.8Gy/fraction) daily Monday through Friday for one cycle. (A) Tumor volumes were normalized to the first day of treatment (day 1) and are the mean ± SE of 13-18 tumors per treatment group. (B) The Kaplan-Meier plot illustrates the proportion of tumors tripled in volume within the full 80 day monitoring period. (C) Weights were normalized to the first day of treatment.

Table 3.1

	Condition	RER	Cytotoxicity
A	*MiaPaCa-2 RAD51 shRNA*		
	HRP (no dox)	*1.0*	*1.0*
	AZD6738 (100 nmol/L)	1.14 ± 0.05	0.93 ± 0.07
	Olaparib (10 nmol/L)	1.11 ± 0.04	0.88 ± 0.04
	Olaparib (3 μmol/L)	1.43 ± 0.08[a]	0.80 ± 0.04
	AZD6738 + olaparib (10 nmol/L)	1.40 ± 0.10[a,b]	0.84 ± 0.07
	AZD6738 + olaparib (3 μmol/L)	1.83 ± 0.14[a,b,c]	0.66 ± 0.03
	HRD (+ dox)	*1.0*	*1.0*
	AZD6738 (100 nmol/L)	1.16 ± 0.06	0.98 ± 0.04
	Olaparib (10 nmol/L)	1.17 ± 0.03	0.80 ± 0.05
	AZD6738 + olaparib	1.43 ± 0.11[a]	0.63 ± 0.02
	Panc-1		
	AZD6738 (100 nmol/L)	1.02 ± 0.03	0.96 ± 0.08
	Olaparib (10 nmol/L)	1.03 ± 0.07	0.83 ± 0.09
	Olaparib (3 μmol/L)	1.29 ± 0.06[a]	0.80 ± 0.12
	AZD6738 + olaparib (10 nmol/L)	1.06 ± 0.04	0.87 ± 0.03
	AZD6738 + olaparib (3 μmol/L)	1.67 ± 0.07[a,b,c]	0.94 ± 0.08
	Capan-1		
	AZD6738 (100 nmol/L)	1.14 ± 0.06	0.92 ± 0.04
	Olaparib (10 nmol/L)	1.26 ± 0.06	0.92 ± 0.12
	AZD6738 + olaparib	1.47 ± 0.13[a]	0.87 ± 0.12
B	*MiaPaCa2 – cas 9*	*1.0*	*1.0*
	AZD6738 (100 nmol/L)	1.24 ± 0.05	0.88 ± 0.03
	Olaparib (3 μmol/L)	1.59 ± 0.09	0.93 ± 0.11
	AZD6738 + olaparib	2.10 ± 0.17[d,e]	0.60 ± 0.09
	MiaPaCa2 – PARP1 null	1.31 ± 0.14	0.67 ± 0.03
	AZD6738 (100 nmol/L)	1.55 ± 0.18	0.69 ± 0.03
	Olaparib (3 μmol/L)	1.40 ± 0.19	0.72 ± 0.04
	AZD6738 + olaparib	1.49 ± 0.30 (n=2)	0.64 ± 0.01 (n=2)

P < 0.05 vs. control[a], AZD6738[b], olaparib[c], cas9 control[d], cas9 AZD6738[e].

Table 3.1 Radiosensitization and cytoxocicity of combined ATR and PARP1 inhibition - (A) MiaPaCa2 HRP, MiaPaCa2 HRD, Panc-1, and Capan-1 cells were treated with AZD6738 and/or olaparib beginning one hour prior to radiation. Twenty-four post-radiation, cells were processed for clonogenic survival. Data are the mean radiation enhancement ratio (RER) ± SEM for n=3-6 independent experiments. Cytotoxicity in the absence of radiation treatment was calculated by normalizing the plating efficiencies of drug treated- to non-drug treated cells. (B) MiaPaCa2 Cas9 control cells and MiaPaCa2 PARP1 null cells were treated with AZD6738 and/or olaparib beginning one hour prior to radiation. Twenty-four post-radiation, cells were processed for clonogenic survival. Data

are the mean radiation enhancement ratio (RER) ± SEM for n = 2-3 independent experiments. Cytotoxicity in the absence of radiation treatment was calculated by normalizing the plating efficiencies of drug treated- to non-drug treated cells.

Illustration 3.1

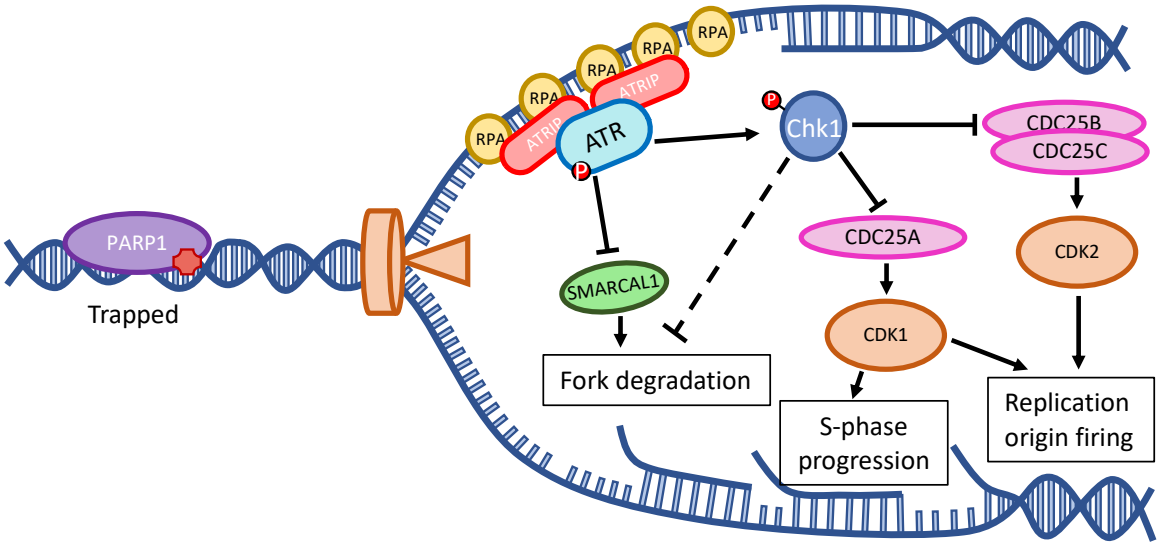

Illustration 3.1 - ATR protects stalled replication forks. When replication forks encounter trapped poly (ADP-ribose) polymerase 1 (PARP1) on chromatin, they stall and expose large sections of single stranded DNA. This is quickly coated by replication protein A (RPA), which recruits ataxia telangiectasia mutated and Rad3-related (ATR) through ATR interacting protein (ATRIP). ATR phosphorylates checkpoint kinase 1 (Chk1) which triggers intra-S phase arrest and inhibits aberrant replication origin initiation through the CDC25-CDK1/2 pathway. Separately, ATR protects the replication fork from degradation through SMARCAL1 and potentially through a second Chk1-mediated pathway.

CHAPTER 4:

Future Directions

The concluding volume of Robert Jordan's epic fantasy series, The Wheel of Time, ends with this message: "This wind, it was not the ending. There are no endings, and never will be, to the turning of the Wheel of Time. But it was an ending." So too with any graduation, publication, or presentation in the scientific world. While we may tie our findings and advancements into neat stories for presentation to our peers and adjudicators, the truth is that these conclusions are imposed on the tale of scientific discovery, and more is left to be done than could be pursued in a lifetime. Personally, as the time has come for me to defend my thesis and return to my clinical studies in the medical school, I am filled with more questions than ever and excited to see how they will be explored in the future.

4.1 Continued exploration of PARP trapping

In this work we have demonstrated that the radiosensitization achieved by PARP inhibitors in HR competent pancreatic cancer models cannot be explained solely by their enzymatic inhibition actions. The disconnection between enzymatic inhibition and radiosensitization became very clear when looking at concentration response curves for the three different PARP inhibitors. However, part of our inference relied on the trapping

potencies for these agents previously described in the literature by other groups. Olaparib reaches an approximate trapping IC50 at 3uM and talazoparib at 50nM, while Veliparib only begins to demonstrate trapping properties at 30uM [208]. Our work would benefit from the establishment of these properties in our own hands and in our own cell lines. One barrier has been the need to handle multiple samples in the same experiment in order to generate these curves and we hope that we will be able to surmount this in the future using the recently-adapted PLA.

In a similar vein, full characterization of two representative cell lines' (MiaPaCa2 and Panc1) concentration-dependent response to different PARP inhibitors was illuminating, but similar work could be expanded to remaining cell lines in the pancreatic cancer toolkit. Subtle molecular alterations exist among many of the commonly used PDAC cell line models, as well as major PARP inhibition-relevant alterations as is the case with BRCA2 status in Capan1-neo [230]. Such an expansion would contribute toward affirming our understanding of how PARP inhibitors radiosensitize in pancreatic cancer, and potentially draw out some new and interesting information given the propensity for DDR inhibitors to synergize with transformative mutations [231]. Among the cell lines interrogated for concentration response to PARP inhibitors should be PARP-null and -reconstituted models created by our group.

I feel that among the work done by our group to genetically tease out the difference between enzymatic inhibition and trapping, we have created a clean and informative system using CRISPR-Cas9 technology to delete PARP1 from cells. However, there are several drawbacks to this system. One is the potential for adaptation to the permanent loss of PARP1. By that same token, it affords an opportunity to study PARP1 loss as a

potential mechanism of resistance in HRP cancers, discussed later. Complete deletion also limits the ability to interpret comparisons to drug treatment due to temporal concerns. One recurrent theme of radiosensitization has always been the search for optimal scheduling between administration of drug(s) and radiation - both in the relatively simple system of cell culture, to animal models, and to the clinic [232]. How long does it take to achieve target engagement and inhibition? Should the target be engaged during radiation? How long after radiation should we continue therapy to maximize sensitization and minimize toxicity? In the PARP1-null system, enzymatic activity is suppressed prior to treatment all the way through the collection of growing colonies, whereas drug treatments are discontinued upon processing and clonal plating 24 hours following radiation. A system of shRNA under the control of doxycycline would allow for the temporary and reversible knockdown of PARP1 to better replicate schedule-dependent effects of PARP1 enzymatic inhibition.

The confounding effect of increasing concentrations of inhibitor leading both to increased enzymatic inhibition and trapping, albeit with different potencies, has led our comparisons of concentration response to rely heavily on induction. While the ability to cleanly enzymatically inhibit without trapping through genetic deletion has represented an improvement in mechanistic dissection, we have yet to demonstrate trapping in the absence of enzymatic inhibition. Such deduction has so far been beyond the capabilities of our current tools. A study by Steffen *et al*. discovered two mutations in PARP1, W318R and E988A, that impaired catalytic activity and delayed release from chromatin in the presence of NAD^+ [233]. A recent study by Pettit *et al*. using CRISPR-Cas9 to screen for mutations causing PARP inhibitor resistance reported finding mutants with similar

properties [210]. These mutations occurred outside the zinc finger binding domains and did not affect PARP1 recruitment to chromatin. A focused effort to uncover more mutants with decreased chromatin dissociation could yield a tool to genetically induce trapped PARP at sites of DNA damage while still preserving PARP1 enzymatic function in the background of PARP1*wt* cells.

The biology of trapping in the context of radiation warrants further investigation. The phenotypic evidence for trapping with radiation is abundant, impacting radiosensitivity, DNA damage, and cell cycle. However, biochemical assessment of PARP1-DNA complexes remains elusive. Some have suggested that DNA lesions following radiation are not suitable for trapping, yet the cellular effects can be readily observed. As noted in Chapter 2, PARP trapping following radiation by chromatin fractionation was most readily detected 24 hours after RT. This result is surprising given the understanding of PARP1 as a rapidly-recruited mediator of the DDR. Does the potentiation of damage late after irradiation observed by γH2AX and comet assay recruit PARP1 to chromatin? The expansion of our tools to observe trapped PARP may assist in clarifying these questions. Real-time observation of PARP1 and PAR binding domain constructs to sites of damage using a modified version the laser microirradiation assay would provide valuable information about the timing of events in the formation and dissociation of PARP1-DNA complexes after radiation that could significantly inform treatment schedules.

The development of the PLA assay to measure trapped PARP *in situ* has applications beyond answering questions posed by our current study. We hope to further optimize the assay to interrogate fixed tissue slices. In the laboratory, this will allow us to consider the *in vivo* efficacy of different PARP inhibitor doses with respect to trapping in

tumors in mice. Further, it provides us with a model to study the contribution of PARP trapping to clinically described dose limiting toxicities. We will be able to assay for trapping in bone marrow, intestine, skin, and other organs in the context of animal models.

If, as we have suggested in this work, trapping is necessary for the productive radiosensitization of HRP pancreatic cancers, the ability to assay for trapping in fixed tissues will afford us the opportunity to monitor whether we are reaching therapeutic concentrations and "hitting the target" in patients treated with PARP inhibitors. Information provided from patient tissues treated with PARP inhibitors has the opportunity to inform our understanding of the biology of PARP inhibition. Patients enrolled in trials combining veliparib with radiation have experienced hematologic toxicity [234], radiation dermatitis [235], and nausea and vomiting [235], [236]. Despite veliparib's described inability to stabilize DNA-PARP complexes, these events fit the profile of trapping-induced cytotoxicity. Molecular interrogation in these cases may reveal unknown factors that modulate the trapping potential of PARP inhibitors.

Perhaps the most intriguing outstanding question posed by the work presented here remains the exact relationship between the treatments we have investigated and replication fork progression. We began our study with the hypothesis that trapped PARP1 created an impediment to replication forks, which caused stalling and collapse. These forks relied on ATR for stabilization and restart. Combined inhibition, therefore, would lead to persistent DNA damage and increased radiosensitization. Several lines of evidence supported this reasoning: DNA damage caused by PARP inhibitors is most pronounced during the S-phase of the cell cycle [237], trapping concentrations induce markers of replication stress (**Figure 3.5e**), and stabilization of replication forks leads to

PARP inhibitor resistance (discussed in section 4.3). However, this model was challenged by a study by Bartek *et al*. in which they discovered that PARP inhibition seemed to speed, not slow, replication forks, and that it did not lead to fork stalling or collapse [220]. They proposed a model in which cellular PARylation leads to p53 transactivation of p21, which acts to suppress replication forks. They show that PARP inhibition releases this inhibition, leading to increased replication fork velocity, which in turn generates single stranded but not double stranded DNA damage.

We have also observed that PARP inhibition increases replication fork velocity, but several of our observations are not consistent with their model. We only observe the effect on fork velocity at trapping concentrations of olaparib (**Figure 3.5d**). The data presented by Bartek's group also indicate that the effects on replication fork velocity are induced under trapping conditions, suggesting that they are not due simply to changes in cellular PARylation. Additionally, our observations were made in a p53 mutant system, leading us to conclude that the effect must be p53-independent. Finally, we observed that the addition of an ATR inhibitor slows replication fork speed while increasing DNA damage; if replication fork speed were causative of olaparib-induced damage, AZD6738-induced fork slowing should attenuate DNA damage.

We propose an alternative model in which increased replication fork velocity is a downstream consequence of olaparib-induced replication stress and DNA damage (**Illustration 4.1**). ATR is activated by the replication stress, which prevents origin firing through Chk1. Origin number and velocity have a reciprocal relationship, acting to speed up the origins that do initiate. This hypothesis is supported by the frequent observation that PARP inhibition slows S-phase progression and the overall rate of DNA replication.

Combining this effect with ATR inhibition disinhibits aberrant replication origins, massively slowing down fork progression, while still increasing DNA damage.

How does the PARP trapping lesion generate replication stress and DNA damage to begin this cascade? Our data do not suggest a clear answer. Bartek *et al*. show that PARP inhibition does not lead to fork stalling or collapse, measured by asymmetry of symmetric origins with the DNA fiber combing technique. However, they also did not induce concomitant DNA damage through radiation or genotoxins. It has been demonstrated that different DNA damaging agents have strikingly different effects on fork slowing and asymmetry [238]. It is possible that without the addition of ionizing radiation, PARP trapping does not cause appreciable replication fork stalling and collapse, and leads to milder DNA damage in the form of SSBs. Our experiments with radiation were able to produce significant elevation in DSBs. While we also did not observe replication fork asymmetry, we only measured 24 hours after radiation. At this time point, all cells in the population have cycled through S-phase at least once. One plausible hypothesis is that the deleterious effects of olaparib and radiation on replication forks are limited to the first S-phase after radiation. Any cells still cycling 24 hours later will display the effects of olaparib alone, which are milder. Therefore, the optimal window to assay for fork asymmetry would be 2-4 hours following radiation. Further investigation will bring us closer to understanding the mechanistic significance of trapped PARP versus enzymatic inhibition.

4.2 PARP2 and PARP3

The primacy of PARP1 in the cellular environment and DNA damage response has led to an overwhelming focus on it as the therapeutically relevant target of PARP inhibitors. In reality, however, all clinically investigated PARP inhibitors also inhibit PARP2, and olaparib, talazoparib, and rucaparib also inhibit PARP3 with varying potencies [239], [240]. Indeed, observations in our own work not shown here demonstrate that these other family members may play significant roles in the absence of PARP1. In our PARP1-null model, after multiple passages in culture the level of cellular PARylation returned to that seen in Cas9 control cells, with no indication of a reversion mutation or presence of the protein. These levels of PAR were sensitive to treatment with olaparib, suggesting that PARP2 or PARP3 could increase in abundance and/or activity in the absence of PARP1 protein. However, due to limitations of time and availability of quality detection reagents we were not able to pursue this line of inquiry.

Structurally, PARP2 and PARP3 share ~60% amino acid sequence homology with PARP1 [241]. Both feature the C-terminal WRG and catalytic domains of PARP1, but differ in their shorter N-termini, which lack DNA binding ZF and autoregulatory BRCT domains. Rather they display preferential activation by 5' phosphorylated DNA ends, suggesting a more limited role in backbone repair [242], [243].

The importance of PARP2 in the DNA damage response is underscored by its upregulation in response to DNA damaging agents [244], [245]. It has been shown to cooperate with PARP1 in response to SSB lesions [246], [247] and genomic and replication stability [149], [248]. PARP2 also assists in the recruitment of APLF to chromatin through PARP1-dependent branch chain formation at damage sites [249].

On its own, there is evidence that PARP2 function contributes to the DSB repair pathway choice [250]. The question of why cells choose to repair certain lesions by NHEJ or HR is one for which many mediators and signaling events have unsatisfyingly benn described but not answered. Does the cell know that a lesion has taken place in the middle of nowhere and can be repaired “quick and dirty” simply to ensure the integrity of the molecule, or if it has taken place among highly sensitive genetic material that merits time and attention from HR machinery? The work by Fouquin *et al*. demonstrates that PARP2 prevents the accumulation of 53BP1 at sites of DNA damage, allowing strand resection by CtIP and progression of homology directed repair. As veliparib had no effect on this process, they concluded that this function of PARP2 was independent of its PARylation. Crucially, though, it has been demonstrated that PARP2 can be trapped on chromatin like PARP1 [194], and it will be illuminating to see if this pathway choice can be disrupted through the inhibition of PARP2 with a stronger trapper such as olaparib or talazoparib.

A recent study also demonstrated that PARP2 facilitates androgen receptor (AR) signaling in prostate cancer through interaction with FOXA1 [251]. PARP2 levels are elevated in prostate cancer relative to normal tissue, and even further in castration resistant prostate cancer (CRPC), where the AR signaling pathway frequently employs mutations and truncations to evade inhibition by antiandrogens. If these results remain robust in more prostate cancer models, this could represent an exciting new therapeutic opportunity, especially considering the frequent activation of FOXA1 signaling [252].

PARP3 has been less extensively studied than PARP1 and PARP2. Nevertheless, it has been ascribed some functions in the DNA damage response, and its loss promotes

sensitivity to chemotherapeutic drugs [253]. Interestingly, PARP3 seems to promote NHEJ pathway choice by promoting the accumulation and activity of APLF [254], [255] and ADP-ribosylation of Ku80 [256]. Taken together with the pathway choice actions of PARP2, these studies suggest that we may be able to pharmacologically tip genomic repair toward HR or NHEJ through our choice of PARP inhibitor, to say nothing of future developments in pharmacology that target these other PARPs even more specifically.

4.3 PARP inhibitor resistance

The genomic and mutational instability hallmark of cancer [28] means that cancer cells are quick to adapt to selective pressures. These advances can be difficult to anticipate at the bench because the classic tools we use to model malignancy often fail to capture the heterogeneity of mutational landscapes within patients' tumors. In cancer treatment, this fluidity frequently leads to treatment failure in the form of acquired resistance. Broadly, there are four categories of PARP inhibitor resistance that have been observed in the laboratory or the clinic: reversion to HR proficiency, alterations in the target, replication fork stabilization, and increased drug efflux.

The upregulation of ATP-binding cassette transporters is a common and nonspecific form of drug resistance for many therapies. Specifically for PARP inhibitors, the upregulation of P-glycoprotein transporter was modeled as a mechanism of acquired resistance in murine models of olaparib resistance [257], [258]. However, affinity for the transporter varies among inhibitors [259], and is especially low for recently developed agent AZD2461 [260]. Vigilance for this mechanism of resistance would allow for the seamless transition between agents if the need should arise clinically.

Overwhelmingly, the cancers displaying acquired resistance to PARP inhibition in the clinic have done so through reacquisition of proficient homologous recombination. As discussed previously, tumors deficient in HR are exquisitely sensitive to PARP inhibition. The major mutations conferring HR deficiency were first described as inactivating mutations in the BRCA1 and BRCA2 genes. Correspondingly, secondary mutations restoring functionality have been seen in these genes in breast, ovarian, prostate, and even pancreatic cancers [261]–[266]. Reversion mutations have been observed in other genes that confer “BRCA-ness” such as PALB2 [265], RAD51C and RAD51D [267]. PARPi sensitivity conferred by low expression of BRCA1 in patient derived xenograft models has been overcome in the laboratory through demethylation of the promoter region and re-expression of the protein [268].

One major and surprising method by which BRCA1 mutant cancers subvert their PARPi sensitivity preclinically is through inactivation of the 53BP1 pathway [269]–[271]. While the exact downstream mediators of its effects are still being illuminated, studies have shown that 53BP1 is involved in the cell’s choice of DSB repair pathway promoting NHEJ in opposition to BRCA1 [272]. Thus, loss of 53BP1 resulted in rescue of DNA end resection and partial restoration of HR [269], [270].

While restoration of homologous recombination in previously deficient cancers clearly reduces sensitivity to PARP inhibition, one could argue with the characterization of this state as entirely resistant. As we and others have demonstrated, opportunities abound for treatment of HRP cancers with PARP inhibitors, albeit with a narrower therapeutic window and rarely as a monotherapy. To harness the full potential of these treatments, though, drug selection and dosage must be adjusted to harness trapping

potential in combination with radiation or other targeted agents. In fact, these cancers may have provided us with one small advantage; in restoring HR they have improved their genetic integrity and given up some of the very plasticity that lent them malignancy in the first place.

Beside reversion mutations that confer HR, the only other mechanism of acquired PARPi resistance observed so far clinically was a mutation in the WRG domain of PARP1 leading to decreased trapping capability [210]. The study by Pettit *et al*. used CRISPR-Cas9 mutagenesis to further screen for other PARP1 mutations that would confer resistance to talazoparib. They found that mutations in the zinc finger domain attenuated the ability of PARP1 to localize to DNA and decreased sensitivity to talazoparib. Other mutations discovered in their screen were mapped to residues observed to interact with DNA binding domains. Their observation bolsters the hypothesis that PARP inhibitor cytotoxicity is mediated by trapping in the setting of HR proficiency and that in these cancers PARP1 mutation, downregulation, or genetic loss could be a major mechanism of resistance [194], [210], [273], [274].

It has also been demonstrated that cellular PARylation can be rescued by the loss of PAR glycohydrolase (PARG), the enzyme that depolymerizes chains of PAR [275]. Even in the absence of HR restoration and presence of PARP inhibition, the amplification of residual PARP1 activity by PARG loss was sufficient to transform these cells to a resistant phenotype. However, this very adaptation rendered cells sensitive to temozolomide due to increased PARP1 retention on chromatin and the induction of trapping. While PARG loss has been observed in treatment-naive breast and ovarian

cancers [275], it remains to be seen whether it will lead to PARP inhibitor resistance clinically.

Recent studies have proposed several mechanisms by which PARP inhibitor resistance derives from alterations in the response to replication stress. Loss of PTIP was shown to rescue stalled replication forks from MRE11-mediated degradation following PARP inhibition [276]. Similar protection of replication fork stability was promoted by EZH2 loss or inhibition, disrupting its ability to recruit MUS81 nuclease to stalled forks. Another study demonstrated that lethal replication fork block induced by PARPi is mediated by SLFN11 [277]. Absence of SLFN11 promotes productive completion of replication an entry into G2.

However, while these mutations protect cells from PARP inhibition, they allow replication to proceed under stress, presenting a therapeutic opportunity. Work has already shown that resistance arising from fork protection can be overcome with the addition of an ATR inhibitor [278], [279], consistent with its role as a master regulator of the response to replication stress [223]. These results are encouraging for the combination of PARP and ATR inhibitors in other settings both as a demonstration of induced sensitivity and in anticipation of treatment failure. However, the difference in how ATR inhibition can sensitize HRD cells in the context of replication fork stabilization and inherently resistant HRP cells to PARP inhibition offers a window into their biology. The necessity for PARP trapping for combined sensitivity in HRP cells suggests that cellular context may determine the type of DNA lesion for which ATR directs productive repair.

4.4 Immunomodulation and the DNA damage response

It does not receive a mention in this work until now, but the DDR including PARP and ATR, have important immune modulatory functions that are further enhanced by radiation as a therapy. Indeed, immunotherapy has become so ubiquitous that during the preparation of this thesis, I heard an advertisement on NPR from the Dana Farber Cancer Institute touting the availability of PD-L1 inhibition at their center. To provide a perspective on all of immunotherapy would be its own manuscript and well beyond the scope of our focus here (see review by Ribas *et al*. [280]). Instead, I will provide some context for the use of immunotherapy with radiation and the ways it may be employed with other inhibitors of the DNA damage response.

Even without pharmacologic manipulation, there are many ways in which radiation has been described to dovetail with the immune system. The first of these involves several effects that render the tumor more visible to immune surveillance by the host. It has been demonstrated that radiation can facilitate the generation and release of neoantigens from tumors ([281], [282]). Presentation of these antigens is also enhanced by an upregulation of MHC class I molecules on the tumor surface after radiation[283], [284], counteracting a common mechanism of immune evasion.

Radiation is also known to activate the innate immune response through its induction of Type I interferon via the cGAS-STING pathway [285]. Radiation induces the release of nuclear DNA in the cytosol and formation of micronuclei [286], [287], which in turn triggers the viral pattern recognition receptor responses and the production of type I interferons. Inside the cell, radiation has also been demonstrated to increase immune checkpoint proteins [284] and has even been suggested to involve DNA DSB signaling from

ATM/ATR [288]. These effects can be observed in the clinical setting by the induction of anti-tumor responses outside the treatment field of locoregional radiation [289]–[291].

These factors have combined to generate interest in whether immune modulation could be used to sensitize cancers to radiation. The most common of these therapies is immune checkpoint blockade (ICB). Proteins mediating immune checkpoints function physiologically to dampen the immune response and protect the normal tissues of the body from attack by T cells and NK cells. Among the earliest of these to be targeted was cytotoxic T-lymphocyte associated protein 4 (CTLA-4), whose inhibitory antibody ipilimumab was approved for use in metastatic melanoma in 2011 [292]. Two other major targets major targets were quickly discovered: programmed cell death 1 (PD-1) and its ligand PD-L1. Antibodies inhibiting PD-1 were first approved by the FDA in 2014 (Pembrolizumab and nivolumab) and PD-L1 in 2016 (Atezolizumab) and 2017 (Avelumab and Durvalumab) (reviewed in [293]).

Anti-tumoral activity can be readily appreciated in the combination of immune blockade and radiation. A study by Dewan *et al*. showed that the addition of CTLA-4 blockade synergized with radiation at the primary tumor site and induced an abscopal effect outside the radiation field [294]. Similarly, anti-PD-1 and anti-PD-L1 therapy were shown to combine with radiation for increased response [295], [296]. Promising results have also been delivered by combining inhibitors of both major ICB pathways with radiation [297], overcoming T-cell exhaustion by PD-L1 upregulation as a mechanism of resistance to CTLA-4 therapy.

In addition to the immune stimulatory effects of radiation discussed briefly above, there is evidence that sensitization by these modalities could operate in both directions.

ICB agents have been demonstrated to help modulate the tumor microenvironment by increasing tumor vascularity and perfusion [298], [299], which in turn could combat the radioprotective effects of hypoxia [300], [301].

A growing body of evidence suggests that improvement in the efficacy of immuno-radiotherapy through the addition of targeted DNA damage response inhibitors may represent the next frontier of therapy. Consistent with the findings described above implicating DNA DSB pathway proteins in the regulation of immune modulatory proteins, studies have found that ATR inhibition possesses inherent immunostimulatory effects. Treatment with ATRi reduces PD-L1 expression and enhanced anti-tumor T cell activity [302], [303]. In combination with radiation, it has also been found to increase the immunostimulatory effects of radiation alone described above, including immune cell infiltration, innate immune recognition of cytoplasmic DNA, and increased antigen processing and presentation [304]. Dillon *et al*. attribute many of these findings to increased DNA damage, though our own findings suggest that ATR inhibition alone may only modestly increase damage. The addition of a PARP inhibitor may further potentiate this effect. The addition of targeted checkpoint blockade to the intrinsic activity of ATRi could deliver vast benefits due to the non-redundant checkpoint pathways [297].

The overlapping but separate functions of ATM make it an intriguing avenue for further investigation into the DDR master regulator inhibition as a combination with radiation. A study from our group recently demonstrated the efficacy of ATM inhibition to induce the innate immune response and sensitize to anti-PD-L1 therapy [305].

On its own, PARP inhibition was demonstrated to upregulate PD-L1 expression in cell culture models and sensitized murine tumors to PD-L1 inhibition *in vivo* [306]. A single

arm clinical trial assessing the combination of niraparib and pembrolizumab demonstrated high response rates regardless of BRCA status [307].

Further investigation is warranted into the combination of targeting the DNA damage response and immune checkpoint inhibition. On its own, elevated DNA damage by the combination of ATR and PARP inhibition with radiation has the potential to potentiate the immunostimulatory effects of ATR inhibition alone. Given the contrasting effects of ATRi and PARPi on PD-L1 expression in previous studies it will be important to determine the dominant phenotype of this effect when they are combined. Studies with radiation suggest ATR inhibition will act to counteract the effect of PARPi-mediated PD-L1 upregulation. Finally, we will determine whether the addition of immune checkpoint blockade will potentiate the radiosensitizing effects of combined ATR/PARP inhibition with radiation.

Broadly, the rapid development of immunomodulating therapies has opened up new and exciting avenues of investigation for those of us who have studied the DNA damage response. As we learn more about the involvement of the DNA damage response in modulating immune surveillance in cancer, our hard-won knowledge about these pathways in the setting of radiation will be ready-made to apply for the benefit of our patients.

Illustration 4.1

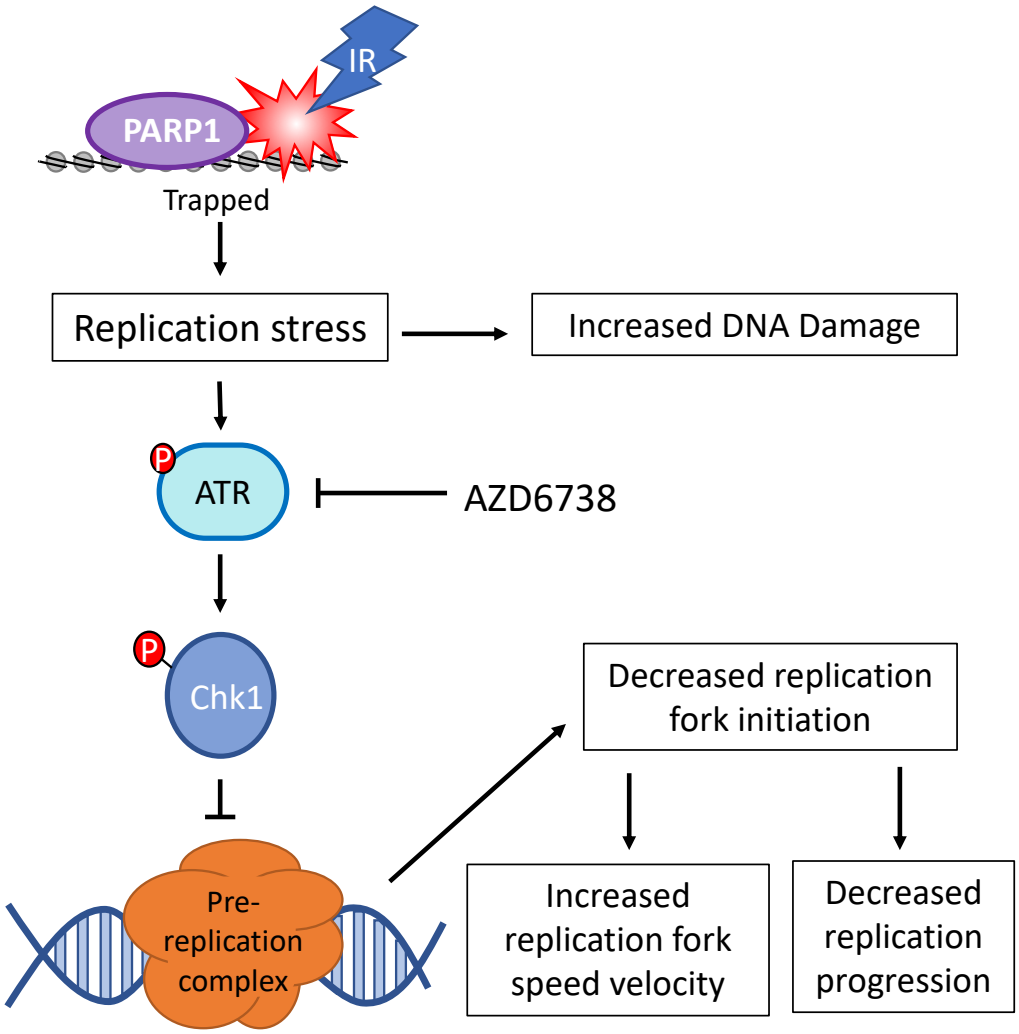

Illustration 4.1 - Proposed model of how PARP trapping leads to changes in replication fork velocity. In response to the combination of ionizing radiation (IR) and talazoparib or micromolar olaparib, poly (ADP-ribose) polymerase 1 (PARP1) becomes trapped on DNA. This PARP1-DNA complex leads to replication stress (RS), which is converted to increased DNA damage. Ataxia telangiectasia mutated and Rad3-related (ATR) is activated by RS and phosphorylates activates checkpoint kinase 1 (Chk1). Chk1 acts on pre-replication complexes to inhibit the initiation of aberrant replication origins. Fewer active origins of replication decreases overall DNA replication speed but reciprocally increases the velocity of replication forks that do fire. ATR inhibition by AZD6738 disinhibits pre-replication complexes and leads to decreased replication fork velocity.

REFERENCES

[1] J. Kleeff *et al.*, “Pancreatic cancer.,” *Nat. Rev. Dis. Prim.*, vol. 2, p. 16022, Apr. 2016.

[2] R. L. Siegel, K. D. Miller, and A. Jemal, “Cancer statistics, 2018.,” *CA. Cancer J. Clin.*, vol. 68, no. 1, pp. 7–30, Jan. 2018.

[3] J. He *et al.*, “2564 resected periampullary adenocarcinomas at a single institution: trends over three decades.,” *HPB (Oxford).*, vol. 16, no. 1, pp. 83–90, Jan. 2014.

[4] B. Zhou *et al.*, “Early detection of pancreatic cancer: Where are we now and where are we going?,” *Int. J. cancer*, vol. 141, no. 2, pp. 231–241, Jul. 2017.

[5] N. B. Merchant, “Eat When You Can, Sleep When You Can, and Don’t Mess with the Pancreas,” *Surg. Oncol. Clin.*, vol. 25, no. 2, pp. xv–xvi, Apr. 2016.

[6] C. Hu *et al.*, “Association Between Inherited Germline Mutations in Cancer Predisposition Genes and Risk of Pancreatic Cancer.,” *JAMA*, vol. 319, no. 23, pp. 2401–2409, Jun. 2018.

[7] B. J. Raphael *et al.*, “Integrated Genomic Characterization of Pancreatic Ductal Adenocarcinoma,” *Cancer Cell*, vol. 32, no. 2, pp. 185-203.e13, Aug. 2017.

[8] S. Jones *et al.*, “Core signaling pathways in human pancreatic cancers revealed by global genomic analyses.,” *Science*, vol. 321, no. 5897, pp. 1801–6, Sep. 2008.

[9] A. V Biankin *et al.*, “Pancreatic cancer genomes reveal aberrations in axon guidance pathway genes.,” *Nature*, vol. 491, no. 7424, pp. 399–405, Nov. 2012.

[10] N. Waddell *et al.*, “Whole genomes redefine the mutational landscape of pancreatic cancer.,” *Nature*, vol. 518, no. 7540, pp. 495–501, Feb. 2015.

[11] A. K. Witkiewicz *et al.*, “Whole-exome sequencing of pancreatic cancer defines genetic diversity and therapeutic targets.,” *Nat. Commun.*, vol. 6, p. 6744, Apr. 2015.

[12] P. Bailey *et al.*, “Genomic analyses identify molecular subtypes of pancreatic cancer,” *Nature*, vol. 531, no. 7592, pp. 47–52, Mar. 2016.

[13] Cancer Genome Atlas Research Network. Electronic address: andrew_aguirre@dfci.harvard.edu and Cancer Genome Atlas Research Network, “Integrated Genomic Characterization of Pancreatic Ductal Adenocarcinoma.,”

Cancer Cell, vol. 32, no. 2, pp. 185-203.e13, 2017.

[14] S. K. Dougan, “The Pancreatic Cancer Microenvironment.,” *Cancer J.*, vol. 23, no. 6, pp. 321–325.

[15] K. C. Valkenburg, A. E. de Groot, and K. J. Pienta, “Targeting the tumour stroma to improve cancer therapy,” *Nat. Rev. Clin. Oncol.*, vol. 15, no. 6, pp. 366–381, Jun. 2018.

[16] M. Binnewies *et al.*, “Understanding the tumor immune microenvironment (TIME) for effective therapy,” *Nat. Med.*, vol. 24, no. 5, pp. 541–550, May 2018.

[17] X. Chen and E. Song, “Turning foes to friends: targeting cancer-associated fibroblasts,” *Nat. Rev. DRUG Discov.*, vol. 18, no. 2, pp. 99–115, Feb. 2019.

[18] T. A. Sohn *et al.*, “Resected adenocarcinoma of the pancreas-616 patients: results, outcomes, and prognostic indicators.,” *J. Gastrointest. Surg.*, vol. 4, no. 6, pp. 567–579, 2000.

[19] A. Teague, K.-H. Lim, and A. Wang-Gillam, “Advanced pancreatic adenocarcinoma: a review of current treatment strategies and developing therapies.,” *Ther. Adv. Med. Oncol.*, vol. 7, no. 2, pp. 68–84, Mar. 2015.

[20] T. Conroy *et al.*, “FOLFIRINOX versus gemcitabine for metastatic pancreatic cancer,” *N. Engl. J. Med.*, vol. 364, no. 19, pp. 1817–1825, May 2011.

[21] S. Gourgou-Bourgade *et al.*, “Impact of FOLFIRINOX compared with gemcitabine on quality of life in patients with metastatic pancreatic cancer: Results from the PRODIGE 4/ACCORD 11 randomized trial,” *J. Clin. Oncol.*, vol. 31, no. 1, pp. 23–29, Jan. 2013.

[22] D. D. Von Hoff *et al.*, “Increased survival in pancreatic cancer with nab-paclitaxel plus gemcitabine,” *N. Engl. J. Med.*, vol. 369, no. 18, pp. 1691–1703, 2013.

[23] P. Hammel *et al.*, “Phase II LAPACT trial of nab-paclitaxel (nab-P) plus gemcitabine (G) for patients with locally advanced pancreatic cancer (LAPC).,” *J. Clin. Oncol.*, vol. 36, no. 4_suppl, p. 204, 2018.

[24] P. Hammel *et al.*, “Effect of chemoradiotherapy vs chemotherapy on survival in patients with locally advanced pancreatic cancer controlled after 4 months of gemcitabine with or without erlotinib the LAP07 randomized clinical trial,” *JAMA - J. Am. Med. Assoc.*, vol. 315, no. 17, pp. 1844–1853, May 2016.

[25] P. J. Loehrer *et al.*, “Gemcitabine alone versus gemcitabine plus radiotherapy in patients with locally advanced pancreatic cancer: An Eastern Cooperative Oncology Group trial,” *J. Clin. Oncol.*, vol. 29, no. 31, pp. 4105–4112, Nov. 2011.

[26] C. A. Lacobuzio-Donahue *et al.*, “DPC4 gene status of the primary carcinoma correlates with patterns of failure in patients with pancreatic cancer,” *J. Clin. Oncol.*, vol. 27, no. 11, pp. 1806–1813, Apr. 2009.

[27] D. Hanahan and R. A. Weinberg, “The hallmarks of cancer,” *Cell*, vol. 100, no. 1.

pp. 57–70, 07-Jan-2000.

[28] D. Hanahan and R. A. Weinberg, “Hallmarks of cancer: The next generation,” *Cell*, vol. 144, no. 5. pp. 646–674, 04-Mar-2011.

[29] M. A. Morgan and T. S. Lawrence, “Molecular pathways: Overcoming radiation resistance by targeting DNA damage response pathways,” *Clin. Cancer Res.*, vol. 21, no. 13, pp. 2898–2904, Jul. 2015.

[30] G. Iliakis, “The role of DNA double strand breaks in ionizing radiation-induced killing of eukaryotic cells.,” *Bioessays*, vol. 13, no. 12, pp. 641–8, Dec. 1991.

[31] R. Dueva and G. Iliakis, “Alternative pathways of non-homologous end joining (NHEJ) in genomic instability and cancer,” *Transl. Cancer Res.*, vol. 2, no. 3, pp. 163–177, 2013.

[32] M. LEVINE, “The action of colchicine on cell division in human cancer, animal, and plant tissues.,” *Ann. N. Y. Acad. Sci.*, vol. 51, no. 8, pp. 1365–408, Mar. 1951.

[33] H. E. Skipper, J. B. Chapman, and M. Bell, “The anti-leukemic action of combinations of certain known anti-leukemic agents.,” *Cancer Res.*, vol. 11, no. 2, pp. 109–12, Feb. 1951.

[34] C. Heidelberger *et al.*, “Studies on fluorinated pyrimidines. II. Effects on transplanted tumors.,” *Cancer Res.*, vol. 18, no. 3, pp. 305–17, Apr. 1958.

[35] D. S. Childs, C. G. Moertel, M. A. Holbrook, R. J. Reitemeier, and M. Colby, “Treatment of unresectable adenocarcinomas of the stomach with a combination of 5-fluorouracil and radiation.,” *Am. J. Roentgenol. Radium Ther. Nucl. Med.*, vol. 102, no. 3, pp. 541–4, Mar. 1968.

[36] C. G. Moertel, D. S. Childs, R. J. Reitemeier, M. Y. Colby, and M. A. Holbrook, “Combined 5-fluorouracil and supervoltage radiation therapy of locally unresectable gastrointestinal cancer.,” *Lancet (London, England)*, vol. 2, no. 7626, pp. 865–7, Oct. 1969.

[37] C. G. Moertel *et al.*, “Therapy of locally unresectable pancreatic carcinoma: A randomized comparison of high dose (6000 rads) radiation alone, moderate dose radiation (4000 rads + 5-fluorouracil), and high dose radiation + 5-fluorouracil. The gastrointestinal tumor study group,” *Cancer*, vol. 48, no. 8, pp. 1705–1710, 1981.

[38] M. H. Kalser and S. S. Ellenberg, “Pancreatic cancer. Adjuvant combined radiation and chemotherapy following curative resection.,” *Arch. Surg.*, vol. 120, no. 8, pp. 899–903, Aug. 1985.

[39] J. P. Hoffman *et al.*, “A pilot study of preoperative chemoradiation for patients with localized adenocarcinoma of the pancreas.,” *Am. J. Surg.*, vol. 169, no. 1, pp. 71–7; discussion 77-8, Jan. 1995.

[40] T. S. Lawrence, E. Y. Chang, T. M. Hahn, L. W. Hertel, and D. S. Shewach, “Radiosensitization of pancreatic cancer cells by 2’,2’-difluoro-2’-deoxycytidine.,” *Int. J. Radiat. Oncol. Biol. Phys.*, vol. 34, no. 4, pp. 867–72, Mar. 1996.

[41] D. S. Shewach and T. S. Lawrence, “Gemcitabine and radiosensitization in human tumor cells.,” *Invest. New Drugs*, vol. 14, no. 3, pp. 257–63, 1996.

[42] C. H. Crane *et al.*, “Is the therapeutic index better with gemcitabine-based chemoradiation than with 5-fluorouracil-based chemoradiation in locally advanced pancreatic cancer?,” *Int. J. Radiat. Oncol. Biol. Phys.*, vol. 52, no. 5, pp. 1293–302, Apr. 2002.

[43] Z. H. Siddik, “Cisplatin: mode of cytotoxic action and molecular basis of resistance.,” *Oncogene*, vol. 22, no. 47, pp. 7265–79, Oct. 2003.

[44] H. J. Boeckman, K. S. Trego, and J. J. Turchi, “Cisplatin sensitizes cancer cells to ionizing radiation via inhibition of nonhomologous end joining.,” *Mol. Cancer Res.*, vol. 3, no. 5, pp. 277–85, May 2005.

[45] C. R. Sears and J. J. Turchi, “Complex cisplatin-double strand break (DSB) lesions directly impair cellular non-homologous end-joining (NHEJ) independent of downstream damage response (DDR) pathways,” *J. Biol. Chem.*, vol. 287, no. 29, pp. 24263–24272, Jul. 2012.

[46] W. J. Kil *et al.*, “In vitro and in vivo radiosensitization induced by the DNA methylating agent temozolomide.,” *Clin. Cancer Res.*, vol. 14, no. 3, pp. 931–8, Feb. 2008.

[47] A. Chakravarti *et al.*, “Temozolomide-mediated radiation enhancement in glioblastoma: a report on underlying mechanisms.,” *Clin. Cancer Res.*, vol. 12, no. 15, pp. 4738–4746, Aug. 2006.

[48] C. J. McGinn, D. S. Shewach, and T. S. Lawrence, “Radiosensitizing nucleosides.,” *J. Natl. Cancer Inst.*, vol. 88, no. 17, pp. 1193–203, Sep. 1996.

[49] P. Groth, M. L. Orta, I. Elvers, M. M. Majumder, A. Lagerqvist, and T. Helleday, “Homologous recombination repairs secondary replication induced DNA double-strand breaks after ionizing radiation.,” *Nucleic Acids Res.*, vol. 40, no. 14, pp. 6585–94, Aug. 2012.

[50] Y. Liu, G. Vidanes, Y. C. Lin, S. Mori, and W. Siede, “Characterization of a Saccharomyces cerevisiae homologue of Schizosaccharomyces pombe Chk1 involved in DNA-damage-induced M-phase arrest.,” *Mol. Gen. Genet.*, vol. 262, no. 6, pp. 1132–46, Jan. 2000.

[51] L. Busino, M. Chiesa, G. F. Draetta, and M. Donzelli, “Cdc25A phosphatase: combinatorial phosphorylation, ubiquitylation and proteolysis.,” *Oncogene*, vol. 23, no. 11, pp. 2050–6, Mar. 2004.

[52] C. Y. Peng, P. R. Graves, R. S. Thoma, Z. Wu, A. S. Shaw, and H. Piwnica-Worms, “Mitotic and G2 checkpoint control: Regulation of 14-3-3 protein binding by phosphorylation of Cdc25c on serine-216,” *Science (80-.).*, vol. 277, no. 5331, pp. 1501–1505, Sep. 1997.

[53] S. J. Elledge, “Cell cycle checkpoints: preventing an identity crisis.,” *Science*, vol. 274, no. 5293, pp. 1664–1672, Dec. 1996.

[54] M. J. O'Connell, J. M. Raleigh, H. M. Verkade, and P. Nurse, "Chk1 is a wee1 kinase in the G2 DNA damage checkpoint inhibiting cdc2 by Y15 phosphorylation.," *EMBO J.*, vol. 16, no. 3, pp. 545–54, Feb. 1997.

[55] J. Lee, A. Kumagai, and W. G. Dunphy, "Positive regulation of Wee1 by Chk1 and 14-3-3 proteins.," *Mol. Biol. Cell*, vol. 12, no. 3, pp. 551–63, Mar. 2001.

[56] C. S. Sorensen *et al.*, "The cell-cycle checkpoint kinase Chk1 is required for mammalian homologous recombination repair.," *Nat. Cell Biol.*, vol. 7, no. 2, pp. 195–201, Feb. 2005.

[57] M. A. Morgan *et al.*, "Mechanism of radiosensitization by the Chk1/2 inhibitor AZD7762 involves abrogation of the G2 checkpoint and inhibition of homologous recombinational DNA repair.," *Cancer Res.*, vol. 70, no. 12, pp. 4972–4981, Jun. 2010.

[58] R. G. Syljuasen *et al.*, "Inhibition of human Chk1 causes increased initiation of DNA replication, phosphorylation of ATR targets, and DNA breakage.," *Mol. Cell. Biol.*, vol. 25, no. 9, pp. 3553–3562, May 2005.

[59] M. A. Morgan, L. A. Parsels, J. D. Parsels, A. K. Mesiwala, J. Maybaum, and T. S. Lawrence, "Role of checkpoint kinase 1 in preventing premature mitosis in response to gemcitabine.," *Cancer Res.*, vol. 65, no. 15, pp. 6835–6842, Aug. 2005.

[60] C. C. Chen, R. D. Kennedy, S. Sidi, A. T. Look, and A. D'Andrea, "CHK1 inhibition as a strategy for targeting Fanconi Anemia (FA) DNA repair pathway deficient tumors.," *Mol. Cancer*, vol. 8, p. 24, Apr. 2009.

[61] J. P. Shen *et al.*, "Chemogenetic profiling identifies RAD17 as synthetically lethal with checkpoint kinase inhibition.," *Oncotarget*, vol. 6, no. 34, pp. 35755–69, Nov. 2015.

[62] K. D. Davies *et al.*, "Chk1 inhibition and Wee1 inhibition combine synergistically to impede cellular proliferation.," *Cancer Biol. Ther.*, vol. 12, no. 9, pp. 788–796, Nov. 2011.

[63] R. T. Bunch and A. Eastman, "Enhancement of cisplatin-induced cytotoxicity by 7-hydroxystaurosporine (UCN-01), a new G2-checkpoint inhibitor.," *Clin. Cancer Res.*, vol. 2, no. 5, pp. 791–797, May 1996.

[64] S. D. Zabludoff *et al.*, "AZD7762, a novel checkpoint kinase inhibitor, drives checkpoint abrogation and potentiates DNA-targeted therapies.," *Mol. Cancer Ther.*, vol. 7, no. 9, pp. 2955–66, Sep. 2008.

[65] A. J. Massey, J. Borgognoni, C. Bentley, N. Foloppe, A. Fiumana, and L. Walmsley, "Context-dependent cell cycle checkpoint abrogation by a novel kinase inhibitor," *PLoS One*, vol. 5, no. 10, 2010.

[66] S. M. Vance *et al.*, "Selective radiosensitization of p53 mutant pancreatic cancer cells by combined inhibition of Chk1 and PARP1," *Cell Cycle*, vol. 10, no. 24, pp. 4321–4329, Dec. 2011.

[67] Z. Ma, G. Yao, B. Zhou, Y. Fan, S. Gao, and X. Feng, “The Chk1 inhibitor AZD7762 sensitises p53 mutant breast cancer cells to radiation in vitro and in vivo.,” *Mol. Med. Rep.*, vol. 6, no. 4, pp. 897–903, Oct. 2012.

[68] C. G. Engelke *et al.*, “Sensitization of pancreatic cancer to chemoradiation by the Chk1 inhibitor MK8776.,” *Clin. Cancer Res.*, vol. 19, no. 16, pp. 4412–21, Aug. 2013.

[69] M. Schmidt, A. Rohe, C. Platzer, A. Najjar, F. Erdmann, and W. Sippl, “Regulation of G2/M transition by inhibition of WEE1 and PKMYT1 Kinases,” *Molecules*, vol. 22, no. 12. MDPI AG, 01-Dec-2017.

[70] K. Katayama, N. Fujita, and T. Tsuruo, “Akt/protein kinase B-dependent phosphorylation and inactivation of WEE1Hu promote cell cycle progression at G2/M transition.,” *Mol. Cell. Biol.*, vol. 25, no. 13, pp. 5725–37, Jul. 2005.

[71] R. Heald, M. McLoughlin, and F. McKeon, “Human wee1 maintains mitotic timing by protecting the nucleus from cytoplasmically activated cdc2 kinase,” *Cell*, vol. 74, no. 3, pp. 463–474, Aug. 1993.

[72] C. J. Squire, J. M. Dickson, I. Ivanovic, and E. N. Baker, “Structure and inhibition of the human cell cycle checkpoint kinase, Wee1A kinase: An atypical tyrosine kinase with a key role in CDK1 regulation,” *Structure*, vol. 13, no. 4, pp. 541–550, 2005.

[73] N. Watanabe *et al.*, “M-phase kinases induce phospho-dependent ubiquitination of somatic Wee1 by SCFbeta-TrCP.,” *Proc. Natl. Acad. Sci. U. S. A.*, vol. 101, no. 13, pp. 4419–24, Mar. 2004.

[74] D. R. Kellogg, “Wee1-dependent mechanisms required for coordination of cell growth and cell division.,” *J. Cell Sci.*, vol. 116, no. Pt 24, pp. 4883–4890, Dec. 2003.

[75] R. Dominguez-Kelly *et al.*, “Wee1 controls genomic stability during replication by regulating the Mus81-Eme1 endonuclease.,” *J. Cell Biol.*, vol. 194, no. 4, pp. 567–579, Aug. 2011.

[76] H. Beck *et al.*, “Cyclin-dependent kinase suppression by WEE1 kinase protects the genome through control of replication initiation and nucleotide consumption.,” *Mol. Cell. Biol.*, vol. 32, no. 20, pp. 4226–36, Oct. 2012.

[77] M. Krajewska *et al.*, “Forced activation of Cdk1 via wee1 inhibition impairs homologous recombination.,” *Oncogene*, vol. 32, no. 24, pp. 3001–8, Jun. 2013.

[78] H. Hirai *et al.*, “Small-molecule inhibition of Wee1 kinase by MK-1775 selectively sensitizes p53-deficient tumor cells to DNA-damaging agents,” *Mol. Cancer Ther.*, vol. 8, no. 11, pp. 2992–3000, Nov. 2009.

[79] H. Hirai *et al.*, “MK-1775, a small molecule Wee1 inhibitor, enhances antitumor efficacy of various DNA-damaging agents, including 5-fluorouracil,” *Cancer Biol. Ther.*, vol. 9, no. 7, pp. 514–522, Apr. 2010.

[80] N. V Rajeshkumar *et al.*, “MK-1775, a potent Wee1 inhibitor, synergizes with gemcitabine to achieve tumor regressions, selectively in p53-deficient pancreatic cancer xenografts.,” *Clin. Cancer Res.*, vol. 17, no. 9, pp. 2799–806, May 2011.

[81] J. M. Kreahling *et al.*, “Wee1 inhibition by MK-1775 leads to tumor inhibition and enhances efficacy of gemcitabine in human sarcomas.,” *PLoS One*, vol. 8, no. 3, p. e57523, 2013.

[82] J. PosthumaDeBoer *et al.*, “WEE1 inhibition sensitizes osteosarcoma to radiotherapy.,” *BMC Cancer*, vol. 11, p. 156, Apr. 2011.

[83] K. A. Bridges *et al.*, “MK-1775, a novel Wee1 kinase inhibitor, radiosensitizes p53-defective human tumor cells.,” *Clin. Cancer Res.*, vol. 17, no. 17, pp. 5638–48, Sep. 2011.

[84] B. Sarcar *et al.*, “Targeting radiation-induced G(2) checkpoint activation with the Wee-1 inhibitor MK-1775 in glioblastoma cell lines.,” *Mol. Cancer Ther.*, vol. 10, no. 12, pp. 2405–14, Dec. 2011.

[85] T. Kausar *et al.*, “Sensitization of Pancreatic Cancers to Gemcitabine Chemoradiation by WEE1 Kinase Inhibition Depends on Homologous Recombination Repair.,” *Neoplasia*, vol. 17, no. 10, pp. 757–66, Oct. 2015.

[86] M. Aarts *et al.*, “Forced mitotic entry of S-phase cells as a therapeutic strategy induced by inhibition of WEE1.,” *Cancer Discov.*, vol. 2, no. 6, pp. 524–539, Jun. 2012.

[87] D. Karnak *et al.*, “Combined inhibition of Wee1 and PARP1/2 for radiosensitization in pancreatic cancer.,” *Clin. Cancer Res.*, vol. 20, no. 19, pp. 5085–96, Oct. 2014.

[88] C.-J. Busch *et al.*, “G2-checkpoint targeting and radiosensitization of HPV/p16-positive HNSCC cells through the inhibition of Chk1 and Wee1.,” *Radiother. Oncol.*, vol. 122, no. 2, pp. 260–266, Feb. 2017.

[89] K. C. Cuneo *et al.*, “Dose Escalation Trial of the Wee1 Inhibitor Adavosertib (AZD1775) in Combination With Gemcitabine and Radiation for Patients With Locally Advanced Pancreatic Cancer.,” *J. Clin. Oncol.*, vol. 37, no. 29, pp. 2643–2650, Oct. 2019.

[90] D. Cortez, S. Guntuku, J. Qin, and S. J. Elledge, “ATR and ATRIP: partners in checkpoint signaling.,” *Science*, vol. 294, no. 5547, pp. 1713–1716, Nov. 2001.

[91] L. Zou and S. J. Elledge, “Sensing DNA damage through ATRIP recognition of RPA-ssDNA complexes.,” *Science*, vol. 300, no. 5625, pp. 1542–1548, Jun. 2003.

[92] C. A. MacDougall, T. S. Byun, C. Van, M. Yee, and K. A. Cimprich, “The structural determinants of checkpoint activation.,” *Genes Dev.*, vol. 21, no. 8, pp. 898–903, Apr. 2007.

[93] H. Gaillard, T. Garcia-Muse, and A. Aguilera, “Replication stress and cancer.,” *Nat. Rev. Cancer*, vol. 15, no. 5, pp. 276–289, May 2015.

[94] A. Kumagai, J. Lee, H. Y. Yoo, and W. G. Dunphy, “TopBP1 activates the ATR-ATRIP complex.,” *Cell*, vol. 124, no. 5, pp. 943–955, Mar. 2006.

[95] D. A. Mordes, G. G. Glick, R. Zhao, and D. Cortez, “TopBP1 activates ATR through ATRIP and a PIKK regulatory domain.,” *Genes Dev.*, vol. 22, no. 11, pp. 1478–1489, Jun. 2008.

[96] T. E. Bass *et al.*, “ETAA1 acts at stalled replication forks to maintain genome integrity.,” *Nat. Cell Biol.*, vol. 18, no. 11, pp. 1185–1195, Nov. 2016.

[97] P. Haahr *et al.*, “Activation of the ATR kinase by the RPA-binding protein ETAA1.,” *Nat. Cell Biol.*, vol. 18, no. 11, pp. 1196–1207, Nov. 2016.

[98] J. A. Tercero and J. F. Diffley, “Regulation of DNA replication fork progression through damaged DNA by the Mec1/Rad53 checkpoint.,” *Nature*, vol. 412, no. 6846, pp. 553–557, Aug. 2001.

[99] P. Pichierri, F. Rosselli, and A. Franchitto, “Werner’s syndrome protein is phosphorylated in an ATR/ATM-dependent manner following replication arrest and DNA damage induced during the S phase of the cell cycle.,” *Oncogene*, vol. 22, no. 10, pp. 1491–1500, Mar. 2003.

[100] S. L. Davies, P. S. North, and I. D. Hickson, “Role for BLM in replication-fork restart and suppression of origin firing after replicative stress.,” *Nat. Struct. Mol. Biol.*, vol. 14, no. 7, pp. 677–679, Jul. 2007.

[101] F. B. Couch *et al.*, “ATR phosphorylates SMARCAL1 to prevent replication fork collapse.,” *Genes Dev.*, vol. 27, no. 14, pp. 1610–1623, Jul. 2013.

[102] G. Lossaint *et al.*, “FANCD2 binds MCM proteins and controls replisome function upon activation of s phase checkpoint signaling.,” *Mol. Cell*, vol. 51, no. 5, pp. 678–690, Sep. 2013.

[103] A. K. Murphy *et al.*, “Phosphorylated RPA recruits PALB2 to stalled DNA replication forks to facilitate fork recovery.,” *J. Cell Biol.*, vol. 206, no. 4, pp. 493–507, Aug. 2014.

[104] D. Cortez, G. Glick, and S. J. Elledge, “Minichromosome maintenance proteins are direct targets of the ATM and ATR checkpoint kinases.,” *Proc. Natl. Acad. Sci. U. S. A.*, vol. 101, no. 27, pp. 10078–10083, Jul. 2004.

[105] Y.-H. Chen *et al.*, “ATR-mediated phosphorylation of FANCI regulates dormant origin firing in response to replication stress.,” *Mol. Cell*, vol. 58, no. 2, pp. 323–338, Apr. 2015.

[106] Y.-W. Zhang, T. L. Jones, S. E. Martin, N. J. Caplen, and Y. Pommier, “Implication of checkpoint kinase-dependent up-regulation of ribonucleotide reductase R2 in DNA damage response.,” *J. Biol. Chem.*, vol. 284, no. 27, pp. 18085–18095, Jul. 2009.

[107] V. D’Angiolella *et al.*, “Cyclin F-mediated degradation of ribonucleotide reductase M2 controls genome integrity and DNA repair.,” *Cell*, vol. 149, no. 5, pp. 1023–

1034, May 2012.

[108] X. Zhao, E. G. Muller, and R. Rothstein, “A suppressor of two essential checkpoint genes identifies a novel protein that negatively affects dNTP pools.,” *Mol. Cell*, vol. 2, no. 3, pp. 329–340, Sep. 1998.

[109] E. J. Brown and D. Baltimore, “ATR disruption leads to chromosomal fragmentation and early embryonic lethality.,” *Genes Dev.*, vol. 14, no. 4, pp. 397–402, Feb. 2000.

[110] A. de Klein *et al.*, “Targeted disruption of the cell-cycle checkpoint gene ATR leads to early embryonic lethality in mice.,” *Curr. Biol.*, vol. 10, no. 8, pp. 479–482, Apr. 2000.

[111] K. M. Foote, A. Lau, and J. W. M. Nissink, “Drugging ATR: progress in the development of specific inhibitors for the treatment of cancer.,” *Future Med. Chem.*, vol. 7, no. 7, pp. 873–891, 2015.

[112] Y. Ruzankina, D. W. Schoppy, A. Asare, C. E. Clark, R. H. Vonderheide, and E. J. Brown, “Tissue regenerative delays and synthetic lethality in adult mice after combined deletion of Atr and Trp53.,” *Nat. Genet.*, vol. 41, no. 10, pp. 1144–1149, Oct. 2009.

[113] P. M. Reaper *et al.*, “Selective killing of ATM- or p53-deficient cancer cells through inhibition of ATR.,” *Nat. Chem. Biol.*, vol. 7, no. 7, pp. 428–430, Apr. 2011.

[114] L. I. Toledo *et al.*, “A cell-based screen identifies ATR inhibitors with synthetic lethal properties for cancer-associated mutations.,” *Nat. Struct. Mol. Biol.*, vol. 18, no. 6, pp. 721–727, Jun. 2011.

[115] M. Kwok *et al.*, “ATR inhibition induces synthetic lethality and overcomes chemoresistance in TP53- or ATM-defective chronic lymphocytic leukemia cells.,” *Blood*, vol. 127, no. 5, pp. 582–595, Feb. 2016.

[116] A. Schmitt *et al.*, “ATM Deficiency Is Associated with Sensitivity to PARP1- and ATR Inhibitors in Lung Adenocarcinoma.,” *Cancer Res.*, vol. 77, no. 11, pp. 3040–3056, Jun. 2017.

[117] A. Min *et al.*, “AZD6738, A Novel Oral Inhibitor of ATR, Induces Synthetic Lethality with ATM Deficiency in Gastric Cancer Cells.,” *Mol. Cancer Ther.*, vol. 16, no. 4, pp. 566–577, Apr. 2017.

[118] O. Gilad *et al.*, “Combining ATR suppression with oncogenic Ras synergistically increases genomic instability, causing synthetic lethality or tumorigenesis in a dosage-dependent manner.,” *Cancer Res.*, vol. 70, no. 23, pp. 9693–9702, Dec. 2010.

[119] E. Fokas *et al.*, “Targeting ATR in vivo using the novel inhibitor VE-822 results in selective sensitization of pancreatic tumors to radiation.,” *Cell Death Dis.*, vol. 3, p. e441, Dec. 2012.

[120] R. Prevo *et al.*, “The novel ATR inhibitor VE-821 increases sensitivity of

pancreatic cancer cells to radiation and chemotherapy.," *Cancer Biol. Ther.*, vol. 13, no. 11, pp. 1072–1081, Sep. 2012.

[121] M. Murga *et al.*, "A mouse model of ATR-Seckel shows embryonic replicative stress and accelerated aging.," *Nat. Genet.*, vol. 41, no. 8, pp. 891–898, Aug. 2009.

[122] K. Sanjiv *et al.*, "Cancer-Specific Synthetic Lethality between ATR and CHK1 Kinase Activities.," *Cell Rep.*, vol. 14, no. 2, pp. 298–309, Jan. 2016.

[123] J. P. Y. Mak, W. Y. Man, H. T. Ma, and R. Y. C. Poon, "Pharmacological targeting the ATR-CHK1-WEE1 axis involves balancing cell growth stimulation and apoptosis.," *Oncotarget*, vol. 5, no. 21, pp. 10546–10557, Nov. 2014.

[124] R. Josse *et al.*, "ATR inhibitors VE-821 and VX-970 sensitize cancer cells to topoisomerase i inhibitors by disabling DNA replication initiation and fork elongation responses.," *Cancer Res.*, vol. 74, no. 23, pp. 6968–6979, Dec. 2014.

[125] S. V Muralidharan, J. Bhadury, L. M. Nilsson, L. C. Green, K. G. McLure, and J. A. Nilsson, "BET bromodomain inhibitors synergize with ATR inhibitors to induce DNA damage, apoptosis, senescence-associated secretory pathway and ER stress in Myc-induced lymphoma cells.," *Oncogene*, vol. 35, no. 36, pp. 4689–4697, Sep. 2016.

[126] S. V. Muralidharan *et al.*, "BET bromodomain inhibitors synergize with ATR inhibitors in melanoma.," *Cell Death Dis.*, vol. 8, no. 8, p. e2982, Aug. 2017.

[127] H. Kim *et al.*, "Targeting the ATR/CHK1 Axis with PARP Inhibition Results in Tumor Regression in BRCA-Mutant Ovarian Cancer Models.," *Clin. Cancer Res.*, vol. 23, no. 12, pp. 3097–3108, Jun. 2017.

[128] N. R. Jette *et al.*, "Combined poly-ADP ribose polymerase and ataxia-telangiectasia mutated/Rad3-related inhibition targets ataxia-telangiectasia mutated-deficient lung cancer cells.," *Br. J. Cancer*, vol. 121, no. 7, pp. 600–610, Oct. 2019.

[129] B. A. Gibson and W. L. Kraus, "New insights into the molecular and cellular functions of poly(ADP-ribose) and PARPs.," *Nat. Rev. Mol. Cell Biol.*, vol. 13, no. 7, pp. 411–24, Jun. 2012.

[130] F. Y. Feng, J. S. de Bono, M. A. Rubin, and K. E. Knudsen, "Chromatin to Clinic: The Molecular Rationale for PARP1 Inhibitor Function.," *Mol. Cell*, vol. 58, no. 6, pp. 925–934, Jun. 2015.

[131] R. Gupte, Z. Liu, and W. L. Kraus, "PARPs and ADP-ribosylation: recent advances linking molecular functions to biological outcomes.," *Genes Dev.*, vol. 31, no. 2, pp. 101–126, Jan. 2017.

[132] Z. Q. Wang *et al.*, "Mice lacking ADPRT and poly(ADP-ribosyl)ation develop normally but are susceptible to skin disease," *Genes Dev.*, vol. 9, no. 5, pp. 509–520, Mar. 1995.

[133] M.-F. Langelier, J. L. Planck, S. Roy, and J. M. Pascal, “Crystal structures of poly(ADP-ribose) polymerase-1 (PARP-1) zinc fingers bound to DNA: structural and functional insights into DNA-dependent PARP-1 activity.,” *J. Biol. Chem.*, vol. 286, no. 12, pp. 10690–701, Mar. 2011.

[134] M.-F. Langelier, J. L. Planck, S. Roy, and J. M. Pascal, “Structural basis for DNA damage-dependent poly(ADP-ribosyl)ation by human PARP-1.,” *Science*, vol. 336, no. 6082, pp. 728–32, May 2012.

[135] M. Masson, C. Niedergang, V. Schreiber, S. Muller, J. Menissier-de Murcia, and G. de Murcia, “XRCC1 Is Specifically Associated with Poly(ADP-Ribose) Polymerase and Negatively Regulates Its Activity following DNA Damage,” *Mol. Cell. Biol.*, vol. 18, no. 6, pp. 3563–3571, Jun. 1998.

[136] D. M. Chou *et al.*, “A chromatin localization screen reveals poly (ADP ribose)-regulated recruitment of the repressive polycomb and NuRD complexes to sites of DNA damage.,” *Proc. Natl. Acad. Sci. U. S. A.*, vol. 107, no. 43, pp. 18475–80, Oct. 2010.

[137] G.-Y. Li *et al.*, “Structure and identification of ADP-ribose recognition motifs of APLF and role in the DNA damage response.,” *Proc. Natl. Acad. Sci. U. S. A.*, vol. 107, no. 20, pp. 9129–34, May 2010.

[138] F. Teloni and M. Altmeyer, “Survey and summary readers of poly(ADP-ribose): Designed to be fit for purpose,” *Nucleic Acids Res.*, vol. 44, no. 3, pp. 993–1006, 2016.

[139] Q. Zhang *et al.*, “The WD40 domain of FBXW7 is a poly(ADP-ribose)-binding domain that mediates the early DNA damage response,” *Nucleic Acids Res.*, vol. 47, no. 8, pp. 4039–4053, May 2019.

[140] D. D’Amours, S. Desnoyers, I. D’Silva, and G. G. Poirier, “Poly(ADP-ribosyl)ation reactions in the regulation of nuclear functions,” *Biochemical Journal*, vol. 342, no. 2. pp. 249–268, 01-Sep-1999.

[141] M. De Vos, V. Schreiber, and F. Dantzer, “The diverse roles and clinical relevance of PARPs in DNA damage repair: current state of the art.,” *Biochem. Pharmacol.*, vol. 84, no. 2, pp. 137–46, Jul. 2012.

[142] Y. Liu, F. A. Kadyrov, and P. Modrich, “PARP-1 enhances the mismatch-dependence of 5’-directed excision in human mismatch repair in vitro.,” *DNA Repair (Amst).*, vol. 10, no. 11, pp. 1145–53, Nov. 2011.

[143] M. Robu, R. G. Shah, N. Petitclerc, J. Brind’Amour, F. Kandan-Kulangara, and G. M. Shah, “Role of poly(ADP-ribose) polymerase-1 in the removal of UV-induced DNA lesions by nucleotide excision repair.,” *Proc. Natl. Acad. Sci. U. S. A.*, vol. 110, no. 5, pp. 1658–63, Jan. 2013.

[144] C. Beck, I. Robert, B. Reina-San-Martin, V. Schreiber, and F. Dantzer, “Poly(ADP-ribose) polymerases in double-strand break repair: focus on PARP1, PARP2 and PARP3.,” *Exp. Cell Res.*, vol. 329, no. 1, pp. 18–25, Nov. 2014.

[145] J.-F. Haince *et al.*, “PARP1-dependent kinetics of recruitment of MRE11 and NBS1 proteins to multiple DNA damage sites.,” *J. Biol. Chem.*, vol. 283, no. 2, pp. 1197–208, Jan. 2008.

[146] K. Gudmundsdottir and A. Ashworth, “The roles of BRCA1 and BRCA2 and associated proteins in the maintenance of genomic stability.,” *Oncogene*, vol. 25, no. 43, pp. 5864–74, Sep. 2006.

[147] I. Robert, F. Dantzer, and B. Reina-San-Martin, “Parp1 facilitates alternative NHEJ, whereas Parp2 suppresses IgH/c-myc translocations during immunoglobulin class switch recombination.,” *J. Exp. Med.*, vol. 206, no. 5, pp. 1047–56, May 2009.

[148] M. S. Luijsterburg *et al.*, “PARP1 Links CHD2-Mediated Chromatin Expansion and H3.3 Deposition to DNA Repair by Non-homologous End-Joining.,” *Mol. Cell*, vol. 61, no. 4, pp. 547–562, Feb. 2016.

[149] H. E. Bryant *et al.*, “PARP is activated at stalled forks to mediate Mre11-dependent replication restart and recombination.,” *EMBO J.*, vol. 28, no. 17, pp. 2601–15, Sep. 2009.

[150] S. Ying, F. C. Hamdy, and T. Helleday, “Mre11-dependent degradation of stalled DNA replication forks is prevented by BRCA2 and PARP1.,” *Cancer Res.*, vol. 72, no. 11, pp. 2814–21, Jun. 2012.

[151] H. Farmer *et al.*, “Targeting the DNA repair defect in BRCA mutant cells as a therapeutic strategy,” *Nature*, vol. 434, no. 7035, pp. 917–921, Apr. 2005.

[152] H. E. Bryant *et al.*, “Specific killing of BRCA2-deficient tumours with inhibitors of poly(ADP-ribose) polymerase,” *Nature*, vol. 434, no. 7035, pp. 913–917, Apr. 2005.

[153] P. C. Fong *et al.*, “Inhibition of poly(ADP-ribose) polymerase in tumors from BRCA mutation carriers,” *N. Engl. J. Med.*, vol. 361, no. 2, pp. 123–134, Jul. 2009.

[154] C. J. Lord and A. Ashworth, “PARP inhibitors: Synthetic lethality in the clinic.,” *Science*, vol. 355, no. 6330, pp. 1152–1158, Mar. 2017.

[155] C. B. Bridges, “The origin of variations in sexual and sex-limited characters,” *Am. Nat.*, vol. 56, no. 642, pp. 51–63, 1922.

[156] L. H. Hartwell, P. Szankasi, C. J. Roberts, A. W. Murray, and S. H. Friend, “Integrating genetic approaches into the discovery of anticancer drugs.,” *Science*, vol. 278, no. 5340, pp. 1064–1068, Nov. 1997.

[157] E. R. 3rd McDonald *et al.*, “Project DRIVE: A Compendium of Cancer Dependencies and Synthetic Lethal Relationships Uncovered by Large-Scale, Deep RNAi Screening.,” *Cell*, vol. 170, no. 3, pp. 577-592.e10, Jul. 2017.

[158] N. Turner, A. Tutt, and A. Ashworth, “Hallmarks of ‘BRCAness’ in sporadic cancers,” *Nature Reviews Cancer*, vol. 4, no. 10. pp. 814–819, Oct-2004.

[159] A. M. Mendes-Pereira *et al.*, “Synthetic lethal targeting of PTEN mutant cells with PARP inhibitors.,” *EMBO Mol. Med.*, vol. 1, no. 6–7, pp. 315–22, Sep. 2009.

[160] T. Sourisseau *et al.*, “Aurora-A expressing tumour cells are deficient for homology-directed DNA double strand-break repair and sensitive to PARP inhibition.,” *EMBO Mol. Med.*, vol. 2, no. 4, pp. 130–42, Apr. 2010.

[161] R. Sultana *et al.*, “Targeting XRCC1 deficiency in breast cancer for personalized therapy.,” *Cancer Res.*, vol. 73, no. 5, pp. 1621–34, Mar. 2013.

[162] A. A. Rodriguez *et al.*, “DNA repair signature is associated with anthracycline response in triple negative breast cancer patients.,” *Breast Cancer Res. Treat.*, vol. 123, no. 1, pp. 189–96, Aug. 2010.

[163] L. B. Alexandrov *et al.*, “Signatures of mutational processes in human cancer,” *Nature*, vol. 500, no. 7463, pp. 415–421, 2013.

[164] N. J. Birkbak *et al.*, “Tumor mutation burden forecasts outcome in ovarian cancer with BRCA1 or BRCA2 mutations.,” *PLoS One*, vol. 8, no. 11, p. e80023, 2013.

[165] M. Graeser *et al.*, “A marker of homologous recombination predicts pathologic complete response to neoadjuvant chemotherapy in primary breast cancer,” *Clin. Cancer Res.*, vol. 16, no. 24, pp. 6159–6168, Dec. 2010.

[166] A. Mukhopadhyay *et al.*, “Development of a functional assay for homologous recombination status in primary cultures of epithelial ovarian tumor and correlation with sensitivity to poly(ADP-ribose) polymerase inhibitors.,” *Clin. Cancer Res.*, vol. 16, no. 8, pp. 2344–51, Apr. 2010.

[167] M. W. Audeh *et al.*, “Oral poly(ADP-ribose) polymerase inhibitor olaparib in patients with BRCA1 or BRCA2 mutations and recurrent ovarian cancer: a proof-of-concept trial.,” *Lancet (London, England)*, vol. 376, no. 9737, pp. 245–51, Jul. 2010.

[168] A. Tutt *et al.*, “Oral poly(ADP-ribose) polymerase inhibitor olaparib in patients with BRCA1 or BRCA2 mutations and advanced breast cancer: a proof-of-concept trial.,” *Lancet (London, England)*, vol. 376, no. 9737, pp. 235–44, Jul. 2010.

[169] J. Mateo *et al.*, “DNA-Repair Defects and Olaparib in Metastatic Prostate Cancer.,” *N. Engl. J. Med.*, vol. 373, no. 18, pp. 1697–708, Oct. 2015.

[170] E. S. Christenson and E. S. Antonarakis, “PARP inhibitors for homologous recombination-deficient prostate cancer,” *Expert Opinion on Emerging Drugs*, vol. 23, no. 2. Taylor and Francis Ltd, pp. 123–133, 03-Apr-2018.

[171] A. G. Patel, J. N. Sarkaria, and S. H. Kaufmann, “Nonhomologous end joining drives poly(ADP-ribose) polymerase (PARP) inhibitor lethality in homologous recombination-deficient cells.,” *Proc. Natl. Acad. Sci. U. S. A.*, vol. 108, no. 8, pp. 3406–11, Feb. 2011.

[172] P. Gottipati *et al.*, “Poly(ADP-ribose) polymerase is hyperactivated in homologous recombination-defective cells.,” *Cancer Res.*, vol. 70, no. 13, pp. 5389–98, Jul.

2010.

[173] T. Helleday, “The underlying mechanism for the PARP and BRCA synthetic lethality: clearing up the misunderstandings.,” *Mol. Oncol.*, vol. 5, no. 4, pp. 387–93, Aug. 2011.

[174] R. Plummer *et al.*, “Phase I study of the poly(ADP-ribose) polymerase inhibitor, AG014699, in combination with temozolomide in patients with advanced solid tumors.,” *Clin. Cancer Res.*, vol. 14, no. 23, pp. 7917–7923, Dec. 2008.

[175] C. K. Donawho *et al.*, “ABT-888, an orally active poly(ADP-ribose) polymerase inhibitor that potentiates DNA-damaging agents in preclinical tumor models.,” *Clin. Cancer Res.*, vol. 13, no. 9, pp. 2728–37, May 2007.

[176] M. Rouleau, A. Patel, M. J. Hendzel, S. H. Kaufmann, and G. G. Poirier, “PARP inhibition: PARP1 and beyond.,” *Nat. Rev. Cancer*, vol. 10, no. 4, pp. 293–301, Apr. 2010.

[177] J. O’Shaughnessy *et al.*, “A randomized phase III study of iniparib (BSI-201) in combination with gemcitabine/carboplatin (G/C) in metastatic triple-negative breast cancer (TNBC).,” *J. Clin. Oncol.*, vol. 29, no. 15_suppl, pp. 1007–1007, May 2011.

[178] A. G. Patel, S. B. De Lorenzo, K. S. Flatten, G. G. Poirier, and S. H. Kaufmann, “Failure of iniparib to inhibit poly(ADP-Ribose) polymerase in vitro.,” *Clin. Cancer Res.*, vol. 18, no. 6, pp. 1655–62, Mar. 2012.

[179] M. S. Satoh and T. Lindahl, “Role of poly(ADP-ribose) formation in DNA repair.,” *Nature*, vol. 356, no. 6367, pp. 356–358, Mar. 1992.

[180] V. Schreiber *et al.*, “A dominant-negative mutant of human poly(ADP-ribose) polymerase affects cell recovery, apoptosis, and sister chromatid exchange following DNA damage,” *Proc. Natl. Acad. Sci. U. S. A.*, vol. 92, no. 11, pp. 4753–4757, May 1995.

[181] J. Ménissier De Murcia *et al.*, “Requirement of poly(ADP-ribose) polymerase in recovery from DNA damage in mice and in cells,” *Proc. Natl. Acad. Sci. U. S. A.*, vol. 94, no. 14, pp. 7303–7307, Jul. 1997.

[182] A. Chalmers, P. Johnston, M. Woodcock, M. Joiner, and B. Marples, “PARP-1, PARP-2, and the cellular response to low doses of ionizing radiation,” in *International Journal of Radiation Oncology Biology Physics*, 2004, vol. 58, no. 2, pp. 410–419.

[183] A. J. Chalmers, M. Lakshman, N. Chan, and R. G. Bristow, “Poly(ADP-ribose) polymerase inhibition as a model for synthetic lethality in developing radiation oncology targets.,” *Semin. Radiat. Oncol.*, vol. 20, no. 4, pp. 274–81, Oct. 2010.

[184] D. A. Löser, A. Shibata, A. K. Shibata, L. J. Woodbine, P. A. Jeggo, and A. J. Chalmers, “Sensitization to radiation and alkylating agents by inhibitors of poly(ADP-ribose) polymerase is enhanced in cells deficient in DNA double-strand break repair.,” *Mol. Cancer Ther.*, vol. 9, no. 6, pp. 1775–87, Jun. 2010.

[185] K. A. Bridges, C. Toniatti, C. A. Buser, H. Liu, T. A. Buchholz, and R. E. Meyn, “Niraparib (MK-4827), a novel poly(ADP-Ribose) polymerase inhibitor, radiosensitizes human lung and breast cancer cells.,” *Oncotarget*, vol. 5, no. 13, pp. 5076–86, Jul. 2014.

[186] Y. Pommier, M. J. O’Connor, and J. de Bono, “Laying a trap to kill cancer cells: PARP inhibitors and their mechanisms of action.,” *Sci. Transl. Med.*, vol. 8, no. 362, p. 362ps17, 2016.

[187] P. CHAMBON, J. D. WEILL, and P. MANDEL, “Nicotinamide mononucleotide activation of new DNA-dependent polyadenylic acid synthesizing nuclear enzyme.,” *Biochem. Biophys. Res. Commun.*, vol. 11, pp. 39–43, Apr. 1963.

[188] P. M. Goodwin, P. J. Lewis, M. I. Davies, C. J. Skidmore, and S. Shall, “The effect of gamma radiation and neocarzinostatin on NAD and ATP levels in mouse leukaemia cells.,” *Biochim. Biophys. Acta*, vol. 543, no. 4, pp. 576–582, Nov. 1978.

[189] C. J. Skidmore *et al.*, “The involvement of poly(ADP-ribose) polymerase in the degradation of NAD caused by gamma-radiation and N-methyl-N-nitrosourea.,” *Eur. J. Biochem.*, vol. 101, no. 1, pp. 135–142, Nov. 1979.

[190] B. W. Durkacz, O. Omidiji, D. A. Gray, and S. Shall, “(ADP-ribose)n participates in DNA excision repair.,” *Nature*, vol. 283, no. 5747, pp. 593–596, Feb. 1980.

[191] B. W. Durkacz, S. Shall, and J. Irwin, “The effect of inhibition of (ADP-ribose)n biosynthesis on DNA repair assayed by the nucleoid technique.,” *Eur. J. Biochem.*, vol. 121, no. 1, pp. 65–69, Dec. 1981.

[192] B. W. Durkacz, J. Irwin, and S. Shall, “Inhibition of (ADP-ribose)n biosynthesis retards DNA repair but does not inhibit DNA repair synthesis.,” *Biochem. Biophys. Res. Commun.*, vol. 101, no. 4, pp. 1433–1441, Aug. 1981.

[193] B. Golia, H. R. Singh, and G. Timinszky, “Poly-ADP-ribosylation signaling during DNA damage repair.,” *Front. Biosci. (Landmark Ed.*, vol. 20, pp. 440–457, Jan. 2015.

[194] J. Murai *et al.*, “Trapping of PARP1 and PARP2 by clinical PARP inhibitors,” *Cancer Res.*, vol. 72, no. 21, pp. 5588–5599, Nov. 2012.

[195] C. J. LaFargue, G. Z. Dal Molin, A. K. Sood, and R. L. Coleman, “Exploring and comparing adverse events between PARP inhibitors.,” *Lancet. Oncol.*, vol. 20, no. 1, pp. e15–e28, Jan. 2019.

[196] J. K. Litton *et al.*, “Talazoparib in Patients with Advanced Breast Cancer and a Germline BRCA Mutation.,” *N. Engl. J. Med.*, vol. 379, no. 8, pp. 753–763, Aug. 2018.

[197] M. R. Mirza *et al.*, “Niraparib Maintenance Therapy in Platinum-Sensitive, Recurrent Ovarian Cancer.,” *N. Engl. J. Med.*, vol. 375, no. 22, pp. 2154–2164, Dec. 2016.

[198] M. Robson *et al.*, “Olaparib for Metastatic Breast Cancer in Patients with a Germline BRCA Mutation.,” *N. Engl. J. Med.*, vol. 377, no. 6, pp. 523–533, Aug. 2017.

[199] E. Pujade-Lauraine *et al.*, “Olaparib tablets as maintenance therapy in patients with platinum-sensitive, relapsed ovarian cancer and a BRCA1/2 mutation (SOLO2/ENGOT-Ov21): a double-blind, randomised, placebo-controlled, phase 3 trial.,” *Lancet. Oncol.*, vol. 18, no. 9, pp. 1274–1284, Sep. 2017.

[200] T. A. Hopkins *et al.*, “PARP1 Trapping by PARP Inhibitors Drives Cytotoxicity in Both Cancer Cells and Healthy Bone Marrow.,” *Mol. Cancer Res.*, vol. 17, no. 2, pp. 409–419, Feb. 2019.

[201] P. Lesueur *et al.*, “Poly-(ADP-ribose)-polymerase inhibitors as radiosensitizers: a systematic review of pre-clinical and clinical human studies.,” *Oncotarget*, vol. 8, no. 40, pp. 69105–69124, Sep. 2017.

[202] M. Goggins *et al.*, “Germline BRCA2 gene mutations in patients with apparently sporadic pancreatic carcinomas.,” *Cancer Res.*, vol. 56, no. 23, pp. 5360–5364, Dec. 1996.

[203] F. Xia *et al.*, “Deficiency of human BRCA2 leads to impaired homologous recombination but maintains normal nonhomologous end joining,” *Proc. Natl. Acad. Sci. U. S. A.*, vol. 98, no. 15, pp. 8644–8649, Jul. 2001.

[204] B. Fertil, H. Dertinger, A. Courdi, and E. P. Malaise, “Mean inactivation dose: a useful concept for intercomparison of human cell survival curves.,” *Radiat. Res.*, vol. 99, no. 1, pp. 73–84, Jul. 1984.

[205] S. Shahda *et al.*, “Homologous Recombination Deficiency in Patients With Pancreatic Ductal Adenocarcinoma and Response to Chemotherapy,” *JCO Precis. Oncol.*, no. 2, pp. 1–11, 2018.

[206] A. Gupta *et al.*, “Phase I study to determine the bioavailability and tolerability of a tablet formulation of the PARP inhibitor olaparib in patients with advanced solid tumors: Dose-escalation phase.,” *J. Clin. Oncol.*, vol. 30, no. 15_suppl, p. 3051, 2012.

[207] J. Murai *et al.*, “Stereospecific PARP trapping by BMN 673 and comparison with olaparib and rucaparib.,” *Mol. Cancer Ther.*, vol. 13, no. 2, pp. 433–443, Feb. 2014.

[208] T. Hopkins, B. Ainsworth, V. Abraham, D. Maag, E. Johnson, and J. Wilsbacher, “Abstract B26: Development of a proximity ligation assay for the detection of PARP-1 trapped to chromatin,” 2017, pp. B26–B26.

[209] P. L. Olive, P. J. Johnston, J. P. Banath, and R. E. Durand, “The comet assay: a new method to examine heterogeneity associated with solid tumors.,” *Nat. Med.*, vol. 4, no. 1, pp. 103–105, Jan. 1998.

[210] S. J. Pettitt *et al.*, “Genome-wide and high-density CRISPR-Cas9 screens identify point mutations in PARP1 causing PARP inhibitor resistance.,” *Nat. Commun.*,

vol. 9, no. 1, p. 1849, May 2018.

[211] J. Mendez and B. Stillman, “Chromatin association of human origin recognition complex, cdc6, and minichromosome maintenance proteins during the cell cycle: assembly of prereplication complexes in late mitosis.,” *Mol. Cell. Biol.*, vol. 20, no. 22, pp. 8602–8612, Nov. 2000.

[212] L. A. Parsels *et al.*, “PARP1 Trapping and DNA Replication Stress Enhance Radiosensitization with Combined WEE1 and PARP Inhibitors,” *Mol. Cancer Res.*, vol. 16, no. 2, pp. 222–232, Feb. 2018.

[213] E. Ben-Josef *et al.*, “A phase I/II trial of intensity modulated radiation (IMRT) dose escalation with concurrent fixed-dose rate gemcitabine (FDR-G) in patients with unresectable pancreatic cancer,” *Int. J. Radiat. Oncol. Biol. Phys.*, vol. 84, no. 5, pp. 1166–1171, Dec. 2012.

[214] M. A. Morgan, L. A. Parsels, J. Maybaum, and T. S. Lawrence, “Improving the efficacy of chemoradiation with targeted agents,” *Cancer Discovery*, vol. 4, no. 3. American Association for Cancer Research Inc., pp. 280–291, 2014.

[215] C. G. Engelke *et al.*, “Sensitization of pancreatic cancer to chemoradiation by the Chk1 inhibitor MK8776,” *Clin. Cancer Res.*, vol. 19, no. 16, pp. 4412–4421, Aug. 2013.

[216] R. D. Carruthers *et al.*, “Replication stress drives constitutive activation of the DNA damage response and radioresistance in glioblastoma stem-like cells,” *Cancer Res.*, vol. 78, no. 17, pp. 5060–5071, Sep. 2018.

[217] L. M. Karnitz and L. Zou, “Molecular pathways: Targeting ATR in cancer therapy,” *Clin. Cancer Res.*, vol. 21, no. 21, pp. 4780–4785, Nov. 2015.

[218] M. K. Zeman and K. A. Cimprich, “Causes and consequences of replication stress,” *Nature Cell Biology*, vol. 16, no. 1. pp. 2–9, Jan-2014.

[219] E. Petermann, M. L. Orta, N. Issaeva, N. Schultz, and T. Helleday, “Hydroxyurea-stalled replication forks become progressively inactivated and require two different RAD51-mediated pathways for restart and repair.,” *Mol. Cell*, vol. 37, no. 4, pp. 492–502, Feb. 2010.

[220] A. Maya-Mendoza, P. Moudry, J. M. Merchut-Maya, M. Lee, R. Strauss, and J. Bartek, “High speed of fork progression induces DNA replication stress and genomic instability.,” *Nature*, vol. 559, no. 7713, pp. 279–284, 2018.

[221] J. M. Merchut-Maya, J. Bartek, and A. Maya-Mendoza, “Regulation of replication fork speed: Mechanisms and impact on genomic stability.,” *DNA Repair (Amst).*, vol. 81, p. 102654, Sep. 2019.

[222] I. M. Ward and J. Chen, “Histone H2AX is phosphorylated in an ATR-dependent manner in response to replicational stress.,” *J. Biol. Chem.*, vol. 276, no. 51, pp. 47759–62, Dec. 2001.

[223] J. C. Saldivar, D. Cortez, and K. A. Cimprich, “The essential kinase ATR:

Ensuring faithful duplication of a challenging genome," *Nature Reviews Molecular Cell Biology*, vol. 18, no. 10. Nature Publishing Group, pp. 622–636, 01-Oct-2017.

[224] J. X. Zhou, L. J. Feng, and X. Zhang, "Risk of severe hematologic toxicities in cancer patients treated with PARP inhibitors: a meta-analysis of randomized controlled trials.," *Drug Des. Devel. Ther.*, vol. 11, pp. 3009–3017, 2017.

[225] J. T. Ringley, D. C. Moore, J. Patel, and M. S. Rose, "Poly (ADP-ribose) Polymerase Inhibitors in the Management of Ovarian Cancer: A Drug Class Review.," *P T*, vol. 43, no. 9, pp. 549–556, Sep. 2018.

[226] V. Serra *et al.*, "Abstract 3503: Biomarkers for inhibitors of the replication stress response proteins WEE1 and ATR in triple negative breast cancer," *Cancer Res.*, vol. 79, no. 13 Supplement, p. 3503, 2019.

[227] L. Ren *et al.*, "Potential biomarkers of DNA replication stress in cancer.," *Oncotarget*, vol. 8, no. 23, pp. 36996–37008, Jun. 2017.

[228] Z. Chen *et al.*, "Chromosomal instability of circulating tumor DNA reflect therapeutic responses in advanced gastric cancer," *Cell Death Dis.*, vol. 10, no. 10, Oct. 2019.

[229] I. P. Foskolou, D. Biasoli, M. M. Olcina, and E. M. Hammond, "Measuring DNA Replication in Hypoxic Conditions.," *Adv. Exp. Med. Biol.*, vol. 899, pp. 11–25, 2016.

[230] D. J. McConkey, W. Choi, K. Fournier, L. Marquis, V. Ramachandran, and T. Arumugam, "Molecular Characterization of Pancreatic Cancer Cell Lines," in *Pancreatic Cancer*, New York, NY: Springer New York, 2010, pp. 457–469.

[231] P. G. Pilie, C. Tang, G. B. Mills, and T. A. Yap, "State-of-the-art strategies for targeting the DNA damage response in cancer.," *Nat. Rev. Clin. Oncol.*, vol. 16, no. 2, pp. 81–104, Feb. 2019.

[232] T. S. Lawrence, A. Eisbruch, and D. S. Shewach, "Gemcitabine-mediated radiosensitization.," *Semin. Oncol.*, vol. 24, no. 2 Suppl 7, pp. S7-24-S7-28, Apr. 1997.

[233] J. D. Steffen *et al.*, "Targeting PARP-1 allosteric regulation offers therapeutic potential against cancer.," *Cancer Res.*, vol. 74, no. 1, pp. 31–37, Jan. 2014.

[234] L. Kleinberg *et al.*, "Phase I adult brain tumor consortium (ABTC) trial of ABT-888 (veliparib), temozolomide (TMZ), and radiotherapy (RT) for newly diagnosed glioblastoma multiforme (GBM) including pharmacokinetic (PK) data.," *J. Clin. Oncol.*, vol. 31, no. 15_suppl, p. 2065, 2013.

[235] B. G. Czito *et al.*, "Safety and tolerability of veliparib combined with capecitabine plus radiotherapy in patients with locally advanced rectal cancer: a phase 1b study.," *lancet. Gastroenterol. Hepatol.*, vol. 2, no. 6, pp. 418–426, Jun. 2017.

[236] M. P. Mehta *et al.*, "Veliparib in combination with whole brain radiation therapy in patients with brain metastases: results of a phase 1 study.," *J. Neurooncol.*, vol.

122, no. 2, pp. 409–417, Apr. 2015.

[237] J. Michelena, A. Lezaja, F. Teloni, T. Schmid, R. Imhof, and M. Altmeyer, “Analysis of PARP inhibitor toxicity by multidimensional fluorescence microscopy reveals mechanisms of sensitivity and resistance.,” *Nat. Commun.*, vol. 9, no. 1, p. 2678, Jul. 2018.

[238] D. R. Iyer and N. Rhind, “Replication fork slowing and stalling are distinct, checkpoint-independent consequences of replicating damaged DNA.,” *PLoS Genet.*, vol. 13, no. 8, p. e1006958, Aug. 2017.

[239] C. L. Scott, E. M. Swisher, and S. H. Kaufmann, “Poly (ADP-ribose) polymerase inhibitors: recent advances and future development.,” *J. Clin. Oncol.*, vol. 33, no. 12, pp. 1397–1406, Apr. 2015.

[240] A.-G. Thorsell *et al.*, “Structural Basis for Potency and Promiscuity in Poly(ADP-ribose) Polymerase (PARP) and Tankyrase Inhibitors.,” *J. Med. Chem.*, vol. 60, no. 4, pp. 1262–1271, Feb. 2017.

[241] L. Palazzo and I. Ahel, “PARPs in genome stability and signal transduction: implications for cancer therapy.,” *Biochem. Soc. Trans.*, vol. 46, no. 6, pp. 1681–1695, Dec. 2018.

[242] M.-F. Langelier, A. A. Riccio, and J. M. Pascal, “PARP-2 and PARP-3 are selectively activated by 5’ phosphorylated DNA breaks through an allosteric regulatory mechanism shared with PARP-1.,” *Nucleic Acids Res.*, vol. 42, no. 12, pp. 7762–7775, Jul. 2014.

[243] E. Obaji, T. Haikarainen, and L. Lehtio, “Structural basis for DNA break recognition by ARTD2/PARP2.,” *Nucleic Acids Res.*, vol. 46, no. 22, pp. 12154–12165, Dec. 2018.

[244] L. Lin, Y. Zhang, Z.-Y. Chen, Y. Chen, and C.-P. Ren, “The clinicopathological significance of miR-149 and PARP-2 in hepatocellular carcinoma and their roles in chemo/radiotherapy.,” *Tumour Biol.*, vol. 37, no. 9, pp. 12339–12346, Sep. 2016.

[245] Y. H. Kang, K.-A. Lee, J.-H. Kim, S.-G. Park, and D.-Y. Yoon, “Mitomycin C modulates DNA-double strand break repair genes in cervical carcinoma cells.,” *Amino Acids*, vol. 39, no. 5, pp. 1291–1298, Nov. 2010.

[246] V. Schreiber *et al.*, “Poly(ADP-ribose) polymerase-2 (PARP-2) is required for efficient base excision DNA repair in association with PARP-1 and XRCC1.,” *J. Biol. Chem.*, vol. 277, no. 25, pp. 23028–23036, Jun. 2002.

[247] H. Hanzlikova, W. Gittens, K. Krejcikova, Z. Zeng, and K. W. Caldecott, “Overlapping roles for PARP1 and PARP2 in the recruitment of endogenous XRCC1 and PNKP into oxidized chromatin.,” *Nucleic Acids Res.*, vol. 45, no. 5, pp. 2546–2557, Mar. 2017.

[248] J. Menissier de Murcia *et al.*, “Functional interaction between PARP-1 and PARP-2 in chromosome stability and embryonic development in mouse.,” *EMBO J.*, vol.

22, no. 9, pp. 2255–2263, May 2003.

[249] Q. Chen, M. A. Kassab, F. Dantzer, and X. Yu, “PARP2 mediates branched poly ADP-ribosylation in response to DNA damage.,” *Nat. Commun.*, vol. 9, no. 1, p. 3233, Aug. 2018.

[250] A. Fouquin, J. Guirouilh-Barbat, B. Lopez, J. Hall, M. Amor-Gueret, and V. Pennaneach, “PARP2 controls double-strand break repair pathway choice by limiting 53BP1 accumulation at DNA damage sites and promoting end-resection.,” *Nucleic Acids Res.*, vol. 45, no. 21, pp. 12325–12339, Dec. 2017.

[251] B. Gui *et al.*, “Selective targeting of PARP-2 inhibits androgen receptor signaling and prostate cancer growth through disruption of FOXA1 function,” *Proc. Natl. Acad. Sci. U. S. A.*, vol. 116, no. 29, pp. 14573–14582, 2019.

[252] A. Parolia *et al.*, “Distinct structural classes of activating FOXA1 alterations in advanced prostate cancer.,” *Nature*, vol. 571, no. 7765, pp. 413–418, Jul. 2019.

[253] C. Boehler *et al.*, “Poly(ADP-ribose) polymerase 3 (PARP3), a newcomer in cellular response to DNA damage and mitotic progression.,” *Proc. Natl. Acad. Sci. U. S. A.*, vol. 108, no. 7, pp. 2783–2788, Feb. 2011.

[254] S. L. Rulten *et al.*, “PARP-3 and APLF function together to accelerate nonhomologous end-joining.,” *Mol. Cell*, vol. 41, no. 1, pp. 33–45, Jan. 2011.

[255] A. L. Fenton, P. Shirodkar, C. J. Macrae, L. Meng, and C. A. Koch, “The PARP3- and ATM-dependent phosphorylation of APLF facilitates DNA double-strand break repair.,” *Nucleic Acids Res.*, vol. 41, no. 7, pp. 4080–4092, Apr. 2013.

[256] C. Beck *et al.*, “PARP3 affects the relative contribution of homologous recombination and nonhomologous end-joining pathways.,” *Nucleic Acids Res.*, vol. 42, no. 9, pp. 5616–5632, May 2014.

[257] S. Rottenberg *et al.*, “High sensitivity of BRCA1-deficient mammary tumors to the PARP inhibitor AZD2281 alone and in combination with platinum drugs.,” *Proc. Natl. Acad. Sci. U. S. A.*, vol. 105, no. 44, pp. 17079–17084, Nov. 2008.

[258] T. Hay *et al.*, “Poly(ADP-ribose) polymerase-1 inhibitor treatment regresses autochthonous Brca2/p53-mutant mammary tumors in vivo and delays tumor relapse in combination with carboplatin.,” *Cancer Res.*, vol. 69, no. 9, pp. 3850–3855, May 2009.

[259] R. Callaghan, F. Luk, and M. Bebawy, “Inhibition of the multidrug resistance P-glycoprotein: time for a change of strategy?,” *Drug Metab. Dispos.*, vol. 42, no. 4, pp. 623–631, Apr. 2014.

[260] L. Oplustil O’Connor *et al.*, “The PARP Inhibitor AZD2461 Provides Insights into the Role of PARP3 Inhibition for Both Synthetic Lethality and Tolerability with Chemotherapy in Preclinical Models.,” *Cancer Res.*, vol. 76, no. 20, pp. 6084–6094, Oct. 2016.

[261] L. J. Barber *et al.*, “Secondary mutations in BRCA2 associated with clinical

resistance to a PARP inhibitor.," *J. Pathol.*, vol. 229, no. 3, pp. 422–429, Feb. 2013.

[262] E. L. Gornstein *et al.*, "BRCA2 Reversion Mutation Associated With Acquired Resistance to Olaparib in Estrogen Receptor-positive Breast Cancer Detected by Genomic Profiling of Tissue and Liquid Biopsy.," *Clin. Breast Cancer*, vol. 18, no. 2, pp. 184–188, Apr. 2018.

[263] D. Quigley *et al.*, "Analysis of Circulating Cell-Free DNA Identifies Multiclonal Heterogeneity of BRCA2 Reversion Mutations Associated with Resistance to PARP Inhibitors.," *Cancer Discov.*, vol. 7, no. 9, pp. 999–1005, Sep. 2017.

[264] B. Weigelt *et al.*, "Diverse BRCA1 and BRCA2 Reversion Mutations in Circulating Cell-Free DNA of Therapy-Resistant Breast or Ovarian Cancer.," *Clin. Cancer Res.*, vol. 23, no. 21, pp. 6708–6720, Nov. 2017.

[265] J. Goodall *et al.*, "Circulating Cell-Free DNA to Guide Prostate Cancer Treatment with PARP Inhibition.," *Cancer Discov.*, vol. 7, no. 9, pp. 1006–1017, Sep. 2017.

[266] M. J. Pishvaian *et al.*, "BRCA2 secondary mutation-mediated resistance to platinum and PARP inhibitor-based therapy in pancreatic cancer.," *Br. J. Cancer*, vol. 116, no. 8, pp. 1021–1026, Apr. 2017.

[267] O. Kondrashova *et al.*, "Secondary Somatic Mutations Restoring RAD51C and RAD51D Associated with Acquired Resistance to the PARP Inhibitor Rucaparib in High-Grade Ovarian Carcinoma.," *Cancer Discov.*, vol. 7, no. 9, pp. 984–998, Sep. 2017.

[268] P. ter Brugge *et al.*, "Mechanisms of Therapy Resistance in Patient-Derived Xenograft Models of BRCA1-Deficient Breast Cancer," *JNCI J. Natl. Cancer Inst.*, vol. 108, no. 11, 2016.

[269] S. F. Bunting *et al.*, "53BP1 inhibits homologous recombination in Brca1-deficient cells by blocking resection of DNA breaks.," *Cell*, vol. 141, no. 2, pp. 243–254, Apr. 2010.

[270] P. Bouwman *et al.*, "53BP1 loss rescues BRCA1 deficiency and is associated with triple-negative and BRCA-mutated breast cancers.," *Nat. Struct. Mol. Biol.*, vol. 17, no. 6, pp. 688–695, Jun. 2010.

[271] L. Cao *et al.*, "A selective requirement for 53BP1 in the biological response to genomic instability induced by Brca1 deficiency.," *Mol. Cell*, vol. 35, no. 4, pp. 534–541, Aug. 2009.

[272] A. Shibata, "Regulation of repair pathway choice at two-ended DNA double-strand breaks.," *Mutat. Res.*, vol. 803–805, pp. 51–55, Oct. 2017.

[273] I. Bajrami *et al.*, "Genome-wide profiling of genetic synthetic lethality identifies CDK12 as a novel determinant of PARP1/2 inhibitor sensitivity.," *Cancer Res.*, vol. 74, no. 1, pp. 287–297, Jan. 2014.

[274] S. J. Pettitt *et al.*, "A genetic screen using the PiggyBac transposon in haploid

cells identifies Parp1 as a mediator of olaparib toxicity.," *PLoS One*, vol. 8, no. 4, p. e61520, 2013.

[275] E. Gogola *et al.*, "Selective Loss of PARG Restores PARylation and Counteracts PARP Inhibitor-Mediated Synthetic Lethality.," *Cancer Cell*, vol. 33, no. 6, pp. 1078-1093.e12, Jun. 2018.

[276] A. Ray Chaudhuri *et al.*, "Replication fork stability confers chemoresistance in BRCA-deficient cells.," *Nature*, vol. 535, no. 7612, pp. 382–387, Jul. 2016.

[277] J. Murai *et al.*, "SLFN11 Blocks Stressed Replication Forks Independently of ATR.," *Mol. Cell*, vol. 69, no. 3, pp. 371-384.e6, Feb. 2018.

[278] S. A. Yazinski *et al.*, "ATR inhibition disrupts rewired homologous recombination and fork protection pathways in PARP inhibitor-resistant BRCA-deficient cancer cells.," *Genes Dev.*, vol. 31, no. 3, pp. 318–332, Feb. 2017.

[279] J. Murai *et al.*, "Resistance to PARP inhibitors by SLFN11 inactivation can be overcome by ATR inhibition.," *Oncotarget*, vol. 7, no. 47, pp. 76534–76550, Nov. 2016.

[280] A. Ribas and J. D. Wolchok, "Cancer immunotherapy using checkpoint blockade," *Science (80-.).*, vol. 359, no. 6382, SI, p. 1350+, Mar. 2018.

[281] K. W. Mouw, M. S. Goldberg, P. A. Konstantinopoulos, and A. D. D'Andrea, "DNA Damage and Repair Biomarkers of Immunotherapy Response.," *Cancer Discov.*, vol. 7, no. 7, pp. 675–693, Jul. 2017.

[282] M. E. Lomax, L. K. Folkes, and P. O'Neill, "Biological consequences of radiation-induced DNA damage: relevance to radiotherapy.," *Clin. Oncol. (R. Coll. Radiol).*, vol. 25, no. 10, pp. 578–585, Oct. 2013.

[283] F. M. Marincola, E. M. Jaffee, D. J. Hicklin, and S. Ferrone, "Escape of human solid tumors from T-cell recognition: molecular mechanisms and functional significance.," *Adv. Immunol.*, vol. 74, pp. 181–273, 2000.

[284] E. A. Reits *et al.*, "Radiation modulates the peptide repertoire, enhances MHC class I expression, and induces successful antitumor immunotherapy.," *J. Exp. Med.*, vol. 203, no. 5, pp. 1259–1271, May 2006.

[285] T. Li and Z. J. Chen, "The cGAS-cGAMP-STING pathway connects DNA damage to inflammation, senescence, and cancer.," *J. Exp. Med.*, vol. 215, no. 5, pp. 1287–1299, May 2018.

[286] C. Vanpouille-Box *et al.*, "DNA exonuclease Trex1 regulates radiotherapy-induced tumour immunogenicity.," *Nat. Commun.*, vol. 8, p. 15618, Jun. 2017.

[287] S. M. Harding, J. L. Benci, J. Irianto, D. E. Discher, A. J. Minn, and R. A. Greenberg, "Mitotic progression following DNA damage enables pattern recognition within micronuclei.," *Nature*, vol. 548, no. 7668, pp. 466–470, Aug. 2017.

[288] H. Sato *et al.*, “DNA double-strand break repair pathway regulates PD-L1 expression in cancer cells.,” *Nat. Commun.*, vol. 8, no. 1, p. 1751, Nov. 2017.

[289] M. A. Postow *et al.*, “Immunologic correlates of the abscopal effect in a patient with melanoma.,” *N. Engl. J. Med.*, vol. 366, no. 10, pp. 925–931, Mar. 2012.

[290] K. Reynders, T. Illidge, S. Siva, J. Y. Chang, and D. De Ruysscher, “The abscopal effect of local radiotherapy: using immunotherapy to make a rare event clinically relevant.,” *Cancer Treat. Rev.*, vol. 41, no. 6, pp. 503–510, Jun. 2015.

[291] M. T. Yilmaz, A. Elmali, and G. Yazici, “Abscopal Effect, From Myth to Reality: From Radiation Oncologists’ Perspective.,” *Cureus*, vol. 11, no. 1, p. e3860, Jan. 2019.

[292] E. J. Lipson and C. G. Drake, “Ipilimumab: an anti-CTLA-4 antibody for metastatic melanoma.,” *Clin. Cancer Res.*, vol. 17, no. 22, pp. 6958–6962, Nov. 2011.

[293] J. Gong, A. Chehrazi-Raffle, S. Reddi, and R. Salgia, “Development of PD-1 and PD-L1 inhibitors as a form of cancer immunotherapy: a comprehensive review of registration trials and future considerations.,” *J. Immunother. cancer*, vol. 6, no. 1, p. 8, Jan. 2018.

[294] M. Z. Dewan *et al.*, “Fractionated but not single-dose radiotherapy induces an immune-mediated abscopal effect when combined with anti-CTLA-4 antibody.,” *Clin. Cancer Res.*, vol. 15, no. 17, pp. 5379–5388, Sep. 2009.

[295] S. J. Dovedi *et al.*, “Fractionated Radiation Therapy Stimulates Antitumor Immunity Mediated by Both Resident and Infiltrating Polyclonal T-cell Populations when Combined with PD-1 Blockade.,” *Clin. Cancer Res.*, vol. 23, no. 18, pp. 5514–5526, Sep. 2017.

[296] L. Deng *et al.*, “Irradiation and anti-PD-L1 treatment synergistically promote antitumor immunity in mice.,” *J. Clin. Invest.*, vol. 124, no. 2, pp. 687–695, Feb. 2014.

[297] C. Twyman-Saint Victor *et al.*, “Radiation and dual checkpoint blockade activate non-redundant immune mechanisms in cancer.,” *Nature*, vol. 520, no. 7547, pp. 373–377, Apr. 2015.

[298] L. Tian *et al.*, “Mutual regulation of tumour vessel normalization and immunostimulatory reprogramming.,” *Nature*, vol. 544, no. 7649, pp. 250–254, Apr. 2017.

[299] X. Zheng *et al.*, “Increased vessel perfusion predicts the efficacy of immune checkpoint blockade.,” *J. Clin. Invest.*, vol. 128, no. 5, pp. 2104–2115, May 2018.

[300] S. Rockwell, I. T. Dobrucki, E. Y. Kim, S. T. Marrison, and V. T. Vu, “Hypoxia and radiation therapy: past history, ongoing research, and future promise.,” *Curr. Mol. Med.*, vol. 9, no. 4, pp. 442–458, May 2009.

[301] T. W. H. Meijer, J. H. A. M. Kaanders, P. N. Span, and J. Bussink, “Targeting hypoxia, HIF-1, and tumor glucose metabolism to improve radiotherapy efficacy.,”

Clin. Cancer Res., vol. 18, no. 20, pp. 5585–5594, Oct. 2012.

[302] L.-L. Sun *et al.*, “Inhibition of ATR downregulates PD-L1 and sensitizes tumor cells to T cell-mediated killing.,” *Am. J. Cancer Res.*, vol. 8, no. 7, pp. 1307–1316, 2018.

[303] F. P. Vendetti *et al.*, “ATR kinase inhibitor AZD6738 potentiates CD8+ T cell-dependent antitumor activity following radiation.,” *J. Clin. Invest.*, vol. 128, no. 9, pp. 3926–3940, Aug. 2018.

[304] M. T. Dillon *et al.*, “ATR Inhibition Potentiates the Radiation-induced Inflammatory Tumor Microenvironment.,” *Clin. Cancer Res.*, vol. 25, no. 11, pp. 3392–3403, Jun. 2019.

[305] Q. Zhang *et al.*, “Inhibition of ATM Increases Interferon Signaling and Sensitizes Pancreatic Cancer to Immune Checkpoint Blockade Therapy.,” *Cancer Res.*, vol. 79, no. 15, pp. 3940–3951, Aug. 2019.

[306] S. Jiao *et al.*, “PARP Inhibitor Upregulates PD-L1 Expression and Enhances Cancer-Associated Immunosuppression.,” *Clin. Cancer Res.*, vol. 23, no. 14, pp. 3711–3720, Jul. 2017.

[307] P. A. Konstantinopoulos *et al.*, “Single-Arm Phases 1 and 2 Trial of Niraparib in Combination With Pembrolizumab in Patients With Recurrent Platinum-Resistant Ovarian Carcinoma,” *JAMA Oncol.*, vol. 5, no. 8, pp. 1141–1149, 2019.